eman ta zabal zazu

Universidad | Euskal Herriko
del País Vasco | Unibertsitatea

Universidad del País Vasco / Euskal Herriko Unibertsitatea
Facultad de Medicina y Enfermería
Departamento de Neurociencias

How Aging, Seizures and ATP Change the Intrinsic Properties of Adult Hippocampal Neural Stem Cells

Tesis doctoral para optar al grado de Doctor, presentada por

Soraya Martín Suárez

2018

Director de Tesis:

Prof. Juan Manuel Encinas, PhD.

TABLE OF CONTEXT

TABLE OF CONTEXT

1. ABBREVIATIONS

1. ABBREVIATIONS

Act-casp3	Activated caspase 3
ADP	Adenosine diphosphate
AHN	Adult hippocampal Neurogenesis
ANOVA	Analysis of variance
ANP	Amplifiying neuroprotenitors
AP	Antero-Posterior
ASCL-1	Achaete-Scute Family BHLH Transcription Factor 1
ATP	Adenosine triphosphate
ATP-γ	Adenosine 5'-O-(3-thio)triphosphate
BBB	Blood- brain barrier
BDNF	Brain Derived Neurotrophic Factor
BLBP	Brain lipid binding protein
BMP	Bone morphogenetic protein
BRDU	Bromo-deoxyuridine
BSA	Bovine serum albumin
cDNA	Complementary DNA
CNS	Central nervous system
CNT	Control
DAPI	4',6-diamidino-2-phenylindole
DCX	Doublecortin
DG	Dentate gyrus
DMEM	Dulbecco's Modified Eagle's Medium
DNA	Deoxyribonucleic acid
DNAse	Deoxyribonuclease
DS	Dravet Syndrome
DV	Dorsoventral
EC50	Effective concentration
EDTA	Ethylenediaminetetraacetic acid
EEG	Electroencephalogram
EGF	Epidermal Growth Factor
EGFP	Enhanced green fluorescent protein
FACS	Fluorescence-activated cell sorting

ABBREVIATIONS

FBS	Fetal Bovine Serum
FGF	Fibroblast growth factor
FWD	Forward
GABA	Gamma amynobutyric acid
GCD	Granule cell layer dispersion
GCL	Granule cell layer
GFAP	Glial fibrillary acidic protein
GFP	Green fluorescent protein
HBSS	Hank's balanced salt solution
HCl	Hydrochloride acid
HEK	Human embryonic kidney cells 293,
HEPES	4-(2-hydroxyethyl)-1-piperazineethanesulfonic acid
HPA	Hypothalamic-pituitary adrenal (HPA) axis
HPRT	Hypoxanthine guanine phosphoribosyl transferase
IFN	Interferon
IFN-α	Interferon-alpha
IGF	Insulin-like growth factor1
IL	Interleukin
IL-1β	Interleukin 1 beta
IL-4	Interleukin-4
IL-6	Interleukin-6
KA	Kainic Acid
KCl	Potassium chloride
KO	Knock-out
LB*medium	Luria-Bertani medium
LL	Latero-lateral
LPA	Lysophosphatidic acid
LPS	Bacterial lipopolysaccharide
mM	Milimolar
mRNA	Messenger ribonucleic acid
MTLE	Mesial Temporal lobe epilepsy
NaCl	Sodium chloride
NaH2PO4	Sodium phosphate monobasic
NaHCO3	Sodium bicarbonate
NEUN	Neuronal nuclei antigen

ABBREVIATIONS

NEURO2A	Neuroblastoma cells
nL	Nanolitres
NMDA	N-methyl-D-aspartic acid
NPC	Neuroprogenitor cells
NSC	Neural Stem Cells
P—	Post natal
P2X	Purinergic receptor X
P2Y	Purinergic receptor Y
PBS	Phosphate buffered saline
PCR	Polymerase chain reaction
PFA	Paraformaldehyde
POLY I:C	Polyinosinic:polycytidylic acid
Qpcr	Quantitative polymerase chain reaction
REV	Reverse
RMS	Rostral migratory stream
RNA	Ribonucleic acid
React-NSCS	Reactive Neural Stem Cells
RT	Room Temperature
RT-Qpcr	Real Time-Quantitative Polymerase Chain Reaction
RTqPCR	Reverse transcription quantitative polymerase chain reaction
S1OOβ	S100 calcium binding protein b
Sal	Saline
SCN	Sodium voltage-gated channels
SE	Status epilepticus
SGZ	Subgranular zone
SIP	Solution of isotonic percoll
SIV	Simian immunodeficiency virus
SOX2	Sex.RY box 2
SUDEP	Sudden Unexpected Death from Epilepsy
SVZ	Subventricular zone
TBI	Traumatic Brain Injury
TGF	Transforming Growth Factor
TGFβ	Transforming Growth Factor β
TLE	Temporal Lobe epilepsy
TLR	Toll-like receptors

ABBREVIATIONS

TNF	Tumor Necrosis Factor
TNF-α	Tumor Necrosis Factor alpha
TNP-ATP	2',3'-O-Trinitrophenyl-adenosine-5'-triphosphate,
UDP	Uridine diphosphate
UTP	Uridine triphosphate
VEGF	Vascular endothelial growth factor
VSV	Simian immunodeficiency virus
WT	Wild type
μm	Micron

2. RESUMEN/SUMMARY

2. RESUMEN

El cerebro de la mayoría de los mamíferos, incluyendo humanos, es capaz de generar nuevas neuronas a lo largo de la vida adulta mediante un proceso llamado neurogénesis. Estas nuevas neuronas proceden de las células madre neurales (Neural Stem Cells, NSCs).

Las NSCs del hipocampo comparten propiedades con la glía radial responsable de la neurogénesis y la astrogliogénesis (generación de astrocitos) durante el desarrollo; y con los astrocitos como es la expresión de GFAP (glial fibrilary acidic protein), vimentina o BLBP (brain lipid binding protein), además de diversas características morfológicas y electrofisiológicas, son capaces de ser activadas y entrar en el ciclo celular. Las NSCs activadas se dividen mayoritariamente de manera asimétrica dando lugar a progenitores neurales que continúan la cascada neurogénica madurando a neuroblastos postmitóticos hasta diferenciarse progresivamente en neuronas que se integran en los circuitos del hipocampo, finalmente las NSCs comienzan a diferenciarse en astrocitos que migran al hilus o la capa molecular del DG. La proporción de NSCs que salen del estado quiescente y se activan para entrar en ciclo celular se mantiene constante a lo largo de la edad, por lo que en cada momento, la proporción mayoritaria de las NSCs, (independientemente de su número total), está en estado quiescente. Como consecuencia de la activacion, la población de NSCs disminuye progresivamente en el DG y la astroconversión acoplada a la activación explica a su vez por qué la neurogénesis declina con la edad. Debido a que la neurogénesis se ve implicada en el proceso de formación de nuevas memorias en el aprendizaje, la inhibición de la neurogénesis hipocampal adulta acarrea unos déficits cognitivos negativos sobre las tareas dependientes del hipocampo Además, el bloqueo de la neurogénesis afecta negativamente al control hipocampal de estados de ánimo como la ansiedad/depresión y las respuestas al estrés y al miedo.

Este balance entre la activación y la quiescencia deja entrever que la población global de NSCs es heterogénea y que la regulación del nicho depende de las propiedades individuales de las NSCs.

Además, la edad no solo disminuye de forma drástica la población de las NSCs, tal y como se ha explicado anteriormente, sino que el nicho neurogénico presenta un perfil inflamado que influye directamente sobre el comportamiento de las NSCs, y por tanto afecta también a la neurogenesis. Otras condiciones patológicas como la epilepsia también modulan el comportamiento de las NSCS. En un modelo de epilepsia del lóbulo temporal (MTLE), las NSCs del hipocampo se transforman en astrocitos reactivos debido a las convulsiones, contribuyendo directamente a la aparición de la gliosis típica de la esclerosis hipocampal (HS).

RESUMEN/SUMMARY

Es decir, cambian a un fenotipo hipertrófico y multirramificado, y abandonan la quiescencia para entrar masivamente en división celular. Sorprendentemente, las NSCs reactivas cambian además a un modo de división simétrico para generar astrocitos reactivos mientras en paralelo ellas mismas se transforman en astrocitos reactivos. Como consecuencia la neurogénesis queda extinguida y las funciones a ellas se pierden, admás de perderse la capacidad de regenrar las neuronas muertas por excitotoxicidad en las crisis epilépticas.

El objetivo de esta tesis es estudiar las **propiedades de las NSCs del giro dentado y evaluar elefecto de estas alteraciones sobre la neurogénesis, dado que las NSCs constituyen el primer paso de la cascada neurogénica**. En base a esta idea hipotetizamos que las alteraciones sufridas en las propiedades intrínsecas de las células madre hipocampales en condiciones fisiopatológicacs, como la epilepsia o el envejecimiento, son la causa primera de su disfuncionalidad.

Las NSCs del giro dentado del hipocampo son el centro de nuestro nuestro **primer objetivo,** que es el estudio del efecto de las convulsiones sobre las NSCs y el nicho neurogénico. Con este propósito hemos usado un modelo de epilepsia inducido por la administración intahipocampal de KA *in vivo*. Estudiaremos diferentes parámetros como la proliferación, el tipo de división o la supervivencia de las NSCsHemos podido comprobar que las NSCs en condiciones de hiperexcitación neuronal sufren un cambio radical en su función, convirtiéndose en NSCs reactivas (React-NSCs). Este nuevo fenotipo adquirido bajo estas condiciones se caracteriza por salir de su estado quiescente y proliferar de manera masiva. Esta hiperproliferación está acompañada por un cambio morfológico y una pérdida de la capacidad neurogénica ya que las NSCs al trasnformadas en React-NSCs terminan diferenciándose en astrocitos reactivos perdiendo su capacidad deentrar en la cascada neurogénica de manera duradera. Además hemos evaluado la capacidad de las NSCs para participar en el desarrollo y progreso de la patología mediante la el análisis de la liberación de citoquinas pro-inflamatorias demostrando que en efecto las Reac-NSCs por ejemplo pasan a sobrexpresar la interleukina IL1B, un mediado proinflamtorio esencial que además se considera como capaz de ser epileptogénico.

Nuestro **segundo objetivo** ha sido analizar muestras de pacientes epilépticos humanos. Para ello, hemos analizado muestras hipocampales de pacientes humanos terapéuticamente extirpadas como única manera de controlar las crisis tras el fracaso de los tratamientos farmacológiocs. Los estudios realizados en estas muestras muestran además de una clara esclerosis hipocampal con profusión de astrocitos reactivos en todas las áreas del DG y dispersión de la capa granular, la total ausencia de proliferación celular, de

neuroblastos/neuronas inmaduras, y de céluas que pudieran ser consideradas como NSCs. características típicas de esta enfermedad. Además nos ha permitido confirmar que nuestro modelo de ratón es una herramienta que imita perfectamente la fisiopatología humana.

Con intención de comprobar que las alteraciones observadas en las NSCs no son debidas únicamente al modelo en sí de inducción de la epilepsia sino que es un proceso común de las patologías en las que interviene la hipexcitación neuronal, como es el caso de las convulsiones, nuestro **tercer objetivo** se centra en el estudio del síndrome de Dravet (DS). El DS es un tipo de epilepsia genética infantil en la que los niños desarrollan convulsiones durante su primer año de vida. El DS es una epilepsia multifocal e intratable caracterizada por una elevada tasa de mortalidad. Usamos para su estudio un raton trasgenico (Synapsin-Cre Xx floxed stop Scn1a*A1783V) que mimetiza a la perfección las características de esta enfermedad. Estas muestras presentan una elevada gliosis, presencia de React-NSCs y un aumento en la proliferación de las NSCs, estos cambios están acompañados por una dispersión de la capa de células granulares y alteraciones morfologicas en los núcleos que la conforman, perdiendo por completo la circularidad a favor de un un fenotipo irregular casi poliédrico.

Como la epilepsia es una enfermedad compleja en la que la excitación neuronal está acompañada por un proceso inflamatorio, nuestro **cuarto objetivo** ha sido discernir entre el efecto de la neuroinflamación y el efecto de la excitación neuronal. Para ello hemos administrado intrahipocampalmente diferentes agentes proinflamatorios que abarcan desde procesos inflamatorios inducidos por bacterias o virus (LPS, PolyI:C) hasta la administración directa de cotokinas proinflamatorias (como IL6 o iFN-α). Tras analizar la morfología y división de las NSCs podemos confirmar que el proceso de inflamación no transforma las NSCs en NSCs reactivas, de hecho la proliferación de las NSCs puede disminuir sin inducir modificación alguna en su morfología. Hemos estudiado el efecto de la neuroexcitación utilizando un modelo de daño cerebral por trauma (traumatic brain injury, TBI) y la antes mencionada inyección de KA. Ambos modelos inducen un aumento en la proliferación de las NSCs así como la transformación de las NSCs en NSCs reactivas. De este objetivo podemos concluir que mientras la inflamación no es suficiente para inducir la transformación de las NSCs en React-NSCs los modelos de neuroexcitación inducen esta transformación.

Una de las principales características de las convulsiones es la liberación de ATP, por lo tanto pensamos que esta molécula podría estar actuando como mediadora entre las convulsiones y la transformación de NSCs en React-NSCs. Para conocer el efecto del ATP *per se* de esta molécula nuestro **quinto objetivo** fue inyectar ATP intrahipocampalmente. Para

evaluar el efecto del ATP sobre las NSCs analizaremos parámetros como la proliferación o el cambio morfológico. Tras la administración de ATP en diferentes concentraciónes observamos que la proliferación de las NSCs era dosis-dependiente, al igual que su cambio morfológico. A mayor dosis de ATP mayor la inducción de React-NSCs.

Nuestro **sexto objetivo** fue analizar si las NSCs eran capaces de responder directamente al ATP o si era mediada por otras células. Para ello tras aislar NSCs del giro dentado adulto verificamos si las NSCs presentaban receptores purinérgicos. Utilizando la técnica de RT-qPCR confirmamos la presencia de lo varios receptores P2X, confirmando que las NSCs son capaces de reaccionar directamente al ATP.

Como las NSCs *in vivo* se encuentran rodeadas por diferentes tipos celulares que también pueden reaccionar al ATP, no podemos separar el efecto directo del ATP del efecto indirecto que podrán estar alterando las propiedades de las NSCs, por lo tanto decidimos utilizar un modelo *in vitro* de células neuroprogenitoras provenientes del giro dentado del hipocampo. Nuestro **séptimo objetivo** por tanto ha sido analizar el efecto del ATP en cultivos celulares de neuroesferas provenientes del giro dentad del hipocampo adulto. La adminsitración al medio celular de ATP induce un aumento de la proliferación de las células neuroprogenitoras, además de un cambio en el área ocupada por estas células, parámetros equivalentes a los utilizados en vivo.. Además comprobamos nuevamente que las células progenitoras presentan receptores purinérgicos (P2X), confirmándose de nuevo la presencia de los mismos en estas células tanto *in vitro* como *in vivo*. Finalmente administramos un bloqueador de los receptores (TNP-ATP) para comprobar si el efecto del ATP en las neurosferas (proliferación y cecimiento celular) podía ser atenuado. Tras la administración del TNP-ATP la proliferación celular disminuyo así como el área ocupada por las células.

Estos resultados nos llevaron a nuestro **octavo objetivo** que consistió en la elaboración de microRNAs, como herramienta molecular para bloquear la expresión de los receptores purinérgicos ante condiciones de elevadas concentraciones de ATP *in vitro* e *in vivo*. Para ello generamos plámidos que contienen miRNA contra los recepores purinergicos. Estos miRNAg se generaron en colaboracion directa con la Dra. Veerle Baekeland del de Universidad Catolica de Leuven durante la estancia fueron testados *in vitro* en células Neuro2a, confirmando un descenso de la eficiencia. Por tanto la generación de estos constructos se presenta como una herramienta perfecta para bloquear los receptores purinérgico *in vivo*, en un futuro.

Finalmente queríamos investigar las alteraciones que sufren las NSCs en la condición de envejecimiento, que a efectos practicos se considera una situación fisiopatológica. Nuestro

noveno objetivo es el estudio de las propiedades de las NSCs a lo largo de diferentes puntos temporales para monitorizar el envejecimiento en el nicho neurogénico hipocampal. Durante el envejecimiento la población de las NSCs disminuye progresivamente además de sufrir cambios morfológicos y funcionales, afectándose sus propiedades intrínsencas. En base a estos cambios morfológicos hemos descrito una nueva subpoblación de NSCs denominada omega NSCs, caracterizadas por su morfología de tipo reactivo y el aumento de la quiescencia.

Para estudiar las propiedades de las omega NSCs, en nuestro **décimo objetivo**, expusimos a estas células a estímulos pro-activatorios como es la inyección intrahipocampal de KA, que inducen una mayor activación de las NSCs. Observamos que incluso en condiciones de pro-activacion las omega-NSCs se mantienen quiescentes.

El objetivo **décimo primero** fue imitar la inflamación crónica típica de cerebros envejecidos en animales jóvenes para comprobar si las NSCs típicas se transforman en omega-NSCs. Para ello administramos de manera continuada durante un mes IFN-α intraperiotnealmente. En estas condiciones de proinflamacion crónica las NSCs de animales jóvenes se convertían en omega NSCs típicas de cerebros envejecidos.

Tal y como hemos expuesto anteriormente el comportamiento de las NSCs influye directamente sobre a neurogénesis, por lo tanto nuestro **décimo segundo** objetivo fue analizar el nicho neurogénico. Observamos que con la edad hay un descenso en el número de neuroblastos (neuronas inmaduras) así como un aumento en el número de astrocitos dependiente de la zona del DG analizada.

En conclusión, nuestros resultados demuestran que cualquier alteración de las propiedades de las NSCs, ya sea epilepsia, inflamación o envejecimiento, se traduce en una alteración de la neurogénesis. Las NSCs son plásticas y responden de manera diferencial a los estñimulos que llegan al nicho neurogénico, y postulamos que tienen funciones no neurogénicas, o extraneurogénicas, como la de participar, al igual que astrocitos y microglía, en la respuesta inflamatoria ante el daño cerebral.

2. SUMMARY

The brain of most of mammals, probably including humans (Eriksson *et al.*, 1998; Spalding *et al.*, 2013, Boldrini *et al.*, 2018), although this notion is currently subject of hot debate (Sorrell *et al.* 2018; Cipriani *et al.*, 2018; Kempermann *et al.*, 2018) is able to generate new neurons throughout adulthood by a process called adult neurogenesis (Altman and Das, 1965). It is now is well-established and accepted that newborn neurons are continuously produced from neural stem cells (NSCs) in at least two specific regions of the adult mammal brain. Adult neurogenesis is a complex "omnigenic" process (Kempermann *et al.*, 2018) that extends throughout aging in the subventricular zone (SVZ) of the lateral ventricles and the subgranular zone (SGZ) of dentate gyrus (DG) in the hippocampus, being termed in this case adult hippocampal neurogenesis (AHN).

The loss, disruption or alteration of the hippocampal neurogenic cascade arguably results in the impairment of all these tasks (Clelland *et al.*, 2009; Deng *et al.*, 2009; Dupret *et al.*, 2008; Farioli-Vecchioli *et al.*, 2008; Imayoshi *et al.*, 2008; Saxe *et al.*, 2006). In fact, the pathological alteration of the hippocampal cascade has been related to different neurodegenerative diseases as epilepsy, Parkinson's, Alzheimer, Huntington's disease or dementia (Herrup & Yang 2007; Kuhn *et al.* 2007), pathologies in which at least part of the symptoms could be potentially caused or favoured by reduced or altered AHN. The total neurogenic output over the lifespan of an organism depends directly on the properties of NSCs as they represent the first step of the neurogenic cascade and act as a non-renewable source of new neurons.

We therefore hypothesise that the intrinsic properties of NSCs are firstly altered in physiopathological conditions such as epilepsy and aging and that this is the main reason behind neurogenesis been strongly affected in these conditions.

Objective 1: NSCs and seizures.

Objective 1.1. To analyze the effects of seizures on NSCs. For this purpose we will use an *in vivo* mouse model of MTLE based on the intrahippocampal injection of KA. We will analyse NSCs activation, mode of cell division, survival and differentiation by means of confocal microscopy-based quantitative image analysis. We will also analyse NSCs cytokine expression by RT-qPCR after FACS-based isolation.

Objective 1.2. To analyze the hippocampal neurogenic niche in human samples of MTLE. For this purpose we will use therapeutically-resected samples of hippocampi from adult

patients of MTLE. The samples will be analysed by confocal microscopy-based quantitative image analysis.

Objective 1.3. To analyze the hippocampal neurogenic niche in a mouse model of Dravet Syndrome a genetic model of epilepsy. For this purpose we will use samples from the *Synapsin-Cre floxed stop Scn1a*A1783V* transgenic mouse line. The samples will be analysed by confocal microscopy-based quantitative image analysis.

Objective 1.4. To analyze the effect of neuronal hyperexcitation versus inflammation on NSCs. For this purpose we will induce inflammation and neuronal hyperactivity separately in adult mice. We will analyse NSC activation and morphological phenotype by confocal microscopy-based quantitative image analysis.

Objective 1.5. To investigate ATP as main effector driving the conversion of NSCs into React-NSCs *in vivo*. For this purpose we will: a) check the expression of ATP receptors by NSCs using RT-qPCR after FACS-based isolation; and b) inject ATP intrahippocampally in Nestin-GFP mice and analyze cell proliferation, NSCs activation and differentiation by means of confocal microscopy-based quantitative image analysis.

Objective 1.6. To investigate ATP as main effector driving the conversion of NSCs into React-NSCs *in vitro*. For this purpose we will: a) check the expression of ATP receptors by NSCs using RT-qPCR; and b) apply ATP, and TNP-ATP as an antagonist, to neurospheres derived from the adult brain. We will analyse NSCs proliferation and morphological alterations by means of confocal microscopy-based quantitative image analysis.

Objective 1.7. To develop interference RNA-based tools to knock down ATP receptors in NSCs. For this purpose we will generate plasmids containing short-hairpin RNAs against the different ATP receptors expressed by NSCs. We will test their efficiency in cultured cells by RT-qPCR.

Objective 2: NSCs and Aging.

Objective 2.1. To quantify and correlate hippocampal NSCs activation and depletion over aging. For this purpose we will analyse 1, 2, 6 and 12 months-old mice by confocal microscopy-based quantitative image analysis.

Objective 2.2. To analyse the properties of NSCs over aging in Nestin-GFP transgenic mice. For this purpose we will analyse the morphological complexity and the reentry into the cell cycle of activated NSCs by means of confocal microscopy-based quantitative image analysis.

Objective 2.3. To analyze the activation of NSCs in the aged hippocampus under proneurogenic stimulus. For this purpose we will inject KA intrahippocampally in aged Nestin-GFP mice and assess entry into the cell cycle by confocal microscopy-based quantitative image analysis.

Objective 2.4. To analyze the effect of mimicking inflammaging on NSCs. For this purpose we will inject IFN-α for 3 weeks in adult Nestin-GFP mice, and check morphological complexity and NSC activation by confocal microscopy-based quantitative image analysis.

Objective 2.5. To analyse the neurogenic niche during aging in Nestin-GFP transgenic mice. For this purpose we will quantify neuroblasts and astrocytes in 3, 12 and 18 months old animals using specific markers and confocal microscopy-based quantitative image analysis.

Our conclusions extracted from the experimental data are the following:

1. **Seizures induce the conversion of NSCs into React-NSCs in the hippocampal neurogenic niche.**
    I. Neuronal hyperexcitation in the form of EA promote NSC activation and subsequent depletion without changes in differentiation.
    II. In a mouse model of MTLE seizures provoke the massive activation of NSCs and their transformation into a functionally and morphologically reactive phenotype (React-NSCs).
    III. MTLE seizures-induced React-NSCs divide symmetrically and generate reactive astrocytes.

      IV.   MTLE induces in the human hippocampal neurogenic niche alterations comparable with the disruptions found in the neurogenic niche of the MTLE mice.

2. Reactive Neural Stem Cells are present in the Dravet syndrome mouse model

      I.   Cell proliferation and NSCs activation are increased in the mouse model of DS.

      II.   React-NSCs are present in the hippocampal neurogenic niche of DS mice.

      III.   The nuclei of neurons of the GCL present a distorted shape in DS mice.

3. Inflammation does not induce the conversion of NSCs into React-NSCs

      I.   Proinflammatory stimuli or mediators maintain or even reduce NSCs activation.

      II.   Insults that involve neuronal hyperexcitation such as seizures or traumatic brain injury induce NSCs activation and React-NSCs.

4. ATP acts as a mediator in the induction of React-NSCs.

      I.   P2X purinergic receptors are present in the hippocampal NSCs *in vivo* and *in vitro.*

      II.   ATP induces the conversion of NSCs into React-NSCs and their massive activation *in vivo*.

      III.   ATP promotes proliferation and morphological alteration of *in vitro* hippocampus-derived NSPCs and these effects are blocked by the P2X receptor antagonist TNP-ATP.

      IV.   Interference RNA (shRNA) can be used to knock down P2X receptor expression *in vitro.*

5. Aging induces profound functional and morphological changes in hippocampal NSCs.

      I.   The total number of NSCs and activated NSCs decreases with aging but the relative proportion of activated NSCs remains constant over time.

      II.   The activation of NSCs predicts the depletion of the NSCs population over time.

      III.   At least two different populations of NSCs with particular morphology and mitotic capacity coexist in the aging DG.

IV. α-cells represent the most morphologically simple NSCs and account for most of the dividing NSCs over time and after a pro-activation stimulus.

V. Ω-cells are morphologically more complex, and become more quiescent over time even after a proactivation stimulus. α-cells disappear with aging and Ω-cells accumulate (in relative proportion) in the aged DG.

VI. A proinflammatory stimulus can induce, or accelerate, the transformation of α-NSCs into Ω-NSCs in younger mice.

VII. The reactive-like (Ω-like) morphology associates with increased quiescence in a cyclin D2 knock out mouse.

VIII. The number of astrocytes increases differentially with aging in the distinct areas of the DG.

Sierra A, **Martín-Suárez S**, Valcárcel-Martín R, Pascual-Brazo J, Aelvoet S-A, Abiega O, Deudero JJP, Brewster AL, Anderson AE, Baekelandt V, Maletić-Savatić M, Encinas JM. *Neuronal Hyperactivity Leads to Accelerated Depletion of Neural Stem Cells and Impairment of Hippocampal Neurogenesis.* **Cell Stem Cell. 2015** May 7;16(5):488-503. Impact factor 24.

In preparation (to be submitted in 2019):

Martín-Suárez S, Pastor-Alonso O, Valero J, Pineda JR, van Haute C, Veerle Baekelandt V, Encinas JM. *Seizure-induced release of ATP drives the induction of Reactive Neural Stem Cells in the Hippocampus.*

3. INTRODUCTION

3. INTRODUCTION

3.1 Adult Neurogenesis in the Mammal Brain

The brain of most of mammals, probably including humans too (Eriksson *et al.*, 1998, Spalding *et al.*, 2013, Boldrini *et al.*, 2018), although this notion is currently subject of hot debate (Sorrell *et al.* 2018; Cipriani *et al.*, 2018; Kempermann *et al.*, 2018), is able to generate new neurons through adulthood by a process called adult neurogenesis (Altman and Das, 1965). ItAdult neurogenesis is a complex "omnigenic" process (Kempermann *et al.*, 2018) that extends throughout aging in the subventricular zone (SVZ) of the lateral ventricles and the subgranular zone (SGZ) of dentate gyrus (DG) in the hippocampus, being termed in this case adult hippocampal neurogenesis (AHN) (Fig.1).
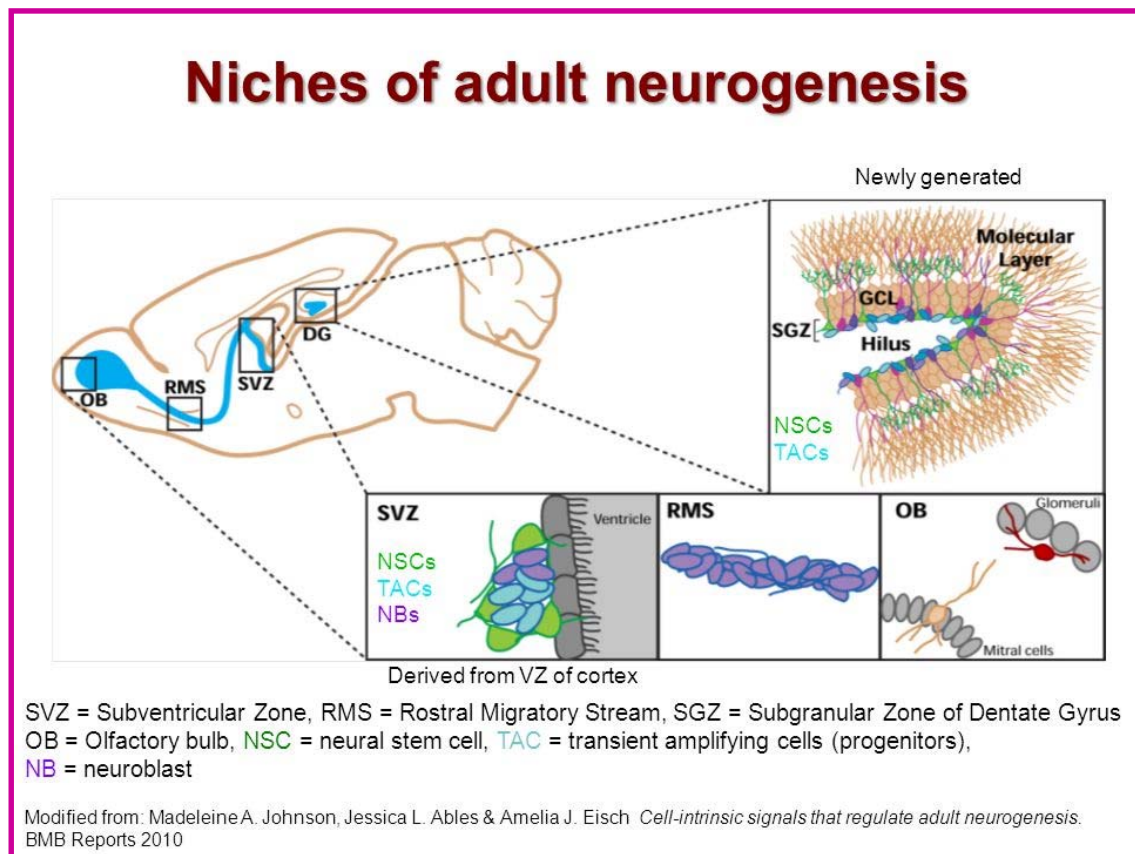
Figure. 1. **Neurogenic niches of the adult rodent brain.**

Briefly, in the SVZ the new-born neuronal precursors migrate rostrally, ensheathed by astrocytes, thus forming the rostral migratory stream (RMS), into the olfactory bulb where they mature mostly into local interneurons (Altman, 1969; Lois and Alvarez-Buylla, 1993; Kornack and Rakic, 2001). In the SGZ of the DG, NSCs give rise to neurons which migrate shortly into the granule cell layer (GCL) and integrate into the hippocampal circuitry (Van Praag *et al.*, 2002; Kemperman *et al.*, 2004; Aimone *et al.* 2014). In a basic view, hippocampal neurogenesis is a multistep process in which quiescent NSCs (or type-1 cells) get activated (enter cell division), in a continuous manner but with low frequency, and then divide asymmetrically giving rise to transient amplifying neural progenitors (ANPs or type-2 cells) which proliferate a few times for 2-4 days and then either die by apoptosis being removed by microglia (Sierra *et al.* 2010) or continue their neurogenic pathway, maturing into post-mitotic neuroblasts that finally differentiate into new neurons. Most of those NSCs that have entered the cell cycle to yield neuronal progeny go back into quiescence and ultimately differentiate into astrocytes exiting the NSC pool. A graphic representation of this process is shown in Fig.2
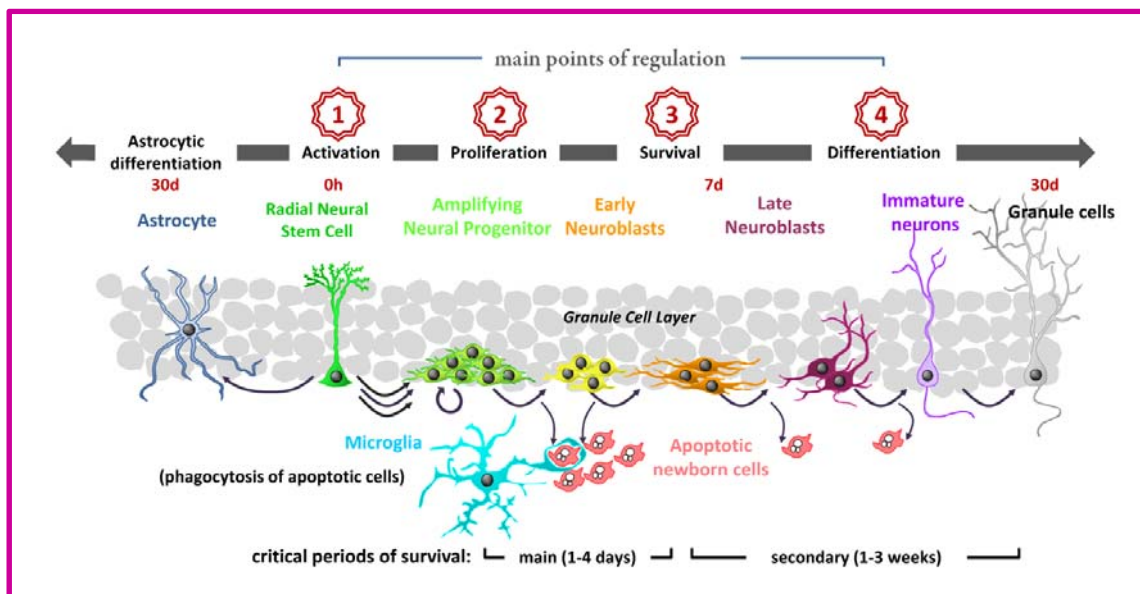
Figure 2. Model of hippocampal adult neurogenesis. NSCs, with radial morphology, are mostly quiescent, but once activated they divide several times consecutively asymmetrically to give rise to ANPs which either die by apoptosis or slowly differentiate into mature granule cells. (Taken from Encinas and Sierra 2012)

In clear contrast with developmental corticogenic neurogenesis, there is not a synchronised neurogenic wave followed by an astrocytic one, but rather NSCs are progressively getting activated in low numbers and the neurogenic and astrocytic cascade takes place continuously. Therefore quiescent and activated NSCs, neural precursors, immature and mature neurons and newborn astrocytes coexist as immediate neighbours in

the hippocampal neurogenic niche in a strict and controlled environment which maintains the correct functioning of the hippocampal neurogenesis.-(Braun and Jessberger 2014).

3.2 Function of Adult Hippocampal Neurogenesis

The generation of fine-tuned genetic tools to ablate neurogenesis after the initial and less precise damage-or pharmacology-based approaches has allowed the detailed analysis of AHN. The addition of new neurons in the DG plays an important role in the formation of new memories (Farioli-Vecchioli *et al.*, 2008), learning (Zhang et al 2008; Deng *et al.*, 2010), responses to stress, anxiety and fear (Santarelli *et al.*, 2003; Saxe *et al.*, 2006; Bergami *et al.*, 2008; Zhang *et al.*, 2008; Aimone *et al.*, 2011; Snyder *et al.*, 2011), as well as in spatial and object recognition memory (Jessberger *et al.*, 2009) and pattern separation (Sahay *et al.*, 2011; Nakashiba *et al.*, 2012). Furthermore, hippocampal neurogenesis dynamically responds to a multitude of extrinsic stimuli and may be important for cognition, behaviour, pathophysiology, brain repair, and response to therapies (Deng *et al.*, 2010; Kempermann *et al.*, 2004; Zhao *et al.*, 2008).

The loss, disruption or alteration of the hippocampal neurogenic cascade arguably results in the impairment of all these tasks (Clelland *et al.*, 2009; Deng *et al.*, 2009; Dupret *et al.*, 2008; Farioli-Vecchioli *et al.*, 2008; Imayoshi *et al.*, 2008; Saxe *et al.*, 2006). In fact, the pathological alteration of the hippocampal cascade has been related to different neurological and neurodegenerative diseases as epilepsy, Parkinson's, Alzheimer, Huntington's disease or dementia (Herrup and Yang 2007; Kuhn *et al.* 2007), pathologies in which at least part of the symptoms could be potentially caused or favoured by reduced or altered AHN.

3.3 Adult Hippocampal Neural Stem Cells

Hippocampal NSCs, were first described as astrocyte-like cells (Seri *et al.*, 2001) and have been termed as radial astrocytes, radial glial-like cells, Type-1, quiescent neural progenitors (QNPs) and Type α cells or α-NSCs (Eckenhoff and Rakic 1984; Encinas *et al.*, 2006; Kempermann *et al.*, 2004; Kosaka and Hama 1986; Kronenberg *et al.*, 2003; Mignone *et al.*, 2004; Seri *et al.*, 2004; Gebara *et al.*, 2016). Under our point of view, even though the neurogenic cascade is highly plastic and subject to regulation at different stages (ANP, proliferation, apoptosis, young neuron differentiation, as it is shown in the Figure 2), NSCs are the most important factor as they are the first step of the process and are a finite (mostly) non-renewable resource. Hippocampal NSCs present astroglial characteristic under electron

and light microscopy and also share the expression of biomarkers with astrocytes, such as glial fibrillary acidic protein (GFAP) , vimentin, Brain Lipid Binding Protein (BLBP) and Sex determining Region Y-box 2 (Sox2) (Kempermann *et al.*, 2004; Kriegstein and Alvarez- Buylla 2009). They also have several morphological (vascular end feet) and electrophysiological (resting potential) similarities with astrocytes (Seri *et al.*, 2001; Fukuda *et al.*, 2004). However, NSCs differentiate from astrocytes in their radial morphology, which is more common with radial glia, the expression of the intermediate filament Nestin (neuroepithelial stem protein) (Lendahl *et al.*, 1990), the expression of Lunatic fringe (Semerci *et al.*, 2017), the expression of Lysofosfatidic acid receptor 1 (LPA1) (Walter *et al.*, 2011), the lack of S100β expression and their ability to naturally generate neurons.

The triangular soma of NSCs is located in the SGZ and from it emerges a single radial process that crosses the GCL and bifurcates and arborizes profusely in a broccoli-like manner in the molecular layer. From the basal part of the soma thin and short cytoplasmic prolongations that extend horizontally (Fukuda *et al.*, 2004; Mignone *et al.*, 2004). These processes are associated to blood vessels forming vascular end-feet as astrocytes do (Gebara *et al.*, 2016). The typical NSCs, type-1 cells have also been termed α-type NSCs or α-NSCs to differentiate from β-type "NSCs" (Gebara *et al.*, 2016). These β-NSCs are morphologically more complex than α-NSCs and are often located out of the SGZ. In reality, β-NSCs should not be considered NSCs as they do not divide and express S100β (a biomarker of mature astrocytes), leading to hypothesis that they are a transient step in the transformation of NSCs into astrocytes (Gebara *et al.*, 2016). Under normal conditions hippocampal NSCs are used only once in the adult life (Encinas *et al.*, 2011; Pilz *et al.*, 2018). Once activated and after a rapid series of divisions (in which they give rise to ANP which differentiate into neuroblasts and finally mature into granule neurons) NSCs differentiate into mature astrocytes abandoning along this process the stem cells properties (Figure 2). Any possible alteration of their intrinsic properties will trickle down the neurogenic cascade thus impacting the total neurogenic output in the lifespan of the organism. A real-life consequence of this prediction is the age-associated decline of AHN.

3.3.1 Hippocampal Neural Stem Cells in Aging

Aging is a natural biological process that is universal and intrinsic to all animals. It is progressive, time-dependent, and deleterious in nature and results ultimately in physiological decline. As we have explained before, under normal conditions neurogenesis gets depleted over time due to the decrease of NSCs population as a natural outcome of the properties

described above. The loss of AHN could contribute to age-related cognitive impairment and aging is actually the most substantial negative regulator of neurogenesis, resulting in reduced cell proliferation, survival and differentiation (Seki and Arai 1995; Kuhn *et al.*, 1996; Cameron and McKay 1999; Hattiangady and Shetty 2008; Leuner *et al.*, 2007; Olariu *et al.*, 2007; Ben Abdallah *et al.*, 2010; Aimone *et al.*, 2014). The underlying cause of the age-related decline of neurogenesis may include an increase in NSCs quiescence, a decrease in their mitotic potential or that of ANPs, reduced survival of their progeny, slowed differentiation, a reduction in neuronal fate commitment, or a loss of NSCs.
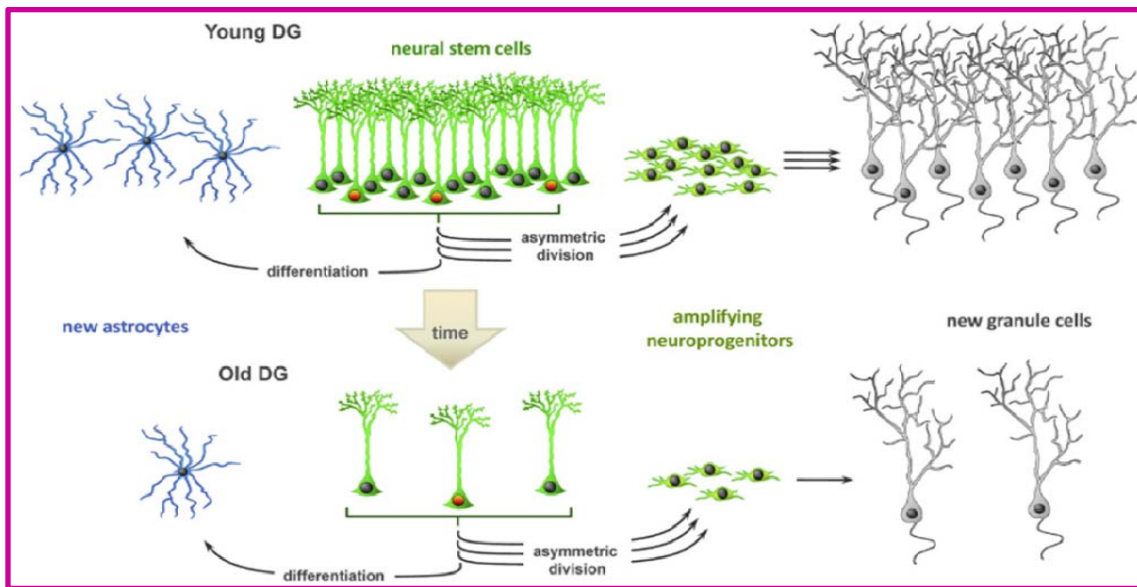
Figure 3. Neural stem cell "deforestation" model of age related decline in adult hippocampal neurogenesis. The NSCs of the dentate gyrus (DG) lose their mitotic potential overtime, resulting in decreased proliferation and neurogenesis in the aged hippocampus.

The loss or depletion of NSCs appears to be the main driving force behind the dramatic reduction of neurogenesis that occurs with aging. Although firstly controversial, the progressive depletion of NSCs population has been often reported (Encinas *et al.*, 2011; Walter *et al.*, 2011; Bonaguidi *et al.*, 2011; Anderson *et al.*, 2014; Gebara *et al.*, 2016). The NSCs depletion can be explained by the differentiation for NSCs into astrocytes after their activation and proneurogenic division (Encinas *et al.* 2011). In fact, prevention of NSCs activation leads to preservation of the NSCs pool over time (Anderson *et al.*, 2014). Although *in vivo* clonal analysis showed that adult NSCs can generate copies of themselves, the frequency of this event is very low (Bonaguidi *et al.*, 2011) and thus may not be quantitatively sufficient to compensate the loss of the NSCs population in aging. In any case, new data using mathematical modelling suggests that only half of the depletion could be explained trough this

gliogenic differentiation and apoptosis has been proposed to explain the rest (Ziebell *et al.*, 2018). However, actual data confirming this hypothesis has not been reported so far.

3.3.2 The aged neurogenic niche

The age-guided decline of NSCs affects the dynamic of depletion of NSCs population during aging. The decline of NSCs is not exponential as in older mice the slope flattens (Encinas *et al.*, 2011). The dynamic of the drop could be explain because of the present of a resilient population of NSCs (Ziebell *et al.*, 2018) that Gebara et al 2016 described as beta NSCs (stable subpopulation of NSCs that do not divide and directly convert into astrocytes), moreover, NSCs increase their quiescence, corresponding to an age-related lengthening of the G0 phase (Ziebell *et al.*, 2018). Stem cell proliferation and maintenance are also regulated by cell cycle checkpoints. The gene p53 is a main regulator of many senescence phenotypes and life span (Tyner *et al.*, 2002). Their downstream activator p21 (Cip1) regulates hippocampal proliferation, although it is in neuroblasts and mature neuron (Pechnick *et al.*, 2008). In addition, telomere shortening and DNA oxidative damage are among the major molecular mechanism in stem cell aging (Sahin and Depinho 2010). The shortening of telomere due to the impairment of telomerase, the enzyme which controls the stability of telomere (Flores and Blasco 2010) provokes chromosomal breakage (Sahin and Depinho 2010).

As we explain above the main reason that explains the decline of neurogenesis is the loss of NSCs population during aging, however this process is not the only one. It is proposed that the age-related decline of neurogenesis could be driven by a chronic inflammatory process associated to aging or "inflammaging". Thus, chronic inflammation (Russo *et al.*, 2011; Monje *et al.* 2003; Ekdahl *et al.*, 2003); increased levels of adrenal corticosteroids (Belanoff *et al.*, 2001; McEwen 1999; Cameron and McKay 1999; Kim *et al.*, 2004; Garcia *et al.* 2004; Cameron and Gould 1994) and decreased levels of growth factors such as Insulin Growth Factor 1 (IGF-1) (Lichtenwalner *et al.*, 2001), Vascular Endothelial Growth Factor (VEGF), Fibroblast Growth Factor-2 (FGF-2) (Bernal and Peterson 2011), Interferon alpha (IFN-α) (Kaneko *et al.*, 2006, Wang *et al.*, 2008) or Reelin (Zhao *et al.* 2008; Knuesel *et al.* 2009) have all been proposed to contribute to the neurogenic decline in the aging hippocampus. Pro-inflammatory cytokines also affects directly the neurogenic function of NSCs. The direct administration of IFN-α abolish directly the mitotic capacity of NSCs (Zheng *et al.*, 2014). In addition, inflammation is a process which involves the active participation of microglia and astrocytes (Lynch 1998; Streit *et al.*, 2004), and as we have recently described that NSCs could also participate in this process (Sierra *et al.* 2015). The increase of inflammation-related genes

and the oxidative stress produces an age-related neuroinflammation which directly reduces neurogenesis (Prolla *et al.*, 2002; Ekdahl *et al.*, 2003; Lynch 2010). During aging microglia increase their proliferation and density (Long *et al.*, 1998) and, moreover, aged microglia change their secretory profile compared with the younger one. The production of greater levels of the typical pro-inflammatory cytokines such as interleukin 6 (IL-6), tumour necrosis factor-α (TNF-α), and interleukin 1 beta IL-1β (Gemma *et al.*, 2007; Bachstetter *et al.*, 2011; Njie *et al.* 2012) is known to prominently inhibit adult neurogenesis (Carpentier and Palmer 2009; Ekdahl *et al.*, 2003). Astrocytes, on their part, showed a pronounced hypertrophy with aging, the hallmark of which is an increase in the amount of protein and mRNA for GFAP (O'Callaghan and Miller 1990; Sloane *et al.*, 2000). The importance of the astrocytic hypertrophy is unknown. Furthermore, the secretion of pro-neurogenic proteins (VEGF, IGF-1, IGF-2, FGF-2 and Wnt 3) commonly secreted by astrocytes, decreases with age (Shetty *et al.*, 2005; Bernal and Peterson 2011; Okamoto *et al.*, 2011; Miranda *et al.*, 2012). However, the production of theses pro-neurogenic proteins is not only limited to astrocytes, IGF-1 and 2 are also produced by microglia, which under inflammatory conditions such as aging decrease their production (Suh *et al.*, 2013), moreover, in NSCs IGF-1 and IGF-2 signal through the IGF-1R regulate their proliferation (Bracko *et al.*, 2012), VEGF probably also regulates the NSCs indirectly through vascular remodelling (Licht *et al.*, 2016). Restoration of the VEGF levels in the brains of aged animals (in this case through conditional transgenic induction) attenuates the age related decline in hippocampal neurogenesis and improves memory performance (Licht *et al.*, 2016).

It is clear that the main factor controlling AHN is the activation of NSCs, because not only the number of new precursors and neurons depends directly on it, also the depletion of NSCs is tightly linked to their activation. Thus, understanding the dynamics and mechanisms of NSCs activation in physiological conditions, aging and pathological conditions such as neuronal hyperexcitation and inflammation in which NSCs is directly altered, is key to unlock the therapeutic potential of NSCs.

3.3.3 Quiescence-Activation. Dinamics of Neural Stem Cells

Although NSCs are mostly quiescent their mitotic potential has been a main poit of attention. The division of NSCs is still a controversial topic, as it was described that NSCs are able to divide symmetrical and asymmetrically. A first model, called "disposable stem cell model" supported the hypothesis that once activated NSCs enter the cell cycle and divide asymmetrically three times (at a population average) consecutively. Immediately after their

division they start to differentiate into astrocytes, which migrate into the hilus or the molecular layer of the DG. As a consequence the population of NSCs diminish progressively in the DG (Encinas *et al.*, 2011), and the astroconversion coupled to the activation of NSCs explains the decrease of neurogenesis with age (Figure 2) (Kuhn *et al.*, 1996). Thus, at the population level, symmetrical division was negligible

On the other hand, another model based on clonal analysis allowing the study of properties of individual cells, defends that there are multiple modes of NSCs activation and cell division, including not only the asymmetric manner but also a symmetric that implies NSC self-renewal. Also, NSCs would able to enter the cell cycle returning later to quiescence to get eventually activated again after some time (Figure 4). This property would have an impact in the dynamics of the depletion of NSCs and neurogenesis.
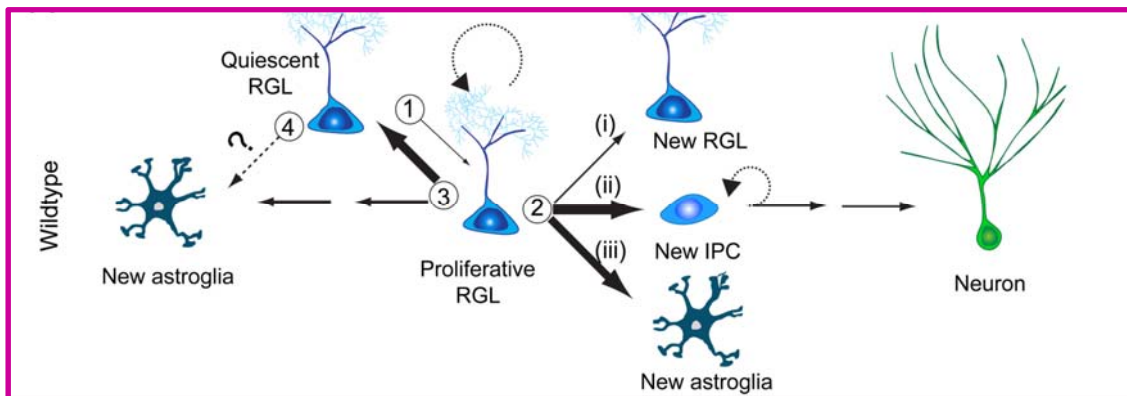
Figure 4. A model of the lineage relationship of RGLs in the young adult mouse hippocampus under basal conditions. There are at least three critical choice points: (1) An RGL decides to remain in quiescence or to become activated and enter the cell cycle, (2) An activated RGL can undergo one of three modes of self-renewal: (i) symmetric self-renewal to expand the RGL pool, (ii) neurogenic or (iii) astrogliogenic asymmetric self-renewal to generate a differentiated progeny while maintaining the RGL pool, (3) The RGL makes a choice between returning to quiescence and maintaining stemness or differentiating into an astrocyte via transition astroglial intermediate. (4) It is also possible that a quiescent RGL can directly differentiate into an astrocyte without cell division. The thickness of the arrow indicates the relative probability of each choice. (Taken from Bonaguidi *et al.*, 2011)

Trying to shed some light on this apparent controversy, mathematical models have been developed. The model produced by Ziebell *et al.*, 2018 took into account both models (Encinas *et al.*, 2011 and Bonagüidi *et al.*, 2011) and concludes that indeed a small proportion of NSCs exit the quiescent state and activate to enter in the cell cycle in a given time point. This proportion remains constant over time, thus in each moment, the majority of the NSCs (regardless of their total number) stay in a quiescent state. The model also confirmed that the population of NSCs gets depleted over time but only a decreased depletion rate of NSCs can reproduce the scenario, suggesting that aged NSCs stay longer in the quiescence stage, but also have a higher probability of reactivation. This model assumed that NSCs can leave the quiescent state through activation or depletion.

This balance between activation and quiescence suggest that the population of NSCs is heterogeneous and the regulation of the niche imply, in turn, an individual regulation of NSCs. The molecular mechanism that triggers the activation of NSCs is not fully elucidated. It seems that Notch1 plays a fundamental role in the regulation of cell cycle entry and exit of NSCs (Guentchev and McKay 2006; Breunig *et al.*, 2007). In addition, Achaete-Scute Family BHLH Transcription Factor 1 (Ascl1) was described as a regulatory key in stem cell activation (Andersen *et al.*, 2014) as this gen is expressed in proliferating NSCs (Breunig *et al.*, 2007; Kim *et al.*, 2011) and its manipulation affects NSCs behaviour. Bone Morphogenetic Proteins (BMPs) are also involved in the maintenance of NSCs quiescence (Mira *et al.*, 2010). GABA is also important as a niche signal to maintain adult NSCs quiescence (Song *et al.*, 2012). Furthermore transcriptomic and genetic studies suggest that NSCs undergo profound changes in their oxygen and lipid metabolisms and cell adhesion properties when they exit quiescence (Knobloch *et al.*, 2013; Martynoga *et al.*, 2013; Renault *et al.*, 2009) although whether manipulating those metabolic processes alter NSCs function has not been addressed yet.

One of the most intriguing aspects regarding the decline in adult neurogenesis is that even in an ever-declining NSC population, the proportion of activated NSCs is small (2-5%), and therefore the potential to maintain neurogenesis at higher levels during aging exits by recruiting higher numbers of NSCs for activation (Encinas and Sierra 2012), something that can be experimentally achieved by increasing neuronal activity through electro-convulsing shock(ECS) (Segi-Nishida *et al.*, 2008), kainic acid (KA) injections (Hüttmann *et al.*, 2003; Lugert *et al.*, 2010; Sierra *et al.*, 2015), or by reducing gamma-aminnobutyric acid (GABA) signalling to NSCs (Song *et al.*, 2012; Giachino *et al.*, 2014). The release of GABA by paravalbumin-expressing interneurons acts directly on NSCs maintaining them in quiescence. The administration of muscimol (a GABA-A receptor agonist) reduces the number of NSCs that enter the cell cycle. Interestingly, blocking the action of GABA in NSCs increases their activation promoting the symmetrical cell division (Song *et al.*, 2012; Gyanchino *et al.*, 2014) or by KA injections (Hüttmann *et al.*, 2003; Lugert *et al.*, 2010), which induces epilepsy. The long term consequences of these stimuli on NSCs and AHN have not been addressed and for us completing these studied would provide insight on the biology of NSCs and the process of AHN itself, but also bring new knowledge to pathological conditions such as epilepsy, which affects more than 50 million people worldwide, with a 30% of them not responding to treatment, a figure that has not changed in decades

3.4 **Epilepsy**

3.4.1 Introduction to epilepsy

Epilepsy is described as a wide spectrum of neurological disorders characterized by spontaneous seizures. It is usually diagnosed after a person has suffered at least two seizures that were not caused by some known medical conditions (Fisher *et al.*, 2005; Savage 2014). Epilepsy affects between 50 and 65 million person in the word, which converts epilepsy into the third most common chronic brain disorder, affecting up to 1% of the population worldwide (Thurman *et al.*, 2011). Not only by its prevalence but also the side effects and comorbidities of this disease such as cognitive impairment, depression, or psychiatric disorder, epilepsy is a major health concern (Gaitatzis *et al.*, 2004).

The etiology of the epilepsy presents a wide ranging of known and unknown risk factors (Eyo *et al.*, 2017). Among these factors we can find genetic factors, traumatic brain injury, fever, tumour, brain infection or neurodegenerative diseases (Ahl *et al.*, 2016). The traditional drug-based treatment of epilepsy only can control the disease symptoms but not cure it (Rassendren and Audinat 2016). In addition, about 30% epileptic patients are pharmacoresistant, or refractory to currently available pharmacological treatments (Schuele and Luders 2008) which aggravates the prognosis. The efficacy of anti-epileptic drugs has not improved in the las 70 years.

Epilepsy can be classified as focal or generalized, according to the brain region where seizures take place (Fisher *et al.*, 2017). Generalized seizures involve the whole brain and usually the patients experience disturbed consciousness often accompanied by tonic-clonic spasms (Ahl *et al.*, 2016). On the other hand, focal epilepsy is initiated in a concrete area of the brain and the symptoms are related to the function of the brain area which is affected (Ahl *et al.*, 2016). One of the main types of focal epilepsy is the mesial temporal lobe epilepsy (MTLE), which affects the hippocampus and tightly associated structures.

3.4.2 Mesial temporal lobe epilepsy.

3.4.2.1 General features of MTLE

The temporal lobe is the most epileptogenic region of the human brain (Tatum 2012) and thus, temporal lobe epilepsy (TLE), is the most common form of epilepsy (Crespel *et al.*, 2002). MTLE is the most common symptomatic focal epilepsy (Wieser *et al.*, 2004; Tatum *et*

al., 2012). In this type of focal epilepsy, seizures arise from the medial aspect of the temporal lobe (Chabardès *et al.*, 2005). This form of epilepsy represents as well the most common form of pharmacoresistant epilepsy (Duveau *et al.*, 2016) and therefore many patients require resection of the epileptic hippocampus as the only means to stop seizuring (Quirico-Santos *et al.*, 2013). The classical clinical history of MTLE patients is stereotypic and can be divided into three main phases:

1- First, an initial precipitating injury occurs in most of the cases in early childhood within the first 2 or 3 years of life but also in some cases in adulthood.

2- Second, the latent phase that lasting several years. This period is also known as the epileptogenesis phase, the process by which the brain becomes epileptic.

3- Third, the appearance of spontaneous recurrent seizures is the indicator of the chronic phase of the disease, which starts usually in adolescence or early adulthood but whit no aggravation with age (Santos *et al.*, 2002).

As a consequence of the recurrent seizures epileptic patient present a case of features which has been hypothesized to affect AHN and as we propose NSCs directly.

3.4.2.2 Pathological features of MTLE

The cognitive functions associated with neurogenesis will be lost or at least substantially impaired in MTLE. As AHN is involved in spatial and associative learning (Clelland *et al.*, 2009; Deng *et al.*, 2009; Dupret *et al.*, 2008; Farioli-Vecchioli *et al.*, 2008; Imayoshi *et al.*, 2008; Saxe *et al.*, 2006), as well as the responses to stress and depression (Snyder *et al.*, 2011), it can be argued that at least some of the symptoms typical of MTLE could be provoked or facilitated by disrupted AHN. It bears mention that epileptic patients have a high incidence of memory impairment (Gargaro *et al.*, 2013) and psychiatric comorbidities, such as anxiety and depression (Heuser *et al.*, 2009).

In the hippocampal epileptic focus cell death and astrogliosis are observed (Zattoni *et al.*, 2011), in addition 45-75 % of MTLE patients present granule cell layer dispersion (GCD) (Lurton *et al.*, 1998; Sierra *et al.*, 2015). GDC is characterized by the enlarge and loss of the boundaries between the dentate gyrus layers, moreover the shape of the GCs changes as well, increasing their size and displaying an elongated and bipolar shape with processes extending vertically within the molecular layer. In epileptic hippocampus with hippocampal sclerosis (gliosis, cell death, GCD), the loss of hilar neurons leads to a differentiation of the granule cell dendrites in the inner molecular layer. The surviving neurons (GCs) and some inhibitory

neurons) sprout axon collaterals and re-innervate empty synaptic sites, with functional connections, giving rise to abnormal hippocampal circuitry (Lurton 1998).

Due to the neuronal hyperexcitation there is neuronal damage and an exacerbation of the immune response (Ekdahl *et al.*, 2003; Kan *et al.*, 2012; Legido and Katsetos 2014; Ravizza *et al.*, 2011). Microglia release pro- and anti- inflammatory molecules after the seizures (Pernhorst *et al.*, 2013) and astrocytes became reactive, disrupting their buffer capacity (Crunelli *et al.*, 2015). More recently, it has been shown that microglia function, phagocytosing specially, can be impaired (Abiega *et al.* 2016). The inability of microglia to efficiently remove cell corpses could exacerbate damage as well.

3.2.2.1. Excitotoxicity

Excitotoxicity is the process by which nerve cells are damaged or killed by excessive stimulation by neurotransmitters such as glutamate (Pickering *et al.*, 2005). Many neurodegenerative diseases exhibit excitotoxicity which leads to cell death by apoptosis or necrosis, depending on its intensity (Bonfoco *et al.*, 1995). The over-activation of glutamatergic receptors induce the entry of high level of Calcium ion ($Ca2+$) into the cells (Jaiswal *et al.*, 2009), then $Ca2+$ activate a number of enzymes which finally damage the structure, membrane and DNA of the cells provoking the cell death (Orrenius *et al.*, 2003).

3.2.2.2. Inflammation

Seizures provoked experimentally in rodents induce a pattern of inflammatory mediators in the brain.

Cytokines and related molecules: Seizures induced either chemically or electrically increase expression and release of cytokines in the rodent brain. The mRNA and protein levels of 1β, TNF-α and IL-6 are rapidly increased after seizures, declining to basal level afterward. Nevertheless some cytokines remains upregulated up to 60 days after the *status epilepticus* (Amor 2010). The release of pro-inflammatory cytokines is accompanied by the synthesis of anti-inflammatory mediators and binding proteins apt to modulate the inflammatory response. Proinflammatory cytokines trigger the transcription of various inflammatory genes which increase the inflammatory response (Kettenmann *et al.*, 2013; Fensterl, *et al.*, 2009).

3.4.3 MTLE mouse model

The most common mouse models of MTLE are based on the chemical induction of seizures based on the administration of pilocarpine, a muscarinic receptor agonist (Vezzani 2009) or the glutamatergic agonist KA (Ben-Ari and Lagowska 1978).

Pilocarpine is usually administered systemically; this treatment is sometimes coupled to lithium pre-treatment in order to lower the threshold for seizure-induction (Eyo *et al.*, 2017). KA can be administered systemically or directly into the brain, into the hippocampus or the amygdale. Both models induce hippocampal sclerosis and mimic the features of human MTLE although pilocarpine works more efficiently and reliably in rats than in mice.

The MTLE mouse model generated by the unilateral injection of a single dose of KA into hippocampus of adult mice (Suzuki *et al.*, 1995) mimics the human MTLE (Bouilleret *et al.*, 1999; Sierra *et al.*, 2015; Abiega *et al.*, 2016) leading as described above to three consecutive phases:

1- Focal SE starts upon awakening from anaesthesia (Riban *et al.*, 2002; Pernot *et al.*, 2011; Sierra *et al.*, 2015). During this phase animals display asymmetric mild chronic movements of the forelimbs, clonic deviations of the head, rotations, and/or immobilization (Riban *et al.*, 2002; Bouilleret *et al.*, 2000). Electroencephalogram (EEG) recording during the SE shows seizure activity consisting of regular, continuous or sub continuous spikes, polyspikes and spike-and-wave concomitant to this characteristic behaviour in both the ipsi and contralateral hippocampi (Pernot *et al.*, 2011; Sierra *et al.*, 2015).

2- The latent period or epileptogenesis phase. The SE is followed by a 2–3 week period during which the activity of the injected hippocampus changes with time (Riban et al 2002).

3- The Recurrent Phase. By the end of the epileptogenesis phase, animals display spontaneous recurrent seizures and enter the chronic phase of the epilepsy. In this phase animals develop severe neuronal cell loss and gliosis in the hippocampus, the neuropathological condition termed hippocampal sclerosis in human patients (Heinrich et al 2011).

Intrahippocampal KA injection is one of the best models to mimic human MTLE, as it replicates the pathophysiological features of this disease. MTLE mice develop recurrent

seizures, hippocampal sclerosis, similar-to-human EEG features, cell death (Eyo *et al.*, 2017) and inflammation (Bouilleret *et al.*, 1999; Sierra *et al.*, 2015; Abiega *et al.*, 2016).
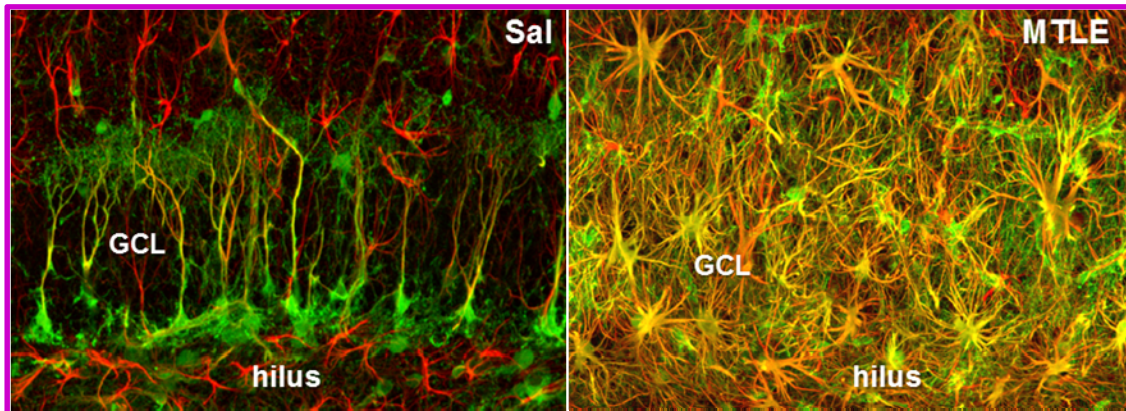
Figure 5. Hippocampal NSCs became reactive after seizures. The left image shows the typical morphology of NSCs, the right image shows the hippocampal sclerosis developed in Nestin-GFP subjected to MTLE after staining for GFP (green) and GFAP (red) Taken from Sierra *et al.*, 2015.

Comparing to pilocarpine model the intrahippocampal injection of KA shows lower animal mortality (Curia *et al.*, 2008; Levesque and Avoli 2013) and is more replicable than the systemic administration mice (McKhann *et al.*, 2003). Therefore this will be our chosen KA-based model to mimic human MTLE.

3.4.4 Epilepsy and Neurogenesis

Seizures induce an immediate overall proliferative response in the DG which in the neurogenic niche is mediated by the activation of NSCs and increased proliferation of neuronal precursors, as a consequence can induce an increase in the generation of new neurons in the short term depending on the MTLE model employed. However, the survival of these seizure-induced new generated neurons is decreased compared with normal conditions (Mohapel *et al.*, 2003). Interestingly, seizures seem to accelerate the maturation and integration of the new born GCs, however, the effect of this process is still unknown (Overstreet-Wadiche *et al.*, 2006). In MTLE neurons present morphological abnormalities. The most typical abnormal features in neurons are the formation of hilar basal dendrites (Ribak et al,. 2000; Dashtipour*et al.* 2003; Shapiro *et al.* 2005) and the ectopic migration of the GCs (Parent *et al.*, 1997; Scharfman *et al.*, 2000). These changes modify the DG connectivity which in turn could be also playing a role in epileptogenesis (Shapiro and Ribak 2006; Scharfman *et al.*, 2000; Parent *et al.*, 2006). However this hypothesis could not be confirmed, as the ablation of seizures-generated new-born neurons did not decrease the frequency of recurrent seizures (Cho *et al.,* 2015) .

In MTLE is common the loss of cognitive functions (Helmstaedter *et al.* 2003; Elger *et al.* 2004) and the worsening of the hippocampal-dependent tasks such as learning or memory (Gargaro *et al.*, 2013) or the development of psychiatric comorbidities (Heuser *et al.*, 2009).
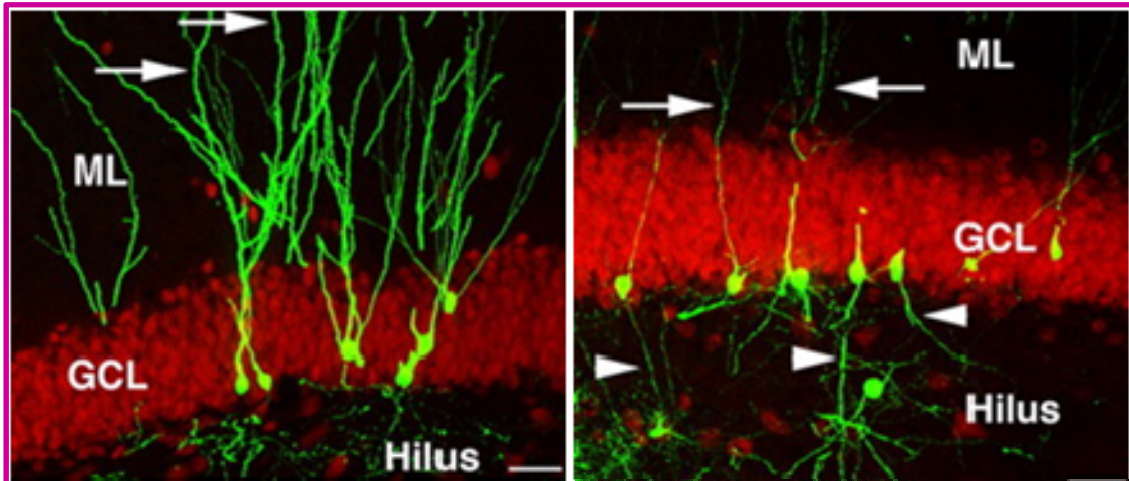
Figure 6. Newborn neurons in normal conditions and after seizures. After seizures nweborn neurons present altered branching and polarity in addition to ectopic localization. Modified from Jesberger *et al.*, 2007.

3.4.5 NSCs in MTLE

Neuronal alterations, as well as reactive astrocytosis, have been proposed as an underlying mechanism driving both pathology and endogenous repair in epileptogenesis (Gibbons *et al.*, 2013), however it has been suggested that hippocampal NSCs are also involved in the epileptic response (Sierra *et al.*, 2015; Lugert *et al.*, 2010).

Epileptic seizures chronically impair hippocampal neurogenesis (Hattiangady *et al.*, 2004; Mathern *et al.*, 2002; Pirttilä *et al.*, 2005; Sierra *et al.*, 2015). It was described that strong enhancers of neuronal activity such as electroconvulsive shock (Segi-Nishida *et al.*, 2008), or the injection KA activate directly NSCs (Hüttmann *et al.*, 2003). In fact, epileptic seizures activate and expand a subset of quiescent NSCs (Lugert *et al.*, 2010). These finding suggest that activation of NSCs is controlled by the levels of activity on the surrounding neural network (Deisseroth *et al.*, 2004). In MTLE neuronal hyperexcitation provokes hyperproliferation on NSCs, besides provokes a dramatic shift in NSCs morphology. Epileptic seizures induce NSCs to become reactive, that is to say, as a consequence NSCs develop a hypertrophic and multibranched phenotype, they divide symmetrically generating copies of themselves that finally differentiate into reactive astrocytes by division nor by direct transformation. Due to these transformation NSCs contribute to the process of hippocampal gliosis and the long-term impairment of neurogenesis (Sierra *et al.*, 2015).

Alternatively, seizure-induced expression of trophic factors, such as brain-derived neurotrophic factor (BDNF), vascular endothelial growth factor (VEGF) and others by surrounding tissue, could indirectly induce NSCs proliferation (Isackson *et al.*, 1991; Gall 1993). When the study is translated to human patient samples the analysis become more difficult since obtaining human sample tissue in good conditions is difficult, especially in the case of control tissue and based on previous studies we can explain in the next section how MTLE injure the hippocampus and the hippocampal NSCs.

3.4.5 Human MTLE

Mesial temporal lobe epilepsy (MTLE) is the most frequent form of focal epilepsy. As described in the mouse model, human pathophysiological features of MTLE include unprovoked seizures and hippocampal sclerosis, including cell death, gliosis, inflammation, and granule cell dispersion (Volmering *et al.*, 2016; Babb *et al.*, 1995; Bouilleret *et al.*, 1999; Heinrich *et al.*, 2006; Kralic *et al.*, 2005; Nitta *et al.*, 2008). An increased expression of pro-inflammatory molecules has been demonstrated in neurons and glia in brain tissue obtained from patients surgically treated for drug resistant epilepsies. Studies in human MTLE patients support the existence of a chronic inflammatory state sustained by microglia, astrocytes, and neurons in the epileptic focus.

Regarding neurogenesis, in human epilepsy the proliferation rate in the dentate gyrus is controversial, some studies describe that proliferation in human increased in the short term but decreased in the long term (Del Bigio 1999; Blümcke *et al.*, 2001; Mathern *et al.*, 2002; Mikkonen *et al.*, 1998; Pirttilä *et al.*, 2005,) however, in young patients an overexpression of neural progenitor markers Nestin and Vimentin in cells of the subgranular area and hilus was observed (Blumcke *et al.* 2001). The data about AHN on humans is hard to interpret as the very existence of NSCs in the adult and aged brain is subject of heated debate. Nevertheless, it is during the early afterbirth period across mammal species, including humans that postnatal neurogenesis peaks. Therefore, we reasoned that hippocampal NSCs and neurogenesis could be of special relevance in infant epilepsies.

3.5 Dravet syndrome

3.5.1 General features of DS

Dravet syndrome (DS), first described in 1978 by Charlotte Dravet (Dravet 1978), is a rare form of epilepsy affecting approximately one in 20.000 (1/2.500). DS is severe infantile multifocal epilepsy and intractable childhood epilepsy characterized by frequent prolonged seizures, developmental delays, speech impairment, and motor/ orthopedic issues including dysautonomia, nutrition issues, characteristics of autism, and a high rate of sudden unexpected death in epilepsy (SUDEP) approximately 10–20% of the afflicted children do not survive (Genton *et al.*, 2011; Sakauchi *et al.*, 2011). Patients with Dravet syndrome often have autism-like behavioural features, and autism spectrum disorder has been associated with seizures in the first year of life.

The severity of its presentation and progression can be variable (Brunklaus *et al.*, 2012; Zuberi *et al.*, 2011). Therefore in adult this syndrome is under-diagnose (Scheffer *et al.*, 2009) and not fully characterized specially in patient in their forties and over. Adults DS features include drug-resistant seizures, interictal epileptiform, nocturnal seizures with focal semiological features and sometimes secondary generalization (Akiyama *et al.*, 2010). The 70-85% of cases with DS presented de novo mutations in the gene encoding the Sodium Voltage-Gated Channel Alpha Subunit 1 (SCNA1) (Depienne *et al.*, 2009; Marini *et al.*, 2009; Mullen and Scheffer 2009; Oguni *et al.*, 2005; Korff and Nordli 2006; Catterall *et al.*, 2009). Sodium channels are essential for action potential generation in excitable cells, including neurons; therefore, it is not surprising that mutations in this gen lead to epilepsy.

Mutations in SCN1B and GABRG2also have been described in DS patients (Patino *et al.*, 2009Harkin *et al.*, 2002). In the case of DS, the mutations lead to a loss of function that becomes more prominent in inhibitory neurons (interneurons) thus provoking recurrent seizures. Studies of mouse genetic models described how disinhibition due to reduced excitability of GABAergic inhibitory interneurons without a corresponding change in the activity of excitatory neurons (Yu *et al.*, 2006; Ogiwara *et al.*, 2007; Cheah *et al.*, 2012; Dutton *et al.*, 2012; Kalume *et al.*, 2013; Rubinstein *et al.*, 2014; Tai *et al.*, 2014).

3.6 Inflammation

A key common event in neuropathological disorders and insult to the brain is inflammation, which implication in the development of neurological and neurogendenerative disorders have became more prominent over the years. Inflammation is also a strong modulator of AHN.

3.6.1 Introduction to inflammation

Inflammation is a complex response of the body to stress, injury or infection that attempts to defend against insults, to clear dead and damaged cells and to return the affected area to a normal state (Ferrero-Miliani *et al.*, 2007; Lucas *et al.*, 2006). This respond is performed at cellular and molecular level (Whitney *et al.*, 2009).

Inflammation can be triggered by a variety of stimuli including pathogens, such as bacteria, fungi, parasites, and viruses (Nayak *et al.*, 2014). In the brain this response is different, the presence of the blood-brain barrier (BBB) which selectively allows the entering or exits of certain molecules and cells protects the brain against insult (Whitney *et al.*, 2009). In physiological conditions, only macrophages and dendritic cells can enter the CNS (Hickey 1999), however, after brain injury, disease associated proteins, environmental toxins, and uncontrolled death (Block and Hong 2005), an inflammatory process is initiated by the resident microglia, astrocytes and in most of the cases the infiltrating peripheral macrophages and lymphocytes. These cited cells in response to inflammation release a plethora of anti and pro-inflammatory molecules, among which stand out cytokines (Tumour necreosis factor α (TNF-α),Interleukin 1β (IL-1β), Interleukin 6 (IL-6), chemokines and neurotransmitters (such as glutamate, ATP) and reactive oxygen species (i.e, nitric oxide) (Whitney *et al.*, 2009; Nayak *et al.*, 2014).

Among all these factors, cytokines play a central role. Cytokines are low-molecular-weight regulatory proteins or glycoproteins secreted by various cells in the body in response to an inflammatory stimulus (Dinarello 2000). Many cytokines are referred to as interleukins (ILs), a name indicating that they are secreted by some leukocytes and act on other similar cell types (Brocker *et al.*, 2010). Two other important types of cytokine include interferons (IFNs), which have the ability to activate immune cells such as natural killer cells and macrophages (Fensterl and Sen 2009), and TNFs, which have been implicated in causing cell death. Cytokines can be categorized as pro-inflammatory or anti-inflammatory:

-Pro-inflammatory cytokines. The most commonly studied pro-inflammatory cytokines are IL-1β, TNFα, and IL-6 (Vezzani *et al.*, 1999). Most of the neurodegenerative diseases associated to neuroinflammation overexpress IL-1β, TNFα, and IL-6.

-Anti-inflammatory cytokines: These cytokines play a fundamental role controlling the pro-inflammatory cytokines (Opal and DePalo 2000; Loftis, *et al.*, 2010) and the resolution of the inflammatory insults (Vezzani *et al.*, 2013). The most classically studied anti-inflammatory cytokines are interleukin 4 (IL-4), interleukin 10 (IL-10), and transforming growth factor β (TGFβ).

3.6.2 Models of Inflammation

Several models have been used in order to mimic the inflammatory process. Here we explain 4 of them:

-Lipopolysaccharides (LPS). LPS is a pro-inflammatory agent derived from gram-negative bacteria, lipopolysaccharides are made up of a hydrophobic lipid, lipid A, which is responsible for the toxic properties of the molecule (Musaelyan *et al.*, 2018). LPS produces an acute innate response through activation of TLR4. Leading to a variety of responses in immune cells, including the production of pro-inflammatory cytokines (such as IL-1β, IL-6 and TNF-α) (Dantzer 2009) and chemokines and the activation of antigen-presenting cell functions to promote recruitment of the adaptive immune system (Uematsu and Akira 2006).

-Polyinosinic–polycytidylic acid (Poly I:C): Synthetic Double-stranded RNA analog and is well-established agent for inducing innate antiviral response through binding to TLR3. The effects of poly(I:C) include inducing the expression of interferon-γ (IFN-γ) and other major inflammatory mediators such as IL-1β, IL-6 and TNF-α (Matsumoto*et al.*, 2008).

-Interleukin 6: IL-6 is a pro-inflammatory cytokine secreted in the brain under pathological conditions (Munoz- Fernandez and Fresno 1998). Administration or overexpression of IL-6 promotes inflammation (Campbell *et al.*, 1993).

-Interferon alpha(IFN-α): IFN-α is a pro-inflammatory cytokine with antiviral and antiproliferative effects (Platanias 2005). IFN induces the activation of a broad set of cytokines and chemokines in the brain, including IL-1β, IL-6, TNF-α (Hayley *et al.*, 2013; Wichers *et al.*, 2007).

3.6.3 Inflammation & Neurogenesis

The severity and the profile of the inflammation from mild and acute to chronic, results in different responses in the brain. Although, inflammation is a protective response against insults, the uncontrolled expression of cytokines in the dentate gyrus inhibits neurogenesis. This inhibition can takes place by a variety of mechanisms, including stimulation of the hypothalamic-pituitary adrenal (HPA) axis with subsequent elevation of glucocorticoids, alterations in the relations between progenitor cells and cells of the neuro-vasculature, or direct effects of activated microglia on the precursor cells (Monje *et al.*, 2003; Monje *et al.*, 2002; Ekdahl *et al.*, 2003; Borsini *et al.*, 2014). Cytokines present different mechanisms of action, depending on their nature, briefly, IL-1α promotes neurogenesis and increase gliogenesis whereas IL-6, IFN-α, and IFN-g IL-1β all reduce proliferation but do not have effect on gliogenesis, finally, TNF-α increases proliferation and gliogenesis, but inhibits neurogenesis.

Inflammation induces the reduction of hippocampal neurogenesis in the models we used above. As neurogenesis is a multistep process which start with the activation of NSCs we hypothesized that inflammation could affect directly to NSCs, therefore we focus the next section on describing the effect of inflammation on NSCs.

3.6.4 Inflammation & Neural Stem Cells

Inflammatory signals influence directly NSCs affecting their proliferation, migration and differentiation (Widera *et al.*, 2006; Sun *et al.*, 2004; Nakanishi *et al.*, 2007; Barkho *et al.*, 2006; Ben-Hur 2008). It has been described that NSCs constitutively express receptors for cytokines (Green *et al.*, 2012), the presence of these receptors allows NSCs to sense the levels of cytokines directly. *In vitro* and *in vivo* experiments have shown that pro-inflammatory cytokines suppress NPCs proliferation. (Zonis *et al.*, 2013; Ben-Hur *et al.*, 2003; Iosif *et al.*, 2006; Monje *et al.*, 2003; Cameron and Glover 2015).

In addition, experiments using a cocktail of cytokines, chemokines, prostaglandins, and other inflammatory molecules and hormones act cooperatively in the course of acute or chronic peripheral inflammation (Ekdahl *et al.*, 2003; Monje *et al.*, 2003; Borsini *et al.*, 2015).

Finally, NSCs are able to respond to inflammation in more unexpected way, such as releasing trophic factors (Ourednik *et al.*, 2002), ameliorate chronic inflammation (Einstein *et al.*, 2003; Pluchino *et al.*, 2005), inhibiting T-cell activation (Einstein *et al.*, 2007) or secreting inflammatory cytokines (Covacu *et al.*, 2009).

3.7 .ATP

3.7.1 ATP functions

Adenosine triphosphate or adenosine-5'- triphosphate (ATP) is a nucleotide that has been considered as a neurotransmitter and modulator in the central nervous system for more than 30 years (Edwards *et al.*, 1992; Evans *et al.*, 1992; Zimmermann 1999; Nearly *et al.*, 1996; Burnstock 1997). Probably in the evolution, ATP was the first extracellular signalling molecule because of its universal availability and thus virtually every known cell or single cell organism has a form of ATP sensitivity (Burnstock and Verkhratsky 2010).

The purinergic signalling is a primitive system that is involved in many non-neuronal and neuronal mechanisms, in both short-term and long-term (trophic) events, including exocrine and endocrine secretion (Burnstock and Verkhratsky 2009; Burnstock 2006). ATP is a ubiquitous modulator of cellular functions in the CNS, the most common functions are:

-7.2.1 Cell proliferation. ATP induces astroglial cell proliferation and the formation of reactive astrocytes, as demonstrated by the increased expression of the astroglial-specific marker GFAP and the elongation of GFAP-positive processes (Abbracchio *et al.*, 1996).

-7.2.2 Neuroprotection and pathophysiology. Some of the responses to ATP released during brain injury are neuroprotective, but in some circumstances ATP contributes to the pathophysiology initiated after trauma (Neary *et al.*, 2003). Autocrine and paracrine ATP signalling can contribute to cellular response to pathogens, such as the production and release of inflammatory mediators, including cytokines. Released ATP is thus a pro-inflammatory signal during the acute inflammation that occurs in damaged or infected tissues. ATP signalling in response to pathogens stimulates apoptosis through activation of P2X7 receptors, perhaps as an attempt to fight infection (Ferrari *et al.*, 1997; Solini *et al.*, 2004). Finally, ATP controls and regulates many pathological reactions of glia, for example reactive gliosis or microglial motility and activation, the latter is specifically controlled by P2Y6 and P2Y12 receptors (Abbracchio *et al.*, 2008).

-7.2.4 Neurological disorders. Adenosine controls hyperexcitability and epileptogenesis (Malva *et al.*, 2003), and the release of glutamate from astrocytes has been implicated in epileptogenesis (Tian *et al.*, 2005).

3.7.2 Purinergic receptors

Extracellular ATP exerts a wide range of cellular effects by activating plasma membrane–localized receptors that belong to one of two classes: heterotrimeric guanine nucleotide–binding protein (G-protein)–coupled P2Y receptors (Abbrachio *et al.*, 2006), and ion channel P2X receptors. In mammalian cells eight P2Y receptor subtypes, regulated through the heterotrimeric G proteins and seven P2X receptors (Khakh *et al.*, 2001) have been described.
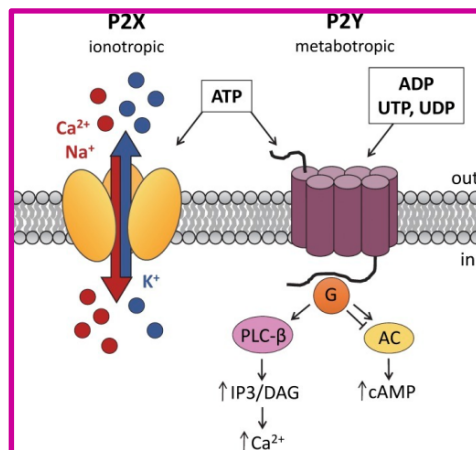
Figure 7. Purinergic signaling. Binding of ATP to P2X channels causes a conformational change that opens the pore and allows Ca2+ and/or Na+ to enter and K+ to leave the cell (Hattori and Gouaux 2012). Binding of ATP, ADP, UTP, or UDP to P2Y receptors activates different G protein signaling pathways, depending on the specific G protein associated with the receptor (Burnstock 2012). Taken from Björkgren and Lishko, 2016

7.3.2 P2X receptors: P2X receptors are classical cationic ligand-operated channels that upon ATP binding open their pore permeable to Na^+, K^+ and $Ca2^+$ (Abbracchio *et al.*, 2008). The P2X receptors are trimers (Nicke *et al.*, 1998) formed from individual subunits encoded by seven distinct genes (designated P2X1 to P2X7). The concentration of activation depends on the subtype, whereas P2X7 receptors are activated at 100–1000 mM ATP concentrations the rest of receptors (P2X1 to P2X6) activate at 1– 10 mM. Their expression varies in the different regions of the brain and cell types. All P2X receptors are permeable to $Ca2^+$, the ratio of $Ca2^+$ to monovalent cations with their permeability varying between 1 and 5–10 for the various P2X subunit combinations. Stimulation of P2X receptors triggers cytosolic $Ca2^+$ signals in many CNS neurons, and P2X-mediated presynaptic $Ca2^+$ signals can regulate neurotransmitter release (Pankratov *et al.*, 2008) .

7.3.3 P2Y receptors: P2Y receptors belong to the seven transmembrane- domain G-protein-coupled receptors. All of them are activated by nucleotides like ATP, ADP, UTP, UDP and UDP-

glucose. P2Y receptors can be classified in two different subgroups base on their ligand binding and selectivity of G-protein coupling. P2Y1, P2Y2, P2Y4, P2Y6 and P2Y11 use Gq/G11 to activate the phospholipase C/inositol triphosphate (InsP3) endoplasmic reticulum $Ca2^+$-release pathway. In the other hand P2Y12, P2Y13, and P2Y14 receptors almost exclusively couple to Gi/o, which inhibits adenylyl cyclase and modulate ion channels (Abbrachio *et al.*, 2006). As the response of the P2Y responses is based on the generation of second messenger molecules their responses are slower than the responses mediated by P2X receptors (Franke *et al.*, 2006).

3.7.3 ATP & NSCs

P2Y and P2X receptors are present at the level of mRNA and protein levels in embryonic NSCs and in adult NSCs (Tang and Illes 2017). Hippocampal radial glial NSCs were found to express P2X receptors (Nestin immunoreactivity and NTPDase2 immunoreactivity overlapping in 64% of the radial cell processes). It is thus possible that the NTPDase2-positive population corresponds largely to the P2X receptor-expressing NSCs population (Shukla *et al.*, 2005).

Recently, using Single-cell RNA sequencing that generates gene expression profiles at the resolution of an individual cell it has been confirmed that P2X3, P2X4, P2X6, P2X7, P2Y1, P2Y4, P2Y12 and P2Y14 mRNA is present in adult NSCs isolated form the adult hippocampus (Shin *et al.*, 2015). P2X7 receptors have been particularly the focus of studied in the hippocampus as their expression was upregulated in the hippocampus in pathological conditions such as in temporal-lobe epilepsy. It has been hypothesised that this receptor could be involved in maintaining the balance between neurogenic proliferation and cell death in adult progenitor cells (Engel *et al.*, 2012).

3.7.4 Toxic effects of ATP

The extracellular concentration of ATP is maintained in the millimolar range, which means that abrupt changes in their concentration transform ATP into excitotoxin. The abnormal release into the extracellular space of ATP as it happens in epilepsy (Burnstock 2006), ischemia or mechanical forces result in tissue damaging (Lutz and Kabler 1997). CNS injury actively released ATP which can act as diffusible 'danger signal' to trigger responses to damage and start repair (Abbracchio *et al.*, 2008). Further, by activation of the respective receptors, ATP release may alter transmitter release and induce further functional responses including necrosis, apoptosis, and as previously documented, regeneration processes (Franke *et al.*, 2006). The strong interaction between ATP and glutamatergic systems suggests that the

ATP-evoked release of glutamate might contribute to the deleterious consequences of high ATP concentration (Choi *et al.*, 1998). Moreover, overstimulation of the N-methyl-D-aspartate (NMDA) receptor by glutamate results in an excessive influx of $Ca2^+$ that culminates in the activation of a plethora of potentially neurotoxic mechanisms, such as kinases, phosphatases, proteases, phospholipases, endonucleases, NOS, and free radical production (Watkins *et al.*, 1994). The excessive stimulation of P2 receptors can also acts as an indirect mechanism to activate macrophage, microglia or astrocytes (Franke *et al.*, 2006). The excess of extracellular ATP produces reactive astrogliosis. Morphogenic and mitogenic changes of astrocytes may be induced by synergistic interactions of purines and pyrimidines with growth factors (Abbracchio *et al.*, 1995). High concentration of purines induces the microglial realised of inflammatory cytokines such as IL-1β, IL-6 or TNF-α (Franke *et al.*, 2006). As a consequence the overstimulation of P2 receptors and high concentration of ATP drives to cellular damage.

4. HYPOTHESIS AND OBJECTIVES

4. HYPOTHESIS AND OBJECTIVES

Adult hippocampal neurogenesis, or in particular the total neurogenic output over the lifespan of an organism, depends directly on the properties of NSCs as they represent the first step of the neurogenic cascade and act as a non-renewable source of new neurons.

We therefore hypothesise that the intrinsic properties of NSCs are firstly altered in physiopathological conditions such as epilepsy and aging and that this is the main reason behind neurogenesis been strongly affected in such conditions.

Objective1 : NSCs and seizures.

Objective 1.1. To analyze the effects of seizures on NSCs. For this purpose we will use an *in vivo* mouse model of MTLE based on the intrahippocampal injection of KA. We will analyse NSCs activation, mode of cell division, survival and differentiation by means of confocal microscopy-based quantitative image analysis. We will also analyse NSCs cytokine expression by RT-qPCR after FACS-based isolation.

Objective 1.2. To analyze the hippocampal neurogenic niche in human samples of MTLE. For this purpose we will use therapeutically-resected samples of hippocampi from adult patients of MTLE. The samples will be analysed by confocal microscopy-based quantitative image analysis.

Objective 1.3. To analyze the hippocampal neurogenic niche in a mouse model of Dravet Syndrome a genetic model of epilepsy. For this purpose we will use samples from the *Synapsin-Cre floxed stop Scn1a*A1783V* transgenic mouse line. The samples will be analysed by confocal microscopy-based quantitative image analysis.

Objective 1.4. To analyze the effect of neuronal hyperexcitation versus inflammation on NSCs. For this purpose we will induce inflammation and neuronal hyperactivity separately in adult mice. We will analyse NSC activation and morphological phenotype by confocal microscopy-based quantitative image analysis.

Objective 1.5. To investigate ATP as main effector driving the conversion of NSCs into React-NSCs *in vivo*. For this purpose we will: a) check the expression of ATP receptors by NSCs using RT-qPCR after FACS-based isolation; and b) inject ATP intrahippocampally in Nestin-GFP

mice and analyze cell proliferation, NSCs activation and differentiation by means of confocal microscopy-based quantitative image analysis.

Objective 1.6. To investigate ATP as main effector driving the conversion of NSCs into React-NSCs *in vitro*. For this purpose we will: a) check the expression of ATP receptors by NSCs using RT-qPCR; and b) apply ATP, and TNP-ATP as an antagonist, to neurospheres derived from the adult brain. We will analyse NSCs proliferation and morphological alterations by means of confocal microscopy-based quantitative image analysis.

Objective 1.7. To develop interference RNA-based tools to knock down ATP receptors in NSCs. For this purpose we will generate plasmids containing short-hairpin RNAs against the different ATP receptors expressed by NSCs. We will test their efficiency in cultured cells by RT-qPCR.

Objective 2: NSCs and Aging.

Objective 2.1. To quantify and correlate hippocampal NSCs activation and depletion over aging. For this purpose we will analyse 1, 2, 6 and 12 months-old mice by confocal microscopy-based quantitative image analysis.

Objective 2.2. To analyse the properties of NSCs over aging in Nestin-GFP transgenic mice. For this purpose we will analyse the morphological complexity and the reentry into the cell cycle of activated NSCs by means of confocal microscopy-based quantitative image analysis.

Objective 2.3. To analyze the activation of NSCs in the aged hippocampus under proneurogenic stimulus. For this purpose we will inject KA intrahippocampally in aged Nestin-GFP mice and assess entry into the cell cycle by confocal microscopy-based quantitative image analysis.

Objective 2.4. To analyze the effect of mimicking inflammaging on NSCs. For this purpose we will inject IFN-α for 3 weeks in adult Nestin-GFP mice, and check morphological complexity and NSC activation by confocal microscopy-based quantitative image analysis.

Objective 2.5. To analyse the neurogenic niche during aging in Nestin-GFP transgenic mice. For this purpose we will quantify neuroblasts and astrocytes in 3, 12 and 18 months old animals using specific markers and confocal microscopy-based quantitative image analysis.

5. EXPERIMENTAL PROCEDURES

5. EXPERIMENTAL PROCEDURES

5.1 Animals

All the animals were housed with ad libitum food and water access, in 12:12h light cycle. All procedures were approved by the University of the Basque Country EHU/UPV Ethics Committees (Leioa, Spain) and Diputación foral de Bizkaia under protocol M20/2015/236. All procedures followed the European directive 2010/63/UE and NIH guidelines.

Nestin-GFP transgenic mice, were generated in the laboratory of Dr. Grigori Enikolopov at Cold Spring Harbor Laboratory (Cold Spring Harbor, NY, USA) (Mignone *et al.*, 2004). The strain was kindly provided by Dr. Enikolopov and were crossbred with C57BL/6 mice for at least 10 generations. In Nestin-GFP mice, GFP is expressed under the regulatory elements of the intermediate filament Nestin, expressed in neural stem and progenitor cells.

LPA1-EGFP transgenic mice, generated by the GENSAT project at Howard Hughes Medical Institute (The Rockefeller University, NY, USA) (Gong *et al.*, 2003), were provided by Dr. Gerd Kempermann at Center for Regenerative Therapies Dresden (Technische Universität Dresden, Dresden, Germany) and crossbred with C57BL/6 mice for at least 10 generations. In LPA mice EGFP is expressed under the lysophosphatidic acid receptor 1 and in the adult hippocampus is exclusively expressed in NSCs (Walker et., al 2016).

Cyclin D2 mutant mice, generated in the laboratory of Dr. Anja Urbach Jena University Hospital (Germany). The cyclin D2 gene was inactivated by excision of exons I and II. Mice were kept as heterozygotes on C57Bl/6J background. The line was then kept as cyclin D2 heterozygotes (+/−) and their homozygous progeny, −/− (cD2 KO) and +/+ (WT) littermates, were used in all experiments.

Scn1a*A1783V transgenic mice were kindly provided by Dr. Onintza Sagredo. These mice are bred to mice that express cre recombinase; resulting offspring express the A1783V mutation in the cre-expressing tissues. Depending on the genetic background of the Cre line used, mice display a lethal seizure phenotype at about three weeks of age: greater than 80% of heterozygotes survive with a ubiquitous Cre on a 129 background, but less than 40% survive on a pure B6 background. Viable mice exhibit spontaneous seizures, motor stereotypies, and hyperactivity.

The experiments of aging, MTLE, inflammation and ATP were performed in Nestin-GFP mice (Mignone *et al.*, 2004; Encinas, Vaahtokari *et al.*, 2006; Lagace *et al.*, 2007). For the FACS

experiments LPA1-EGFP mice were used. For the experiment of Neurogenesis C57BL/6 mice (Harlan, Boxmeer, The Netherlands) were used. Finally, for the study of the DS Synapsin-Cre Xx floxed stop Scn1a*A1783V mice were used.

5.2 Human Samples

Resected samples of hippocampi from adult drug-resistant MTLE patients were obtained from the Basque Biobank at the Cruces University Hospital (Bilbao, Spain) with the patient's written consent and with approval of the University of the Basque Country Ethics committee (CEISH/154/2012). After the surgery the tissue was immediately immersed in saline and refrigerated until transported to Pathology Unit of the Hospital (under 40 min), where it was manually sectioned in 1–2 mm thick coronal sections and transferred to 4% paraformaldehyde (PFA) in PBS, pH 7.4 for 30 min, afterward the tissue was store at 4ºC in PBS+PFA 4%.

5.3. Surgical Procedures

5.3.1. Intrahippocampal injections

For the intrahippocampal injections mice were anesthetized intraperitoneally with Ketamine (Ketolar, Pfizer)/xylazine (Sigma) (10:1 mg/kg) and received a single dose of the analgesic buprenorphine (1mg/kg) (Buprecare, Animalcare Lted) subcutaneously. In brief, the hair over the scalp was shaved and povidone iodine was applied to clean and disinfect. The mice were positioned in the stereotaxic apparatus, an incision was made in the skin over the scalp to localized Bregma (the point of intersection between the coronal suture and the sagittal suture) next the hippocampus was localized using the coordinates: anteroposterior (AP) -1.8mm, laterolateral (LL) -1.6mm. Next, a 0.6mm whole was drilled at the point of the coordinates taken from Bregma, and a pooled glass microcapillary was inserted at -1.9mm dorsoventrally (DV). The drugs were injected in the right hippocampus using a nanoinjector (Nanoject II, Drummond Scientific, and Broomal, PA, USA). After 2 minutes to avoid the reflux the capillary was retracted. Finally, the mice were sutured and place in a thermal blanket until recovered from anesthesia.

The induction of epilepsy was achieved by the administration of 50nL of KA, at 0.74mM and 20 mM, (KA, Sigma-Aldrich, St Louis, MO, USA), a kainate receptor agonist (Bouilleret *et al.*, 1999).

The increase proliferation of NSCs in aging mice (12 months old) was achieved injecting 50 nL of saline or KA at 0.74 mM.

Inflammation was induced by the administration of different drugs. In order to mimic bacterial infection LPS (8mg/ml; Sigma) was injected in the right hippocampus. Poly I: C (2µg/µl; Invivogen) was used to induce viral infection. To stimulate the immune response IFN-α (4*10^5 IU/Kg; Miltenyi Biotec) was administrated in the right hippocampus, and IL6 (IL6 mouse recombinant 1mg/ml; 10µg) was used to increase the levels of cytokines in the dentate gyrus.

Adenosine-5'-(γ-thio)-triphosphate tetralithium salt, a non-degradable form of Adenosine triphosphate (100mM in 1 µL; Tocris), was injected at pH-balanced solutions in 2 month old animals.

5.3.2 Electrode implantation and EEG recordings

Nestin-GFP mice were implanted with platinum iridium, Teflon-coated deep electrodes (PlasticsOne, Roanoke, VA, USA) after intrahippocampal injection of saline or KA. Four recording electrodes were positioned at -1.6mm AP, +1.8mm LL, -1.8mm DV (left hippocampus); -1.6mm AP, -1.8mm LL, - 1.8mm DV (right hippocampus); -0.1mm AP, -1.8mm LL, -2mm DV (right cortex): -0.1mm LL, +1.8mm 12 LL, -2mm DV (left cortex). The reference electrode was placed in the frontal lobe at +0.1mm AP, +0.1mm LL, - 0.5mm DV, and the ground electrode was positioned over the cervical paraspinal area (Sierra, *et al.* 2015). Four hours after implantation, mice were attached to a Nicolet video-electroencephalogram (vEEG) system (NicView 5.71, CareFusion, San Diego, CA, USA), and were recorded in 4h sessions. The same protocol was used every two days for the next week and once a week for another 7 weeks.

5.3.3 Traumatic Brain injury

For the Traumatic Brain injury (TBI) (Scheff *et al.*, 1997; Sullivan *et al.*, 1999) mice were anesthetized intraperitoneally with Ketamine (Ketolar, Pfizer)/xylazine (Sigma) (10:1 mg/kg) and received a single dose of the analgesic buprenorphine (1mg/kg) (Buprecare, Animalcare Lted) subcutaneously. In brief, the hair over the scalp was shaved and povidone iodine was applied to clean and disinfect. The mouse was positioned in the stereotaxic apparatus, and midline incision was made in the skin over the scalp. Next, a 4mm craniotomy was made lateral to the sagittal suture and centered between bregma and lambda. The skull cap was removed without damaging the dura. The pneumaticcaly controlled contusion was driven by an impactor fitted with a rounded stainless steel tip of 3mm of diameter (Precision Systems

and Instrumentation, Fairfax, VA). The impact compressed the cortex to a depth of 0.5mm (mild) or 1.0mm (severe) at a velocity of 3.5m/sec and 400ms duration. After the surgery, the skull cap was replaced and the mice were sutured and placed in a thermal blanket until recovered from anesthesia.

5.4. Intraperitoneal Injections

5.4.1 BrdU administration.

BrdU (Sigma, St Louis, MO) was diluted in sterile saline and administered intraperitoneally at 150mg/kg. For the epilepsy experiment all the mice received four injection separated by 2 hours intervals in the same day (Sierra *et al.*, 2015). For study the type of division the mice were sacrificed 16 hours after the first injection of BrdU to increase the probability to find dividing NSCs in the stages of late karyokinesis or early cytokinesis stages (Encinas *et al.*, 2011). For the aging experiment, all the BrdU-injected mice received 4 injections separated by intervals of 2 hours in the same day and sacrificed 15 hours after the last injection.For ATP and inflammation , mice received 2 injections separated by 6 hours the first and the second day after the surgery. The animals were sacrificed 15 hours after the last injection, on the third day post surgery

In vitro: For the neurospheres proliferation experiment BrdU at 15mg/ml was added at 1:1000 dilution directly in the cell culture 13 hours before the fixation.

5. 4.2 IFN-α administration

Interferon alpha (IFN-α) (Miltenyi Biotec) was diluted in sterile saline and administered intraperitoneally at 4×10^5 IU/Kg. All IFN-α mice received during 20 days one injection of IFN-α or saline in the vehicle mice and sacrificed after the last injection.

5.5. Cells Cultures

5.5.1 Adult Neurospheres cultures.

2 months old mice were sacrificed and the brains were extracted and placed in a cold PBS-Glucose 30% solution to reduce the cellular metabolism. The dentate gyrus was extracted as previously described (Walker and Kempermann 2014), and cut into small pieces of approximately 2 mm. Next, the sample was placed into a 15ml tube. The supernatant was removed and afterwards, a preheated (37ºC and 5% CO2) papain-DNase based enzymatic

solution (20.000 U; 195 U/µL) was added. The sample with the enzymatic solution was incubated at 37ºC during 15 minutes. Afterwards, the enzymatic solution was removed and 950 µl of ovomucocoid (inhibitor of papain) was added and the tissue was mechanically disggregated by carefully pipeting. Next, the cell suspension was filtered into a 15 ml tube and cells were centrifuged 10min 200G, the pellet was resuspended in 500 µl of proliferation medium (Neurocult enriched with 10% proliferation supplement, 2 % B27, 0.24%Heparin, 0.8%EGF and 0.2%FGF of the total volume) and placed in T25 flask with 5 ml of the previous metioned medium.

5.5.2 ATP mediated proliferation and differentiation assays

Isolated cells were counted and plated at density of 80.000 cells/wells on laminin-coated glass coverslips in 24-well plates. Neuroprogenitors cells (NPCs) were allowed to adhere overnight. For the proliferation experiment, NPCs were treated with ATP-γ at 25, 50, 100, 200, 300mM or 500 mM for 15 hours. 2 hours after the incorporation of ATP-γ, BrdU (1:1000) was added to label proliferating NPCs. After 15 hours on of ATP incorporation cells were fixed with PFA 4% during 30 min and cells were store at 4ºC in PBS.

The blockade of the P2X receptors was performed using TNP-ATP (triethylammonium salt (2', 3'-O-(2, 4, 6-Trinitrophenyl) adenosine-5'-triphosphate tetra (triethylammonium) salt). TNP-ATP was added to the plated cells at 30, 50 or 100 µM 3 hours before the addition of ATP-γ which was in the cell culture during hours. 5 hours after the addition of NTP-ATP BrdU was incorporated to the proliferation medium and finally cells were fixed with PFA 4% during 30 min.

5.6. FACS Sorting

For mRNA expression experiments, Neural Stem Cells were isolated from the dentate gyrus of 2 month old Nestin-GFP or LPA-1 hippocampi as described previously (Walker and Kempermann 2014). The DG were dissected and placed in enzymatic solution (116mM NaCl, 5.4mM KCl, 26mM NaHCO$_3$, 1mM NaH$_2$PO$_4$, 1.5mM CaCl$_2$, 1mM MgSO$_4$, 0.5mM EDTA, 25mM glucose, 1mM L-cysteine) with papain (20U/ml) and DNAse I (150U/µl, Invitrogen) for the tissue digestion at 37ºC for 15 min. After mechanic and enzymatic homogenization, cell suspension was filtered through a 40µm nylon strainer to a 15 ml Falcon tube containing 3ml of HBSS and 1 ml of fetal bovine Serum (FBS; Gibco) to stop the enzymatic reaction. In order to enriched cell population the myelin was removed by using a Percoll gradient. For this purpose, NSCs were centrifuge for 5 min at 200G and resuspended in 20% Solution of Isotonic Percoll

(20% SIP; in HBSS) obtained from a previous stock of 100% SIP (9 parts of Percoll and 1 part of PBS 10X). Next, HBSS was slide very slowly down by fire-polished pipettes in order to obtain a density gradient to separate the myelin from the cell suspension. Afterward, the samples were centrifuged for 20 min at 100G with minimum acceleration and no deceleration in order not to disrupt the interphase. After the centrifugation myelin was removed from the interphase and cells were washed with HBSS and centrifuged again 5 minutes at 200G. After centrifugation the cell pellet was resuspended in 500µl sorting buffer (25mM HEPES, 5mM EDTA, 1% BSA, in HBSS).

The NSCs sorting was performed by FACS Jazz (BD), in which the population of green fluorescent cells (GFP+ cells) was selected, collected in Lysis Buffer (Qiagen) containing 0.7% 2-mercaptoethanol and stored at -80ºC until processing. Nevertheless, if the experiment was carried out with Nestin-GFP mice, NSCs were stained with Prominin-1 (anti CD-133) before the sorting. For the staining, cells were incubated in PBS containing anti-CD133 conjugated to the red fluorophore Phycoerythrin (1:250; eBioscience) for 30 min at 4°C, followed by 2 washing steps in PBS. Nestin NSCs sorting was used the same gating strategy that in LPA1 after confirm the double staining. For the analysis of purinergic receptors LPA-EGFP mice were used. For the analysis of the cytokines mRNA levels Nestin-GFP injected mice (Saline, KA; 50mM or ATP-γ; 100mM) were used.

5.7 miRNA Production

For the experiment of knockdown P2X receptors in NSCs, sh-RNAs were used. The design of the primers was based on previous protocols with some modifications (Sun *et al.*, 2006)

5.7.1 Plasmid construction

In brief, first both primers were annealed to generate the double strand DNA. 5 µg of in-house-made Simian immunodeficiency virus (SIV) transfer plasmid was digested by incubating (2 hours at 37ºC) the SIV-transfer plasmid with the back bound mix which contains the restriction enzyme Esp3I. After the digestion, the ligation of the purified-digested-transfer-plasmid was performed. For the ligation the digested plasmid was mixed with T4DNase and T4 buffer and incubated for 2 hours at room temperature. To inactivate the enzymatic activity the mix was incubated 10 minutes at 65ºC.

5.7.2 Transformation

The transformation is the process by which foreign DNA is introduced into a cell. For the transformation we used DH5α cells (E-coli cells that maximize the efficiency of the transformation). We incubate the ligation mix with DH5α for 45 second at 42ºC, (this heat-shock allowed the entrance of the plasmid into the cells) and immediately transferred into ice for 5 minutes. Next, the cells were incubated in Luria-Bertan (LB) medium for 1 hours at 37ºC (shaking at 160 rpm). Afterwards, the sample was centrifuged 5 minutes at 5000 rpm and afterward the medium was removed except for the last 100 µl in which the cells were resuspended and plated in an ampicillin treated (100µg/ml) agar-plate. The plates were incubated overnight at 37ºC. Single colonies were picked up and placed in 15ml falcon tube with 2 ml of LB medium with ampicillin (100µg/ml), the tube was incubated shaking(160rpm) at 37ºC overnight.

Next, the DNA plasmid was extracted using Miniprep Kit (Sigma) following manufacturer's instructions. After, the DNA was subjected to digestion control process by incubating the DNA with the control digestion mix (with two restriction enzymes NcoII and Hind III) and then agarose gel was ran to verify the process (40min, 135 V). The DNA, obtained from the last step, was again transformed using DH5α. The was added to de cells DH5α, heated for 45 minutes at 42ºC and immediately transferred to ice and added to an ampicillin (100µg/ml) treated agar-plate and incubate shaking (160rpm) overnight at 37ºC.

Afterwards a single colony was picked up and placed it in 15ml falcon tube with 2 ml of LB medium with ampicillin (100µg/ml), the tube was incubated shaking at 37ºC overday, then it was transferred into a bigger volume of LB medium with ampicillin(100µg/ml) and incubated overnight at 37ºC (shanking 160 rpm). Afterwards, the DNA plasmid was isolated using Maxiprep Kit (sigma) following manufacturer's instructions. The DNA was subjected to a second digestion control process by incubating the DNA with the control digestion mix. Then, agarose gel (40min, 135 V) was run as a control of the process. The DNA sequence was verified in all cloning steps (data not shown).

5.7.3 Lentiviral vector (LV) production

Transfection is the process of deliberately introducing naked or purified nucleic acids into eukaryotic cells. For that purpose we used HEK293T cells (is a human cell line, derived from the HEK 293 cell line, which expresses a mutant version of the SV40 large T antigen). The DNA plasmid obtained from the Maxiprep was mixed with SIV-packaging (the packing plasmid) and VSV-G (envelope glycoprotein forms complexes with plasmid DNA and

MLV retrovirus-like particles in cell-free conditions that enhances DNA transfection) and added to HEK293T cells. HEK293T cells were maintained in Dulbecco's modified Eagle's medium (DMEM, Invitrogen, Merelbeke, Belgium) and supplemented with FBS and antibiotics. The cells were incubated overnight at 37ºC 5% CO2, and then the medium was changed to OptiMEM medium (which has not FBS to allow the use of the vector *in vivo*) and incubated 24 hours overnight. The next 2 days, the medium optimem, enriched in vector particles, was collected and store in 4ºC The enriched-vector medium was centrifuge to concentrate the medium using Vivaspin 15 columns (Vivascience, Han-nover, Germany) to filter and concentrate it. Finally, the obtained vector particles were aliquoted and stored at −80 ◦C.

5.7.4 Transduction

Transduction is the process by which foreign DNA is introduced into a cell by a virus or viral vector. A mouse neuroblastoma cell line Neuro2a (N2a) was used to the transduction. N2a cells were transduced with a serial LV dilution. The LV dilution was selected according to the goal of the experiment. After 48 hours, the antibiotics blastoestimulin was added to the medium (1:1000) in order to select and eliminate all the non-transduced cells. The transduced cells were counted and plated in a new 6 well plate. After 24 hours the RNA was extracted and transcribed to DNA as explained before to analyze the efficiency of the miRNA a RT q-PCR.

5.8 RNA Isolation and RT-qPCR

5.8.1 RNA isolation and RT

5.8.1.1 Dentate gyrus.

The injected (right) dentate gyrus of Nestin-GFP mice was rapidly isolated in cold HBSS. Using a roto-stator homogenizer and Qiagen RNeasy Mini Kit, RNA was isolated following manufacturer's instructions, including a DNAse treatment to eliminate genomic DNA residues. The quantity of RNA was measured using the Nanodrop 2000. Next, 1.5µg of RNA were retrotranscribed using random hexamers (Invitrogen) and Superscript III Reverse Transcriptase kit (Invitrogen), accordingly to manufacturer's instructions in a Veriti Thermal Cycler (Applied Biosystems, Alcobendas, Spain).

5.8.1.2 FACS sorted NSCs

RNA from FACS-sorted NSCs was isolated by RNeasy Plus micro kit (Qiagen) following the manufacturer instructions, and the RNA was retrotranscribed using an iScript Advanced cDNA Synthesis Kit (Biorad) following manufacturer's instructions in a Veriti Thermal Cycler.

5.8.2. RT-qPCR

RT-qPCR was performed following MIQE guidelines (Minimal Information for Publication of Quantitative Real Time Experiments) (Bustin, Benes *et al.* 2009). Three replica of 1.5µl of a 1:3 dilution of cDNA were amplified using Power SybrGreen (Biorad) for dentate gyrus experiments or three replica of 1.5µl of a 1:2 dilution of cDNA were amplified using SoFast EvaGreen Supermix (Biorad) for isolated NSCs experiments in a CFX96 Touch Real-Time PCR Detection System (Biorad). The amplification protocol for both enzymes was 3min 95°C, and 45 cycles of 10sec at 95°C, 30sec at 60°C.

5.8.3. Primers

Primers were designed to amplify exon-exon junctions using Primer express (Thermo Fisher Scientific) or using the Predesigned primers for gene expression analysis (KiCqStart® SYBR® Green Primers) from sigma. The following table shows the sequences of the different Primers.

GENE	GENE BANK	AMPLICON SIZE	SEQUENCE
Reference genes			
HPRT	NM_013556.2	150	Fwd ACAGGCCAGACTTTGTTGGA
			Rev ACTTGCGCTCATCTTAGGCT
Cytokines & Chemokines			
IL-1β	NM_008361	152	Fwd CAACCAACAAGTGATATTCTCCATG
			Rev GATCCACACTCTCCAGCTGCA
IL-6	NM_031168	141	Fwd GAGGATACCACTCCCAACAGACC
			Rev AAGTGCATCATCGTTGTTCATACA
TGFβ1	NM_011577	51	Fwd GCAGTGGCTGAACCAAGGAG
			Rev TGAGCGCTGAATCGAAAGC
TNFα	NM_013693	179	Fwd CATCTTCTCAAAATTCGAGTGACAA
			Rev TGGGAGTAGACAAGGTACAACCC

AQP4	NM_009700.2	114	Fwd ATTGGGAGTCACCACGGTTC
			Rev CGTTTGGAATCACAGCTGGC
Purinergic receptors			
P2XR3			Fwd TACTACAAGATGGAGAATGGC
			Rev AAATTGAGCAGGATGATGTC
P2XR4	NM_011026	52	Fwd TAAGTATGTGGAAGACTACGAGCAGG
			Rev TCACTGGTCCGTCTCTCCG
P2XR7	NM_011027	51	Fwd CTATACCACGAGAAACATCTTGCC
			Rev GAAAGGTACAAGAGCCGTTCATAGTT
P2YR6	NM_183168	82	Fwd ACAGACTCTCCGAGCATAGGAAA
			Rev GGCGGCAAGCCTGGA
P2YR12	NM_027571	88	Fwd GCAGAACCAGGACCATGGAT
			Rev CTGACGCACAGGGTGCTG

The efficiency was calculated using a standard curve of 1:2 dilutions or the software *Line-Reg.*

Two independent reference genes (or housekeeping genes) were compared: HPRT, hypoxanthine guanine phosphoribosyl transfers, which is a transferase that catalyzes conversion of hypoxanthine to inosine monophosphate and guanine to guanosine monophosphate via transfer of the 5-phosphoribosyl group from 5-phosphoribosyl 1-pyrophosphate and OAZ-1, which encodes ornithine decarboxylase antizyme, a rate-limiting enzyme in the biosynthesis of polyamines and recently validated as reference gene in rat and human (Kwon, Oh *et al.* 2009). The expression of HPRT and OAZ-1 remained constant in each treatment (data not shown), validating their use as reference genes.

5.9 Immunofluorescence

5.9.1 Brain tissue sections.

Immunohistochemistry was performed as described before following methods optimized for the use in transgenic mice (Encinas *et al.* 2004; Encinas and Enikolopov 2008; Encinas *et al.* 2011). In brief, animals were transcardially perfused with 30 ml of PBS 1X followed by 30 ml of 4% (w/v) paraformaldehyde in PBS, pH 7.4. Next, the brains were removed and postfixed for 3 hours ar room temperature in the same fixative solution, then transferred to PBS and kept at 4ºC. Serial 50 µm-thick sagittal sections were cut using a Leica VT 1200S vibrating blade microtome (Leica Microsystems GmbH, Wetzlar, Germany). To

carried out the immunostaining the sections were incubated with blocking and permeabilization solution (PBS containing 0.25% Triton-100X and 3% BSA) for 3hr at room temperature, and then incubated overnight with the primary antibodies (diluted in the same solution) at 4ºC. After the incubation, the primary antibody was removed and the sections were washed with PBS three times for 10 minutes. Next, the sections were incubated with fluorochrome-conjugated secondary antibodies diluted in the permeabilization and blocking solution for 3 hr at room temperature. After washing with PBS, the sections were mounted on gelatin coated slides with DakoCytomation Fluorescent Mounting Medium (DakoCytomation, Carpinteria, CA). For the BrdU analysis and Nestin experiments, sections were treated with 2M HCl during 20 minutes at 37ºC and immediately incubated with 0.1M tetraborate for 10 minute at room temperature before the staining. Aferwards, the sections were washed with PBS and the staining followed as describe above. The GFP and YFP signal from the transgenic mice was detected with an antibody against GFP for enhancement and better visualization.

5.9.2 Neurospheres.

Coverslips with disgregated neurospheres were blocked with 0.5% Triton X-100 and 3% BSA in PBS for 40 min. Next, the cells were incubated with the primary antibody diluted in 0.2% Triton X-100 and 3% BSA in PBS for 1.5 hours t RT, washed with PBS and incubated with the secondary antibody containing DAPI in the same solution for 1h at RT. Finally, the coverslips were upside down on glass slides with DakoCytomation Fluorescent Mounting Medium. For the BrdU experiments, the cells were treated before the staining with 2M HCl during 5 minutes at 37ºC and immediately incubated with 0.1M tetraborate for 10 minute at room temperature. Aferwards, the sections were washed with PBS and the staining followed as describe above.

5.9.3 Antibodies

ANTIBODY	COMPANY	DILUTION
Primary antibody		
Chicken anti-GFP	Aves Laboratories	1:1000
Mouse anti-NeuN	EMD Millipore	1:750
Rabbit anti-activated-caspase-3	Cell Signaling Technolo	1:300

Rabbit anti-Ki67	Vector Laboratorie	1:750
Rabbit anti-GFAP	Dako	1:1000
Rabbit anti-S100β	Dako	1:500
Rat anti-BrdU	AbD Serotech	1:400
Goat anti-Doublecortin	St cruz Biotechnology	1:750
Chicken anti-Nestin	Aves Laboratories	1:1000
Rabbit ant-GFP	Abcam	1:1000
Goat anti-GFAP	Abcam	1:1000
Sencondary antibody		
AlexaFluor 488 goat anti-chicken	Molecular Probes	1:500
Alexa Fluor 568 donkey anti-chicken	Invitrogen	1:500
AlexaFluor 647 goat anti-rabbit	Molecular Probes	1:500
Rhodamine Red-X anti-rabbit	Jackson Immunoresearch	1:500
Alexa Fluor 488 Donkey anti-rabbit	Invitrogen	1:500
Alexa Fluor 568 Donkey anti-rabbit	Invitrogen	1:500
AlexaFluor 568 goat anti-rat	Molecular Probes	1:500
Alexa Fluor 568 Donkey anti-goat	Invitrogen	1:500
Alexa Fluor 647 Donkey anti-goat	Invitrogen	1:500
Rhodamine Red-X goat anti-mouse	Jackson Immunoresearch	1:500
DAPI	Sigma	1:1000

5.10 Image Analysis

5.10.1 Image acquisition

All fluorescence immunostaining images were collected using an Leica SP8 laser scanning microscope using a 40X oil-immersion objective except for the quantification of total number of BrdU and NSCs in which the 63X oil-immersion objective was used and a z-step of 0.5μm with zoom of 1.

The signal from each fluorochrome was collected sequentially, and controls with sections stained for single fluorochromes were performed to confirm the absence of signal leaking into different channels and antibody penetration. For tissue sections, 4 20μm-thick z-stacks located at random positions in the DG were collected per hippocampal section, and a minimum of 6 sections per series were analyzed.For neurospheres, 5 of 4 μm-thick random z-stacks of the coversips were collected per sample and condition. Brightness, contrast, and background were adjusted equally for the entire image using the software of the confocal microscopy Leica LAS X Life Sicence. Brightness, contrast and gamma were adjust from the "adjust" options of the software. All images were imported in tiff format.

5.10.2 Quantitative analysis of cell populations

The right hemisphere was sliced sagittally in a lateral-to-medial direction, from the beginning of the lateral ventricle to the middle line, thus including the entire DG. The 50 μm slices were collected in 5 parallel sets, each set consisting of 14 slices, each slice 250μm apart from the next.

Quantitative analysis of cell populations *in vivo* (proliferation) was performed by design-based (assumption free, unbiased) stereology using a modified optical fractionator sampling scheme as previously described (Encinas *et al.* 2004; Encinas and Enikolopov 2008; Encinas *et al.* 2011).

For the absolute number of NSCs, the number of NSCs, excluding those in the upper focal plane, was counted in 100 μm-wide, 50 μm-tall 12 μm deep z-stacks, in GFP and GFAP stained slices from Nestin-GFP mice, using a 40x oil immersion objective. At least 4 z-stacks were obtained from each slice. The values were normalized to the total volume of the SGZ+GCL for each animal. The total volume was obtained by measuring the area of the SGZ+GCL in each slice and measuring the thickness of each slice in at least 3 points. The area of DG in each z-stack was quantified using the Fiji Is Just ImageJ (Fiji) distribution of ImageJ, using the total hippocampal volume. All BrdU cells per slice were counted, with a 63x oil immersion objective to obtain absolute numbers of BrdU cells.The relative proportions of BrdU-positive NSCs types

were referred to the total number of NSCs quantified per animal. Granule cell dispersion was measured in DAPI- and NeuN-stained sections.

The thickness of the GCL was measured at least in three points in each slice. The density was calculated using 10x10x10 µm z-stacks (dissectors) obtained with the 63x oil immersion objective. DAPI/NeuN-positive cells were counted in each dissector excluding those in the uppermost focal plane and those in contact with the left and bottom margins. At least 4 dissectors were analyzed per slice.

For the type of NSC division, the analysis was carried out in flat projections from 20-25 µm-thick z-stacks. Only those pairs of cells whose nuclei were clearly still in contact were scored. Asymmetric cell division was defined as the daughter cell of the NSC bearing none or short (less than 10 µm) and thin (less that 1 µm) processes, and lacking GFAP expression. Symmetric division , the daughter cell presented clearly defined prolongations of at least 10 µm in length and 1 µm in thickness immunostained for GFAP.

For the cell death experiments, apoptotic cells were defined as cells with abnormal nuclear morphology (pyknotic/karryorhectic) and expression of activated caspase 3 (act-casp 3). The number of apoptotic cells was quantified in 2-3 20 µm thick z-stacks per hippocampal slice.

The proliferation of neurospheres was measured by the incorporation of BrdU. The relative proportions of BrdU-positive neuropreogenitor cells were referred to the total number of neuroprogenitor cells quantified per coverslip and conditions (3 coverslip per condition, CNT, ATP-γ, NTP-ATP). The proliferation in all the conditions were refered to the basal proliferation of the control condition.

5.10.3 CELL MORPHOLOGY ANALYSIS

5.10.3.1 *In vivo* NSCs morphology

For the epilepsy experiments, to measure the morphological changes in reactive NSCs, at least 50 cells were randomly selected form 20 µm-thick z-stacks taken form Sal, EA and MTLE mice brain sections immunostained for GFP and GFAP. The quantification was performed in flat projection generated from the z-stacks. Primary processes were considered as these processes emerging directly from the soma and at least 40 µm length; the secondary processes are those branches emerging from the primary processes. The thickness of the primary processes was measured as the width at 2 places at least 10 µm apart.

For the rest of experiments, the morphological changes were also measure by 3D-Sholl analysis. The sholl analysis is an open-source plug-in for Image J, this plug-in performs the

Sholl technique directly on 2D or 3D images of fluorescence labeled cells. 3D reconstructions from confocal stack image was obtained for the morphological analysis of NSCs. Single NSCs were analyzed using 3D Sholl analysis plugin (http://fiji.sc/Sholl_Analysis) as described previously (Schindelin *et al.*, 2012).

In the aging experiment, 3 types of NSCs were described. α-NSCs were defined as radial glia-like cells positive for Nestin-GFP and GFAP with the soma located in the SGZ or the lower third of the GCL and with a process extending from the SGZ towards the molecular layer through the GCL. Ω-NSCs were Nestin-GFP and GFAP positive with a multibranches phenotype and the soma placed out of SGZ.For the analysis of nucleus circularity in the experiment of Dravet Syndrome the program ImageJ was used. In brief, using the "tolerance" of the wand tool in 8-connected mode the nuclei roundness was automatically delimited and saved as a ROI. Afterward, using the "shape description" option of the "measurement" the circularity is measured as $4\pi*area/perimeter2$.

5.10.3.2 Neuroprogenitor cells morphology

For the anaysis of the area occupied by neuroprogenitors cells, an open-source plug-in for ImageJ was used. In brief, the area was measured as the pixels occupied by GFP. Using the "tolerance" of the wand tool in 8-connected mode the area occupied by GFP was automatically selected and saved as a ROI. Afterward, the area was quantified with "measurement" option obtaining the total area occupied by the GFP.

5.11 Statistical Analysis

SigmaPlot (San Jose, CA, USA) was used for statistical analysis. For the analysis of more that two conditions 1- way-ANOVA test was performed. For analysis of pairs of groups, a Student´s t test was performed. For the analysis of cytokine mRNA expression, a logarithmic transformation was performed to comply with ANOVA assumptions (normality and homocedasticity) . In all cases, all-pairwise multiple comparisons (Holm-Sidak method or Tukey test) were used as a posthoc test to determine the significance between groups in each factor.

For the sholl analysis two-way repeated measures ANOVA followed by Bonferroni post-hoc test was performed. Hierarchical clustering was performed using Ward's method and squared Euclidean distances as linkage metric. Only $p<0.05$ is reported to be significant. Data are shown as mean ± SEM (standard error of the mean).

6. RESULTS

6. RESULTS

6.1 Hippocampal Neural Stem Cells Became Reactive in a Mouse Model of MTLE

Previous works described that strong enhancers of neuronal activity such as electroconvulsive shock (Segi-Nishida *et al.*, 2008) or systemic injection of KA, increase the proliferation of NSCs (Hüttmann *et al.*, 2003). Moreover, epileptic seizures activate and even expand a subset of quiescent NSCs (Lugert *et al.*, 2010), suggesting that the activation of NSCs was directly controlled by the activity of the surrounding hippocampal neural network. However, the long–term effect of the seizures-induced alterations on AHN in general, and on NSCs in particular, have not been addressed. In addition, controversial and opposite effects have been reported when studying AHN in the context of epilepsy, most likely reflecting the variety of models vailable but might be also the plastic capability to respond of NSCs and the hippocampalneurogenic niche. We therefore sough to study the effect of seizures, using a validated mouse model of the most common form of epilepsy, MTLE, on NSCs and AHN.
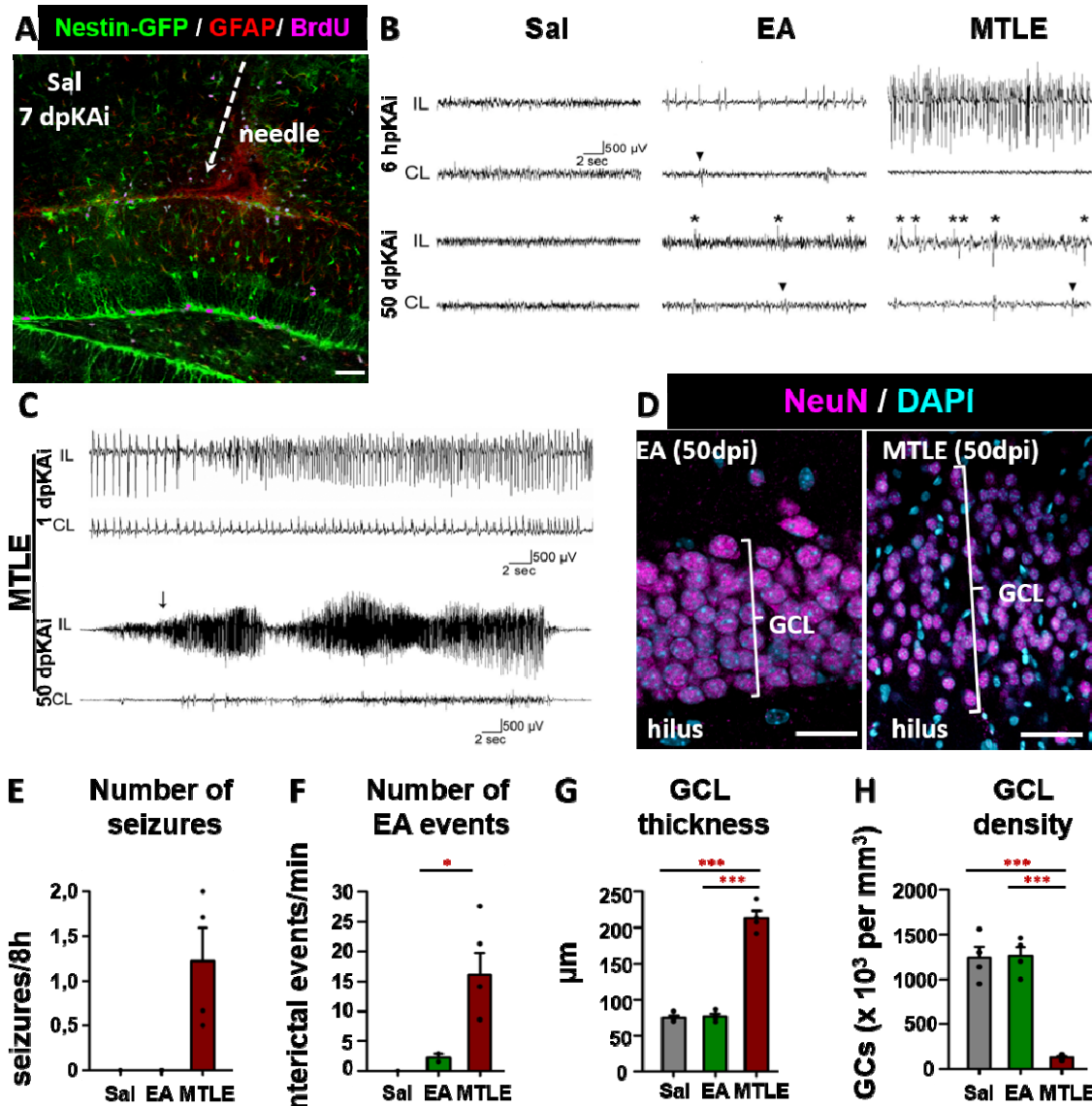
6.1.1. Intra-Hippocampal Injection of KA as a Model of EA and MTLE.

In order to test distinct levels of neuronal hyperactivity in a precisely controlled manner, we resorted to KA, which can be delivered locally into the DG accurately titrated to consistently reproduce the human pathophysiological features of MTLE: unprovoked spontaneous seizures and hippocampal sclerosis, including cell death, gliosis, inflammation, and granule cell dispersion (GCD) (Babb *et al.*, 1995; Bouilleret *et al.*, 1999; Heinrich *et al.*, 2006; Kralic *et al.*, 2005; Nitta *et al.*, 2008).

We confirmed the seizure-inducing effect of 1 nmol of KA in 50 nL of saline (MTLE mice) injected into the DG of Nestin-GFP transgenic mice (Mignone *et al.*, 2004), in which NSCs and ANPs are readily visualized in the SGZ (Figure 1A). EEG recordings from the hippocampus confirmed that MTLE mice developed seizures (repetitive-spike and slow-wave discharges lasting 10 s or more) within 6 hr after the KA injection and later generated seizures spontaneously for the duration of the recordings, which lasted up to 50 days. In addition to MTLE, we developed a model to mimic the abnormal discharges in the forms of spikes, termed EA that occurs between seizures in patients, but that we can here model separateley. For this purpose, we injected a lower dose of KA (0.037 nmol in 50 nL of saline) into the DG of Nestin-GFP mice (EA mice). EA mice did not develop seizures at any time point, but as early as 6 hr after the KA injection they showed epileptiform discharges in the form of spikes that continued intermittently for the duration of the recordings (Figure 1 B-C).

In addition to seizures (Figure 1E), MTLE mice also had EA, in the form of interictal discharges, determined as fast and high amplitude spike events lasting up to 200 ms (Figure 1F). The frequency of interictal epileptiform discharges was significantly higher in the MTLE group as compared with the EA group. Saline-injected controls (Sal mice) did not display seizures or EA at any time during the monitoring (Figure 1F).

In addition to seizures and interictal spikes, MTLE is also characterized by a number of pathological changes in the DG as we mentioned above. One of the most common features of MTLE is GCD or growth or expansion in the GCL length measured between the hilus and the molecular layer (Figure 1D). Accordingly, we found significantly increased GCD in MTLE animals, whereas saline and EA animals did not present any alteration in the GCL (Figure 1G). GCD was accompanied by a decrease of GC density, most likely reflecting neuronal death in addition to the expansion of the layer, in MTLE mice compared with Saline and EA mice. No difference was found between the latter two groups (Figure 1H).

Figure 1. Intra-Hippocampal Injection of KA as a Model of EA and MTLE . (A) Confocal image showing the needle track and the place of delivery of Sal/KA into the hippocampus of a Nestin-GFP mouse at 7 dpKAi. (B) Representative EEG traces from the hippocampus, ipsilateral (IL) and contralateral (CL) to the injection site. During the entire period of monitoring, there were no seizures or interictal spike activity in the saline-treated group (Sal).. Examples at the 6-hr post-KA injection (6 hpKAi) time point are shown. Abnormal interictal spike activity (asterisks) was evident in the EA and MTLE mice but not in the Sal group in the days following de KA injection. Examples are provided for the 50-dpKAi time point.(C) EEG trace from a MTLE mouse showing electrographic seizures at 1 and 50 dpKAi. The arrow indicates the start of the behavioral seizure recorded on video. Scale bar represents 500 μV/2 s. (D) Representative confocal microscopy images showing normal appearance of the GCL in an EA mouse and GCL dispersion and lower neuronal density in a MTLE mouse at 50 dpKAi (E) Quantification of the average number of seizures per 8 hr (2 to 50 dpKAi). No seizures were detected in the Sal or EA mice. (F) Quantification of the average number of EA events per minute (2 to 50 dpKAi). In the EA, only at 50 dpKAi epileptiform discharges were detected. In the MTLE, epileptiform discharges occurred with higher frequency (G) Quantification of the GCL thickness, measured as the distance between the hilus and the molecular layer (H), and of the GC (DAPI$^+$NeuN$^+$cells) density. Bars are shown as mean ± SEM. Dots show individual data. *p < 0.05, after t test.

6.1.2. NSCs Become Reactive as they divide

As we describe above, the epileptic model of MTLE is characterized by recurrent seizures focused on the hippocampus (Tatum 2012; Sharma *et al.*, 2007).

We first noticed that NSCs (Nestin-GFP and GFAP immunopositive cells with a radial process emerging from the soma) had acquired a "reactive-like phenotype" in analogy with reactive astrocytes: their soma was enlarged, their cytoplasmic processes were increased in thickness; abnormal basal branches appeared and overexpression of Nestin (Nestin-GFP) and GFAP was evident. This phenotype lead us to term these cells Reactive NSCs, or React-NSCs (Sierra *et al.*, 2015) as explained in detail below.

At 3 dpKAi, we observed that the majority of the NSCs presented a "reactive phenotype" (Figure 2A), following similar criteria used to describe reactive astrocytes (Sofroniew and Vinters, 2010) we describe this reactive NSCs.   In contrast to the typical single radial process that characterizes NSCs in normal conditions several primary processes emerged from an enlarged soma of the NSCs of MTLE mice (Figure 2B). In addition, the processes were also significantly thicker, and there was a clear increased expression of both Nestin-GFP and GFAP (Figure 2C). Finally, secondary branching, especially in the initial segment of the primary process, was noticeable in the NSCs of MTLE mice (Figure 2D). The quantification of these morphological parameters (number and thickness of the primary processes, and secondary branching) showed significant differences. No differences in NSCs morphology were identified in EA and Sal mice (Figure 2B-D). Thus, after seizures, NSCs acquire a reactive phenotype that shares features with that of reactive astrocytes: increased ramification, hypertrophic cell body, thickened prolongations, and overexpression of Nestin and GFAP.
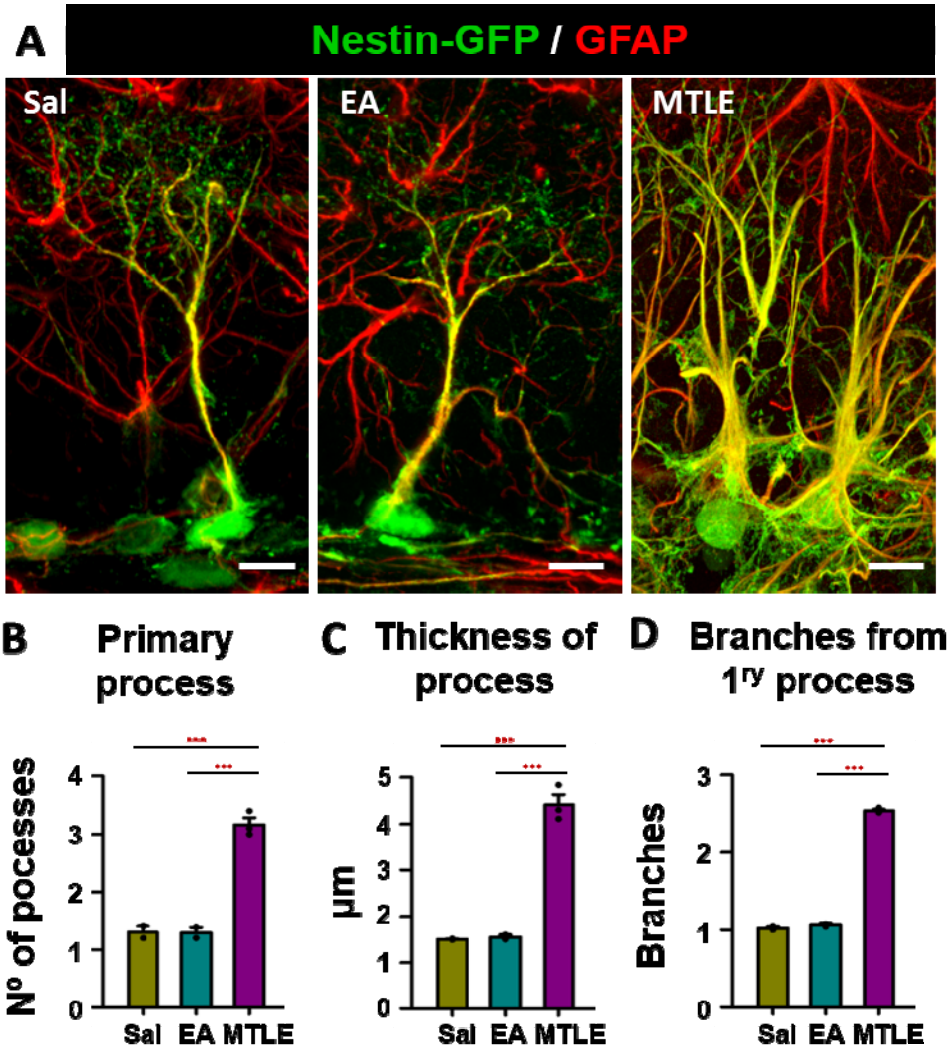
Figure 2. NSCs Become Reactive as they Divide (A) Confocal microscopy images showing typical NSCs present in the SGZ of Sal and EA mice and with a reactive phenotype in MTLE mice. (B) Quantification of the number of NSCs primary processes, defined as those emerging from the soma (C), of the thickness, measured as width in projection from z-stacks of NSCs primary processes (D), and of the number of NSCs secondary processes, defined as those branching from the primary process (F). Scale bar is 10 µm in A. ***$p < 0.001$ by all pairwise multiple comparison by Holm-Sidak post hoc test. Bars show mean ± SEM. Dots show individual data.

In addition to excitotoxicity and inflammation, MTLE is characterized by hippocampal hyperproliferation. To analyze the proliferative capacity of NSCs in the MTLE model (Figure 3A) we administered BrdU 2 days post injection (4 injection 2 hours apart; BrdU is a synthetic analogue of thymidine which is incorporated during the S-phase of the cell cycle substituting for thymidine during DNA replication) and then the animals were sacrificed 15 hours after the first injection of BrdU (Figure 3B). This is a period shorter than the estimated time needed to complete mitosis (Hayes and Nowakowski, 2002; Encinas *et al.*, 2011) so that we could identify NSCs undergoing division (in the stages of telophase, karyokinesis, or cytokinesis) and characterize the morphological and marker-expression features of both the mother and the daughter cell (Figure 3A). Thus, we analyzed only BrdU-stained pairs of cells in which the nuclei

of the NSC and its daughter cell were still in contact and their cytoplasms were still united, performing therefor a *de facto* clonal analysis. Under normal conditions and as we confirmed in the Sal, and in EA mice, NSCs divide mostly asymmetrically, giving rise to ANPs that bear only very short and thin processes and lack GFAP expression (Figure 3 A and C). In contrast, in MTLE mice, we observed that daughter cells being born from React-NSCs had long (10–50 μm) and thick (3–5 μm) processes strongly immunostained for GFAP (Figure 3A), thus presenting also a React-NSCs phenotype. In fact, in MTLE mice most of the daughter cells of React-NSCs gave rise to React-NSCs, strongly suggesting that seizures prompt a switch from predominantly asymmetric neurogenic NSCs division in normal conditions to symmetric division yielding more React-NSCs (Figure 3A and C). We later demonstrated using lineage tracing in inducible transgenic mice that these dividing React-NSCs generated mostly reactive astrocytes and a small proportion of "aberrant" newborn neurons (Sierra *et al.*, 2015).
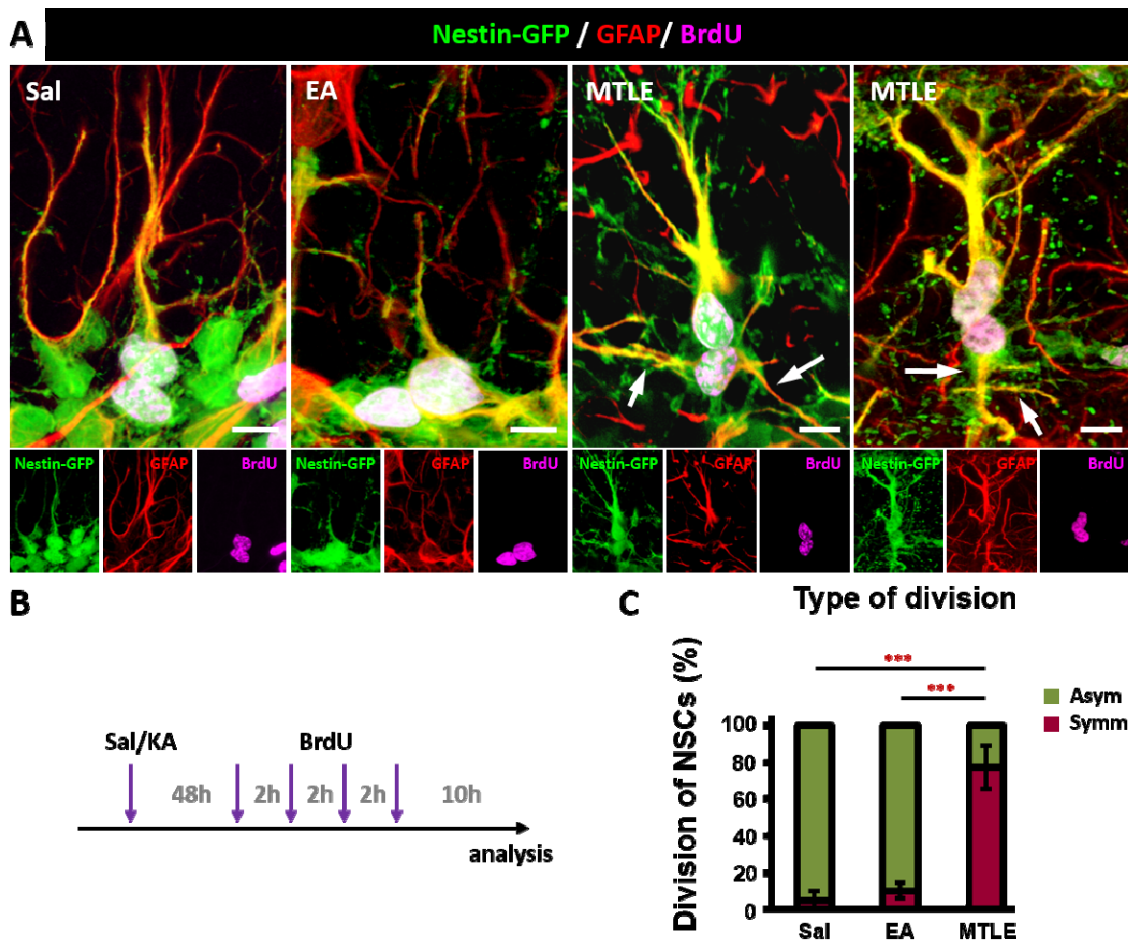
Figure 3 NSCs Become Reactive as They Divide. (A) Confocal microscopy images showing typical asymmetric division of NSCs in Sal and EA mice and symmetric division in MTLE mice. The arrows point at GFAP-immunostained processes of the daughter cells. (B) Experimental paradigm of Sal/KA and BrdU administration designed to increase the probability of capturing cells in telophase, karyokinesis, and cytokinesis. (C) Quantification of the type of NSC cell division. "Asymmetric" cell division was assigned when the daughter cell had no processes or short (less than 10 μm) and thin (less than 1 μm) processes lacking GFAP expression. "Symmetric" division was assigned when the daughter cell had clearly defined

processes of at least 10 μm in length and 1 μm thickness immunostained for GFAP. Only those pairs of cells with the nucleus still in contact were counted. Scale bar is 20 in ***p < 0.001 by all pairwise multiple comparison by Holm-Sidak post hoc test. Bars show mean ± SEM. Dots show individual data

6.1.3. Seizures increase cell death in the DG.

The increased activation of NSCs in EA and MTLE accelerates the depletion of NSCs population over time (Sierra *et al.*, 2015). In the first case the depletion is progressive and consists in an accelerate conversion of the activation-coupled astrocytic differentiation (Sierra *et al.*, 2015). In the MTLE model, the loss of NSCs is fast and almost complete, and could be attributed to the switch to the reactive astrocyte-generating symmetric division of React-NSCs, but it might be also that part of the massive cell death that ensues after seizures corresponds also to death of NSCs or React-NSCs. We therefore analyzed and categorized the apoptotic cells. We considered apoptotic cells as those cells expressing activated-caspase 3 with pyknotic/karryohectuc nuclei (Figure 4A), as carefully detailed before (Sierra *et al.* 2010). 1 day post-KA injection the number of apoptotic cells was higher in MTLE mice comparing to Saline and EA mice (Figure 4B). We also quantified the cell death at 3 dpi and the result was the same than in 1 dpi, in MTLE the number of apoptotic cells was higher than in saline and EA (Figure 4C).By cell types (Figure 4D) we observed that in MTLE, but not in EA mice, there was indeed an increase in apoptotic NSCs, ANPs, and astrocytes (Figure 4E, 4F and 4G respectively). However, the number of apoptotic NSCs was very low and represented only a very small fraction of the total number of apoptotic cells, largely comprised of neuroblasts and GCs (Figure 4H). All together these results let us to confirm that the NSCs population is not exhausted by apoptosis.
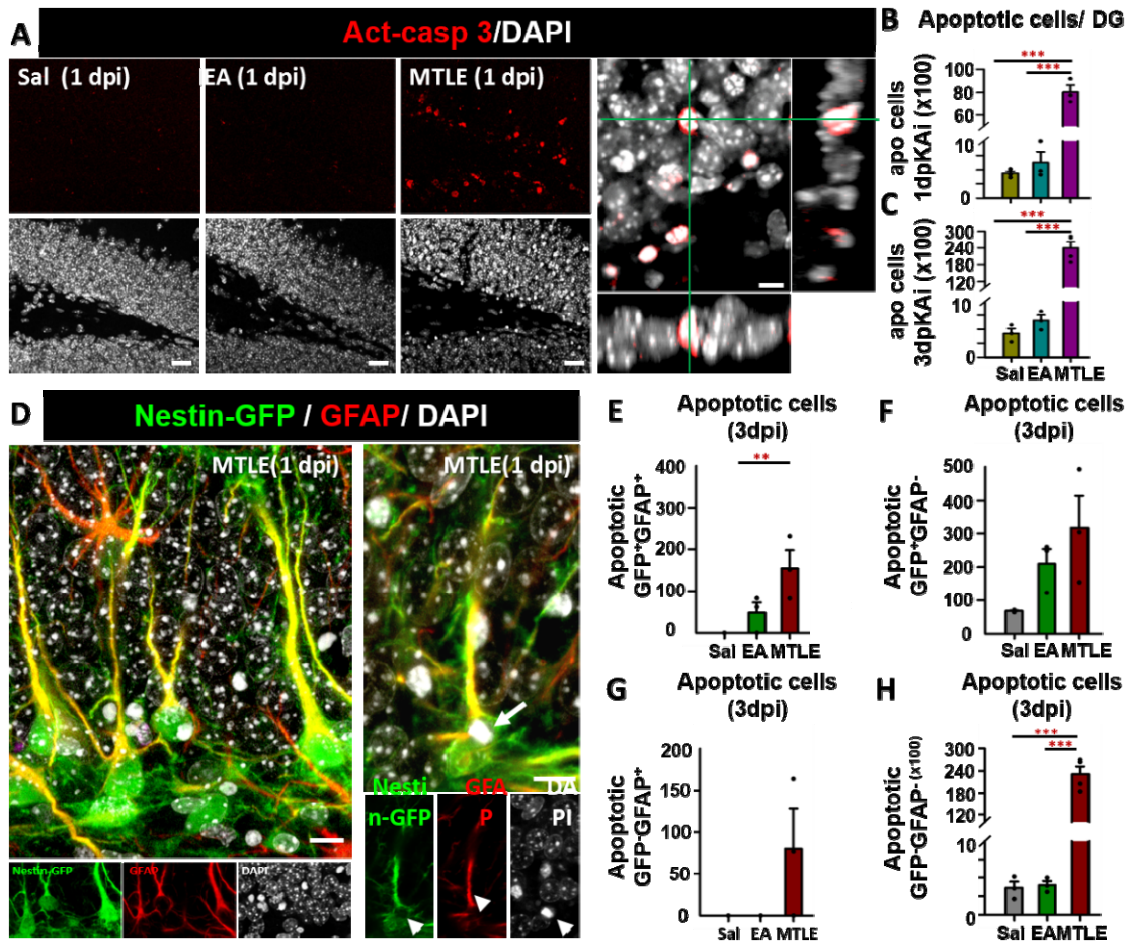
Figure 4. Seizures increase cell death in the DG. Quantification of apoptotic cells by cell types at 3dpKAi. NSCs , ANPs , astrocytes represented a very small proportion of apoptotic cells.(A) Confocal microscopy projections of z-stacks showing DAPI nuclear staining (gray) and immunostaining for the apoptosis marker activated caspase 3 (act-casp3, red) at 1 dpKAi. Note the accumulation of DAPI-stained condensed nuclei, and of act-casp3-immunopositive cells in the MTLE mice (right panel). Orthogonal projection (0.4 μm-thick) showing the co-localization of act-casp3 and condensed DAPI-stained nucleus. Presence of both features was used to unambiguously identify and quantify apoptotic cells in all groups. (B) Quantification of apoptotic cells in the SGZ and the GCL at 1 (C) and 3 dpKAi. A significant increase was found in the MTLE mice in comparison to both the Sal and the EA mice. (D) Confocal microscopy images showing the high number of apoptotic cells in the MTLE mice found in the DG. Example of an apoptotic NSC (arrow). (E) Quantification of apoptotic Nestin-GFP and GFAP positive cells at 3 dpi. (F) Quantification of apoptotic Nestin-GFP positive and GFAP negative cells at 3 dpi (G) Quantification of apoptotic Nestin-GFP negative and GFAP positive cells at 3 dpi (H) Quantification of apoptotic Nestin-GFP and GFAP negative cells at 3 dpi. The vast majority of them were negative for Nestin-GFP and GFAP or positive for Nestin-GFP and negative for GFAP. Scale bar is 25 μm in A and 5 μm in D . . **p < 0.01 ; p<0.001**, by all-pair-wise multiple comparison by Dunn′s (at 3 dpKAi) post hoc tests. Bars show mean ± SEM. Dots show individual data.

We have demonstrated that seizures in a model of MTLE trigger dramatic changes in NSCs (massive activation, acquisition of a reactive phenotype, switch to symmetric division and generation of reactive astrocytes) thus making them part of the brain′s response to insult at least at the tissue level (Figure 5A). In order to evaluate in a more functional manner these new properties of NSCs in a pathophysiological context we isolated by FACS adult NSCs from

MTLE mice (Figure 5B-C) and then we isolated their RNA to performed a RT-qPCR quantification of a panel of pro-inflammatory cytokines (Figure 5D). Interestingly, among them Il1β was highly overexpressed in NSCs form MTLE mice. Il1β is a major proinflammatory cytokine that is also considered pro-epileptogenic (Devinsky *et al.*, 2013). This result confirms that NSCs are indeed contributing functionally to the reactive gliotic response of the hippocampus.

Although the presence of NSCs and neurogeneis in humans is currently a hot topic in the field of AHN, we wanted to explore as much as possible the similarities and differences between the neurogenic niche of our mouse model and that from actual MTLE patients by analayzing human hippocampal samples resected therapeutically.
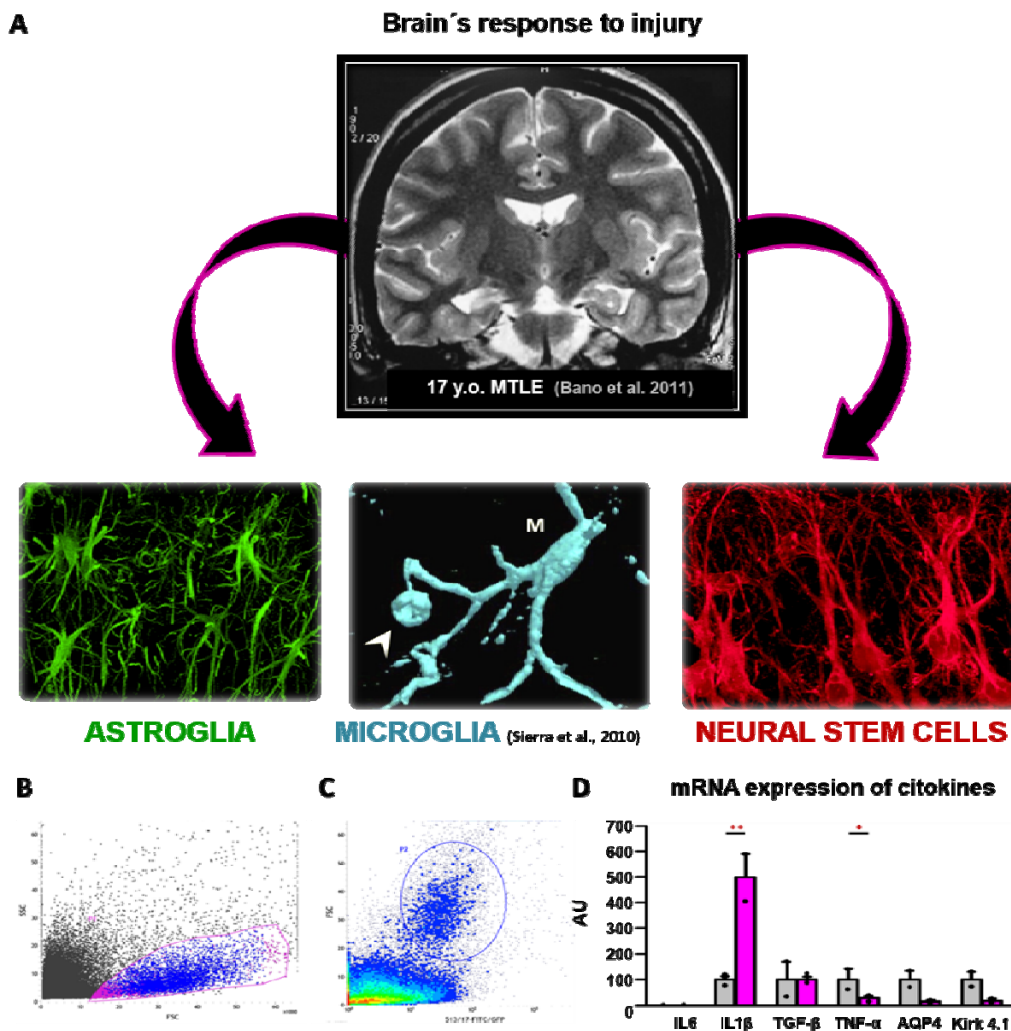
Figure 5. React-NSCs contribute to the MTLE-induced inflammatory response. (A) We hypothesized that NSCs, in the form of React-NSCs are part of the inflammatory process as much as astrocytes and microglia. (B-C) NSCs and React-NSCs were isolated form LPA1-EGFP mice after intrahippocampal injection of saline or KA (MTLE model). (B) Dot plot of sorted event showing the size and the shape of the event. The population of interest is highlight in magenta. (C) Dot plot of the NSCs population showing the size vs the green fluorescence. Blue highlights the population corresponding to the LPA$_1$-EGFP NSCs. (D) RT-qPCR quantification of a panel of pro- inflammatory cytokines showing the significant

increase in the expression of TNF-α and specially of IL1β. * P<0.05, ** p <0.005 by Student's t test. Bars show mean ± SEM. Dots show individual data.

6.1.4. MTLE human sample shows disruption of the neurogenic niche with GCL dispersion and gliosis.

MTLE is one of the most common forms of human epilepsy, and as we described before is characterized by hippocampal sclerosis. MTLE patient are usually resistant to antiepileptic drugs and the only solution is the resection of the focus of the epilepsy, which is usually the hippocampus. Using resected human epileptic brain tissue we analyzed some of the typical parameters we described before, as GDC (Figure 6A), proliferation and hippocampal
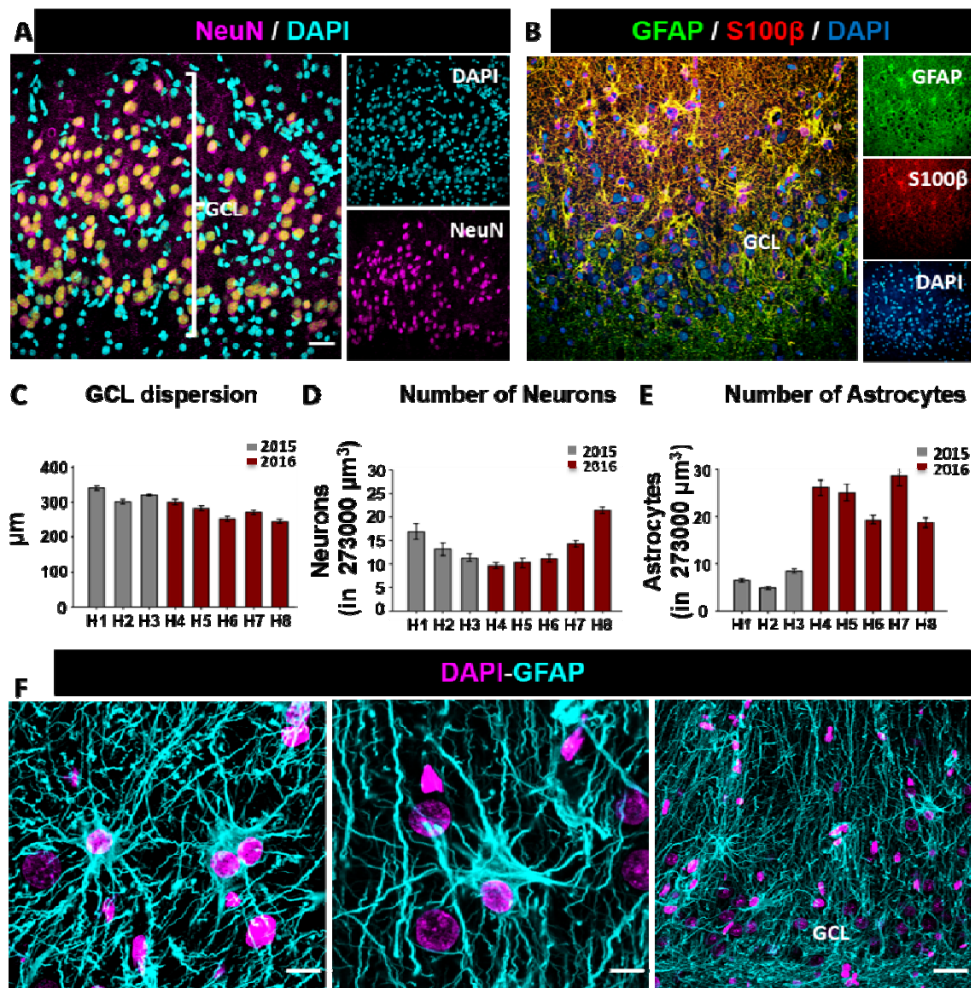
sclerosis.

Figure 6. MTLE human sample shows GCL dispersion and gliosis. (A) Representative confocal microscopy images showing the GCL dispersion in epileptic (MTLE) human samples. The staining shows NeuN (magenta) positive neurons and DAPI (cyan) cells. The dispersion of GCL is characteristic of this type of epilepsy. (B) Representative confocal microscopy images showing the characteristic astrogliosis of the MTLE samples. The staining shows GFAP (green) and S100β (red) positive reactive astrocytes. (C) Quantification of the GCL thickness measured as the distance between the hilus and the molecular layer, showing the CGL dispersion. (D) Quantification of GC density in the GCL. (E) Quantification of astrocytes density in the GCL. (F) Representative confocal microscopy images showing React-NSCs and reactive astrocytes (left and middle panel) and hippocampal gliosis (right panel) in human samples (MTLE) .The

staining shows DAPI (magenta) cells and GFAP (cyan) positive cells. All pairwise multiple comparison by Holm-Sidak. Bars show mean ± SEM. Dots show individual data.

6.1.5. The proliferation is completely lost in the GCL in MTLE human samples.

We next moved on to analyze cell division in the human epileptic neurogenic niche and we did not find proliferation in the SGZ + GCL. The presence of isolated Ki67- positive cells outside of the GCL + SGZ worked as a positive control that validated the use of the antibody (Figure 7A-C). We also studied the neurogenic capacity of these samples, using DCX as a marker of neuroblasts/young newborn neurons. We did not find any DCX positive cells in the neurogenic niche, but found anecdotal DCX positive neurons outside of the GCL that again served as a positive control for the antibody (Figure 7D). These DCX-positive cells resembled interneurons morphologically but investigating their scapes the scope of our study.

The human samples confirm the results obtained in the mouse model where gliosis, GCD go together with lack of cell proliferation and neurogenesis. Whether this result is due to seizures exerting the same effect on the human neurogenic niche as in mice (conversion of NCS on React-NSCs) or is due to human particularities unrelated to epilepsy we cannot tell until we analyse control hippocampal samples obtained in the same manner (directly from surgery) as those from MTLE patients.
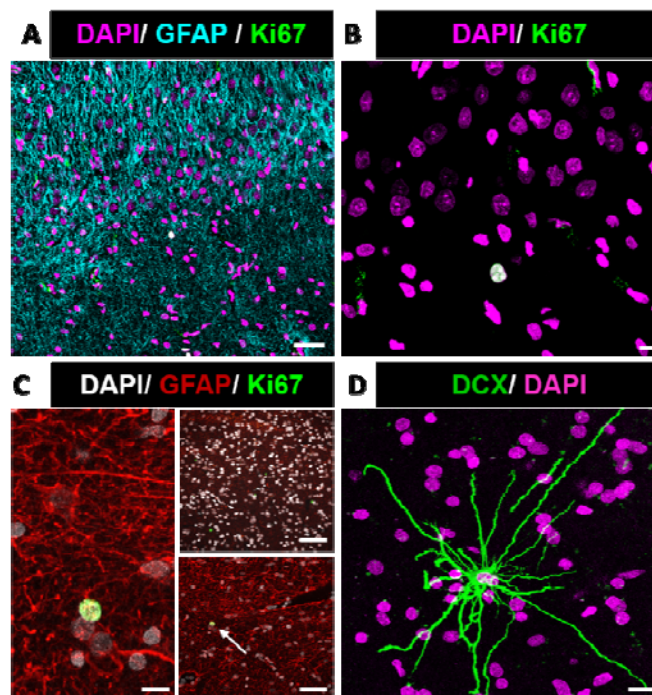
Figure 7. The proliferation is totally lost in the GCL in MTLE human samples. (A) Representative confocal microscopy images showing the GCL dispersion and gliosis in eplileptic (MTLE) human samples, a single Ki67$^+$ cell was found out of the GCL. (B-C) Representative confocal microscopy images showing Ki67$^+$ cell out of the GCL. (D) Representative confocal microscopy images Doublecortin (DCX) positive cell out of the GCL, the DCX cell present an aberrant morphology far from the typical neuroblast.

6. 2 Hippocampal Gliosis and NSCs Reacticity in a Mouse Model of Dravet's Syndrome.

6.2.1. Dravet syndrome mouse model induces reactive NSCs.

We were interested in testing the possibility of our results in MTLE being particular to this mouse model of epilepsy or could be a more generalized response, as we hypothesized that NSCs are also part of the brain´s response to insult as much as astrocytes and microglia. We thus moved on to analyze another model of epilepsy, DS. DS also knows as Severe Myoclonic Epilepsy in infancy is a rare disease that affects 1/20000 of new born children. It is a genetically-provoked epilepsy by in which the 75% of the patient a spontaneous mutation in the SCN1A gene that codifies for a subunit of a sodium channel. These patients present, clonic seizures, ataxia, myoclonus among others alterations and because of its early onset its effect on the developing brain are brutal and long lasting. We used sampled form the mouse model of DS *"Floxed-stop Scn1a*A1783V"* (kindly provided by Dr. O. Sagredo from the group of Javier Fernández-Ruiz,Departamento de Bioquímica y Biología Molecular III, Facultad de Medicina, Universidad Complutenese de Madrid). In contrasts with the wild type the SCN1A cKO mice presented reactive astrogliosis of DG (Figure 8A) and React-NSCs as denoted by the overexpression of GFAP and the thickened processes with the development of basal cytoplasmic expansions (Figure 8B). Focusing on cell proliferation, measured by the expression of the mitotic marker Ki67, we observed that the total number of Ki67 positive cells was higher in cKO mice (Figure 8C) in the SGZ + GCL. When we quantified the percentage of dividing GFAP positive cells with radial-like morphology and located in the SGZ, we found that the proportion of dividing cells was significantly higher in the DS.
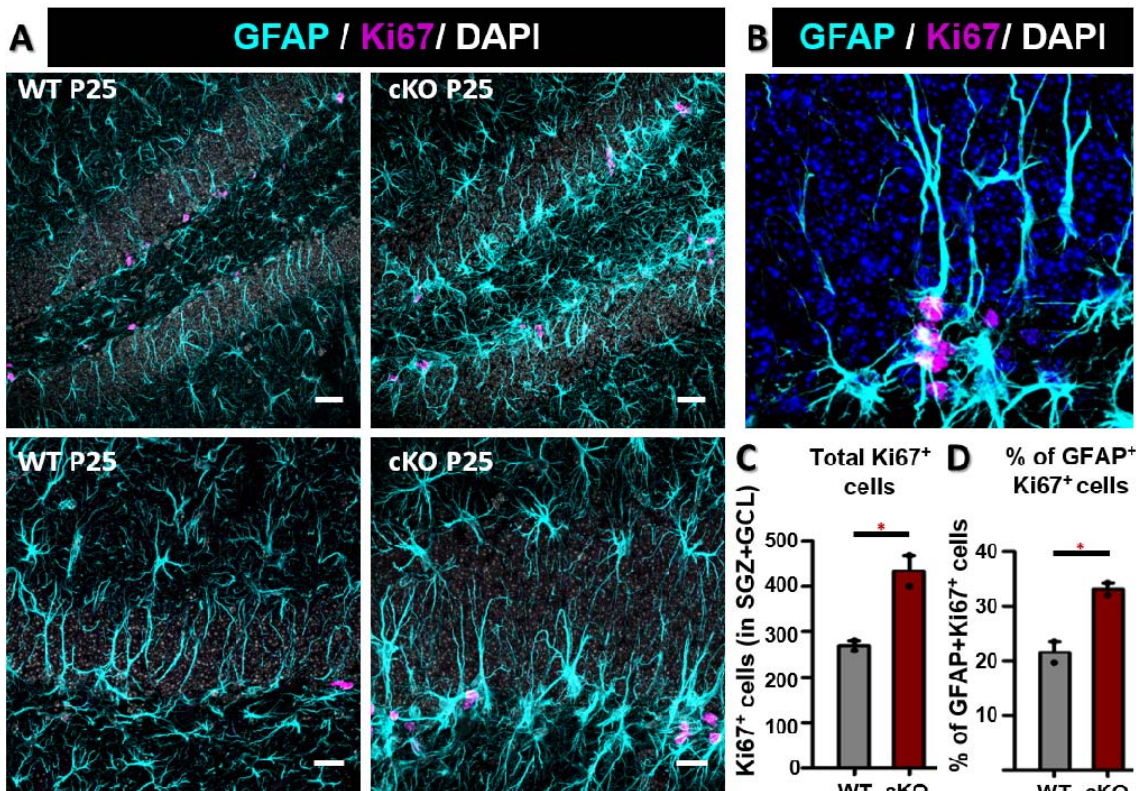
Figure 8. Dravet syndrome mice present Reactive NSCs. (A) Representative confocal microscopy images showing normal dentate gyrus (DG) in WT mice and an epileptic DG in cKO mice. (B) Representative confocal microscopy images showing a reactive NSC in cKO mice stained for GFAP (cyan), Ki67 (magenta) and DAPI (gray). (C) Quantification of the total number of dividing cells measured by the mitotic marker Ki67, there is a significant increase in the dividing cells in the cKO mice. (C) Quantification of the percentage of dividing GFAP positive radial cells measured by the expression of KI67, there is a significant increase in the dividing cells in the cKO mice. Scale bar is 5 μm. *p < 0.001 by Student's t test. Bars show mean ± SEM. Dots show individual data.

Although we were careful with the definition of NSCs we cannot exclude the possibility of some astrocytes with radial morphology also being included in the quantification. Interestingly, we observed React-NSCs dividing also in a symmetric manner, with the daughter also cell bearing long GFAP-expressing proceeses as we described in the adult mouse MTLE model (Figure 8B,D). DS mice also presented significant GCD (Figure 9C) but GC density remained unchanged (Figure 9D). A finding of particular interest was the abnormal shape of the GC nuclei. When we measured the circularity (or how close they are to a perfect circle in the slices) of the nucleus of the GCs we found a significant reduction of this parameter in the DS mice (Figure 9E).
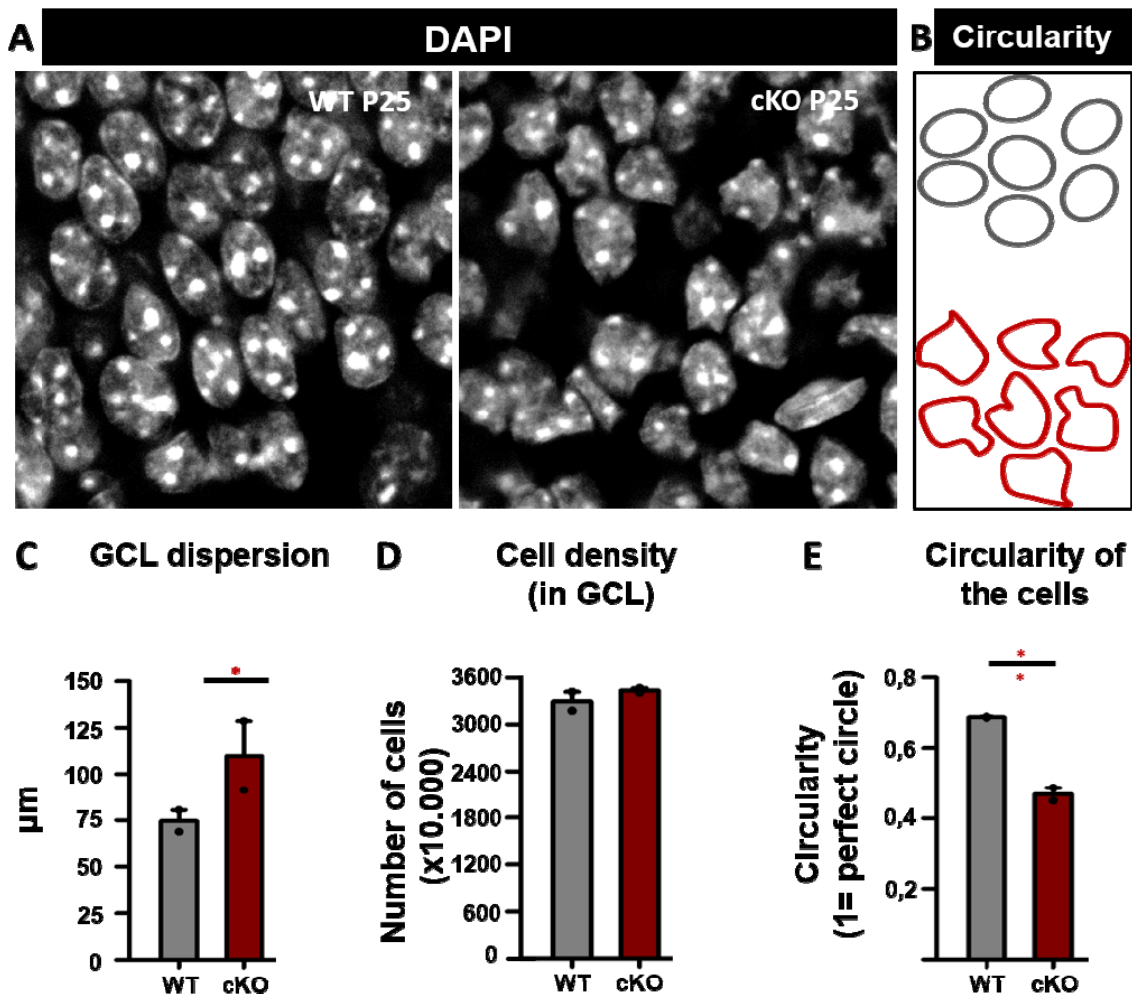
Figure 9. Dravet syndrome mice present reactive NSCs. (A) Representative confocal microscopy images showing normal nuclei (DG) in WT mice and the nuclei in epileptic cKO mice. (B) Schematic representation of the nuclei circularity. (C) Quantification of the GCL thickness measured as the distance between the hilus and the molecular layer ,showing a significant increase of the CGL dispersion in cko mice. (D) Quantification of GC density in the GCL. (E) Measure of the circularity of the nuclei. The perfect circle present a value of 1, WT mice present values higher than cKO mice showing the abnormal morphology of the epileptic nuclei. **p < 0.005 *p < 0.001 by Student's t test. Bars show mean ± SEM. Dots show individual data.

These results confirmed that different levels of neuronal hyperexcitation triggered different response from NSCs. NSCs from MTLE became reactive, generating reactive astrocytes in the dentate gyrus abolishing the neurogenic pathway. In contrast, EA induce an increase in neurogenesis which translates in a long-term depletion of NSCs population. This effect could be comparable to an accelerated aging of the DG with respect to neurogenesis

Thus, after seizures, NSCs acquire a reactive and functional phenotype that shares features with that of reactive astrocytes and that translates into impaired neurogenesis. As we used two very different models of epilepsy we can conclude that this response of NSCs is not a particular on to the injection of KA into the hippocampus and could be a global answer to brain

injury: As epilepsy involves inflammation, which is known to affect NSCs and neurogenesis our next step was to examine whether inflammation alone could be responsible for the epilepsy-induced effect on NSCs.
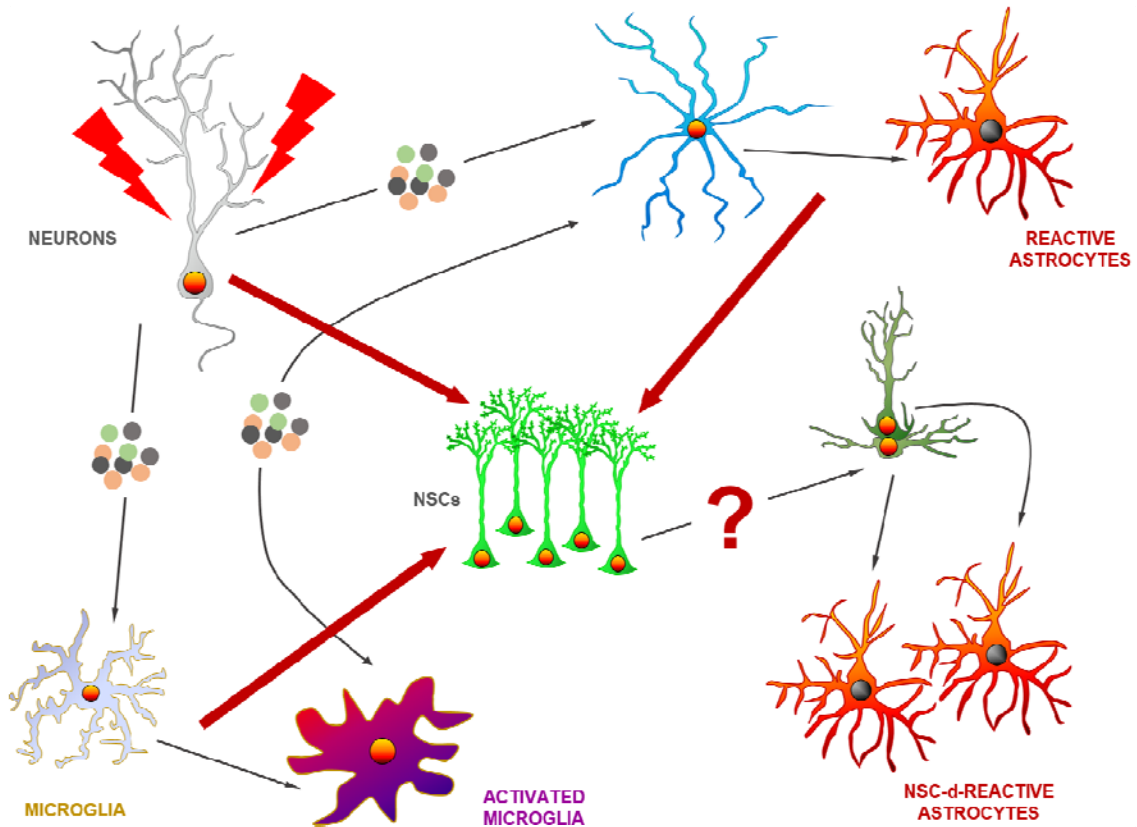
Figure 10. Potential ways of interaction between neurons, astrocytes and microglia to trigger React-NSCs. MTLE induces React-NSCs but what cell type is responsible of instructing NSCs to reprogram remains unknown. Neurons release factors which act on astro and microglia, who in turn release factors that mediatie reciprocal interaction.

6. 3 Reactive Neural Stem is Triggered by ATP *In vivo* and *In vitro*

6.3.1. Neuronal hyperactivity, but not inflammation, is enough to induce React- NSCs.

We resorted to inject different inflammatory agents that mimic viral (POLYI:C), bacterial (LPS) infections or to inject mediators of inflammation (IL6 and IFN-α) directly into the hippocampus of mice and compare it with the effect of insults that involve neuronal hyperactivity such as KA injection (high dose, HKA, as in MTLE) and traumatic brain injury (TBI) (Figure 11A). As readout we focused first on the proliferation of NSCs, measured by the incorporation of administered BrdU (Figure 11B). The quantification of dividing NSCs showed

that the pro-inflammatory drugs (POLY I:C, LPS, IL6, IFN-α) decrease or maintain the proportion of dividing NSCs as in control (non-injected mice) or in saline (injection of saline to discard the effect of injected volume and the damage induced by the canula) conditions, however MTLE or TBI which provoke neuronal hyperexcitation (Sierra *et al.*, 2015; Ding *et al.*, 2011) increase significantly NSCs activation (Figure 11B). As in MTLE hyperproliferation of NSCs is linked with changes in the morphology leading to the reactive phenotype we next analyzed these changes in cell morphology by 3D-sholl analysis (quantification of the number of intersection between virtual spheres of increasing radio and the confocal imaging-based 3D-reconstructions of NSCs) (Figure 11C). We observed a significant increase in the complexity of NSCs in HKA and TBI models, however inflammatory models do not change the morphology and complexity of NSCs (Figure 11C). To facilitate the visualization we separate the figure 11C in two different graphs, inflammatory models (Figure 11 D) and neuronal hyper activity (Figure 11E).

These results strongly suggest that inflammation alone cannot be mediating the induction of Ract-NSCs but rather that neuronal hyperactivity (alone or in combination with inflammation) triggers the induction of React-NSCs. We then hypothesized that hyperactivated neurons are able to directly communicate with NSCs and induce their transformation into React-NSCs. We thought that ATP could be good potential candidate. As we described in the introduction, ATP signalling is important for cell proliferation of NSCs and in reactive gliosis. In addition, ATP release by neurons is a hallmark of seizures (Burnstock 2006). We therefore hypothesized that ATP could be mediating the cell-to-cell communication between neurons and NSCs in MTLE and other types of epilepsy.
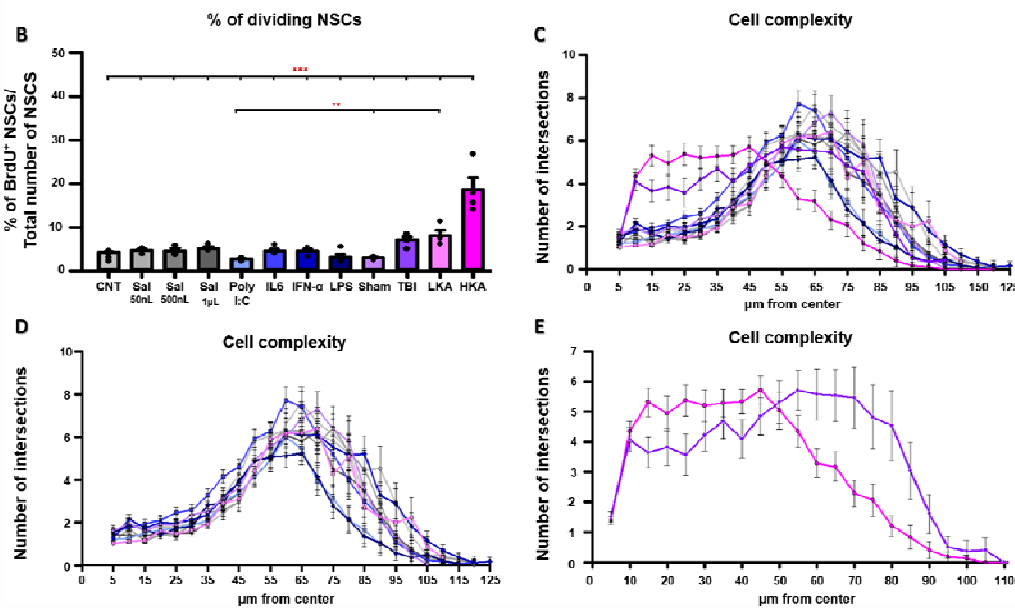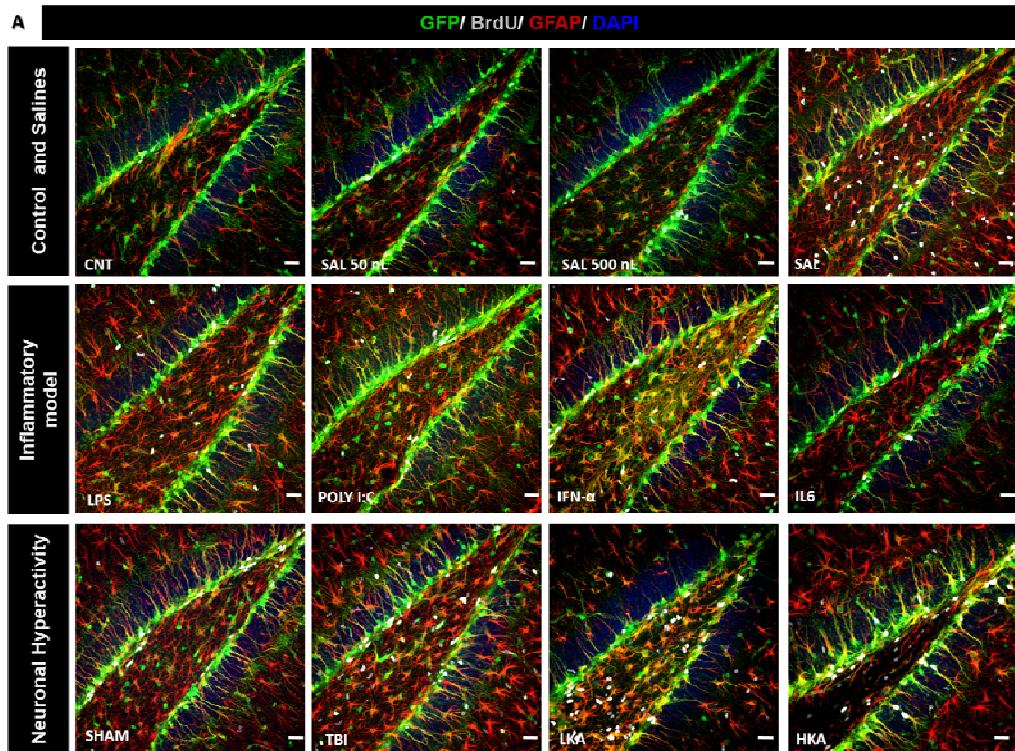
Figure 11. Neuronal hyperactivity is enough to induce the reactive phenotype whereas inflammation fails. (A) Confocal microscopy images showing typical NSCs in the SGZ at 3 dpi of Sal, Cnt, LPS, Poly I:C, IL6, IFN-α,Sham, TBI, LKA and HKA. All NSCs are immunopositive for Nesti-GFP and GFAP and dividing cells are positive for BrdU. (B) Proportion of dividing NSCs among the total population of NSCs. The proinflammatory factors decrease or maintain the proportion of dividing NSCs as in control conditions, whereas low and high KA (LKA and HKA) or TBI, which involve neuronal hyperexcitation increases significantly the proportion of proliferative NSCs. (C) Quantification of the morphological complexity of the NSCs based on the 3D-sholl analysis. This analysis quantify the number of intersections between spheres of different radios and the 3D reconstruction of Nestin-GFP/GFAP NSCs. HKA and TBI induce a high neuronal hyperexcitation and increase the complexity of NSCs whereas the proinflammatory agents or the LKA do not affect the morphology of NSCs. Scale bar is 20 μm in A. * $p<0.05$, **$p < 0.01$, ***$p <0.001$ ANOVA repeated measured followed by Bonferroni post-hoc test in C-E and **$p < 0.01$, ***$p <0.001$ one way ANOVA after all pairwise multiple comparisons by Holm-Sidak post hoc test in B . Bars show mean ± SEM. Dots show individual data.

## 6.3.2. Neural Stem Cells express purinergic receptors at mRNA levels.

To analyze the possibility that ATP is mediating the conversion of NSCs into React-NSCs first we resorted to assess the presence of purinergic receptor in NSCs *in vivo* using NSCs isolated by FACS (Figure 12B). For this purpose we used Nestin-GFP positive mice (Figure 12A) in combination with Prominin-1 staining (Figure12C) a previously validated method to purify the NSCs population (Fischer *et al.*, 2011). Afterward, we assessed the levels of mRNA expression of the P2 receptors (Figure 12G) measured by RT-qPCR using specific primers (Figure 12 D-F and I). We found that NSCs express 3 subtypes of P2X receptors, specifically, P2X3, P2X4 and P2X7 (Figure 12 D-F). In addition to P2Xreceptors NSCs also express 2 of the 11 subtypes of P2Y receptors, specifically, P2Y6 and P2Y12 (Figure 12 H-I). Thus, NSCs are indeed capable to respond to ATP. Our results confirmed those previously reported after single-cell Sequencing of the hippocampal Nesting-GFP population (Shin *et al.*, 2015).
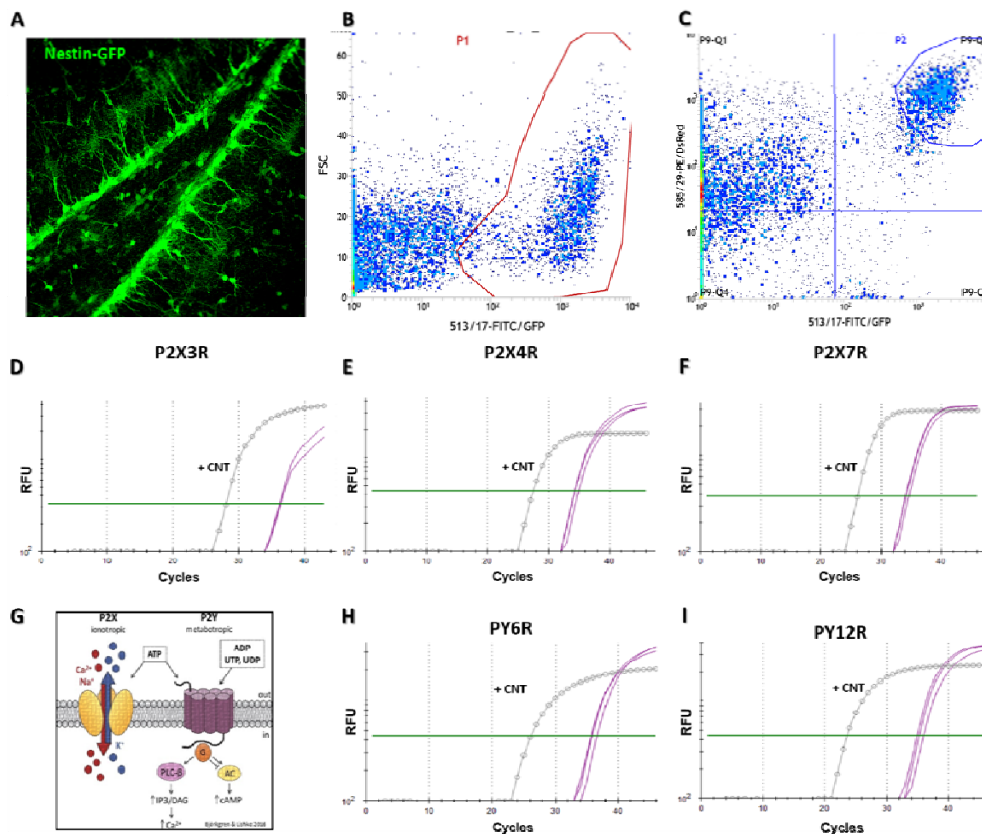
Figure 12. Neural Stem Cells express purinergic receptors. (A) Confocal microscopy images showing the dentate gyrus of Nestin-GFP transgenic mice in which NSCs can be isolated by FACS. (B) Dot-plot of isolated Nestin-GFP positive hippocampal NSCs by FACS.(C) Prominin-PE immunostaining was used isolate NSCs to avoid the isolation of other Nestin-GFP positive populations. (D-F) Amplification graphs of RT-qPCRs. The RNA of the FACS-isolated NSCs was used to analyze the presence of P2XR. NSCs express mRNA for P2X3R, P2X4R and P2X7R. Amplification graphs showing the positive control (total hippocampus) to validate the expression of the gene. (G) Image showing the 2 types of purinergic receptors. (H-I) Amplification graphs of RT-qPCRs. NSCs present 2 types of P2Y receptor, P2Y6 andP2Y12R. Amplification graphs showings the positive control (hippocampus) to validate the expression of the gene.

6.3.3. ATP induces React-NSCs in a dose –dependent manner

To test the possible direct effect of ATP on NSCs *in vivo* we injected ATP directly into the hippocampus of Nestin-GFP mice (Figure 13A) and then we analyzed the most typical features of React-NSCs which are hyperproliferation and morphological changes. Compared to saline the proliferation of NSCs, measured by the incorporation of BrdU, increased significantly with the highest doses of ATP, 50 and 100mM (Figure 13B). In addition, our other readout morphology (complexity) of NSCsalso increased significantly with the highest dose of ATP as measured using 3D-sholl analysis (Figure 13C). These results were obtained at 3 days post injection of ATP. To evaluate the possible effect of ATP in a shorter time we injected the highest dose of ATP (100mM) and analyzed its effect 1 day after the injection (Figure13D). NSCs divide significantly more than in the saline group 1 dpi (Figure13E) although the effect is not as aggressive as at 3 dpi. The complexity of NSCs is also changed 1 day after the ATP injection (Figure13F). Finally we analyzed separately the effect of the highest dose of ATP at 3dpi (Figure 13G). As previously described the proliferation of NSCs in ATP is significantly higher than in saline, being up to 5 fold the value of saline (Figure 13H) . The morphology is also increased in ATP condition, changing the typical morphology into a more branched typical one of the React-NSCs (Figure13I).
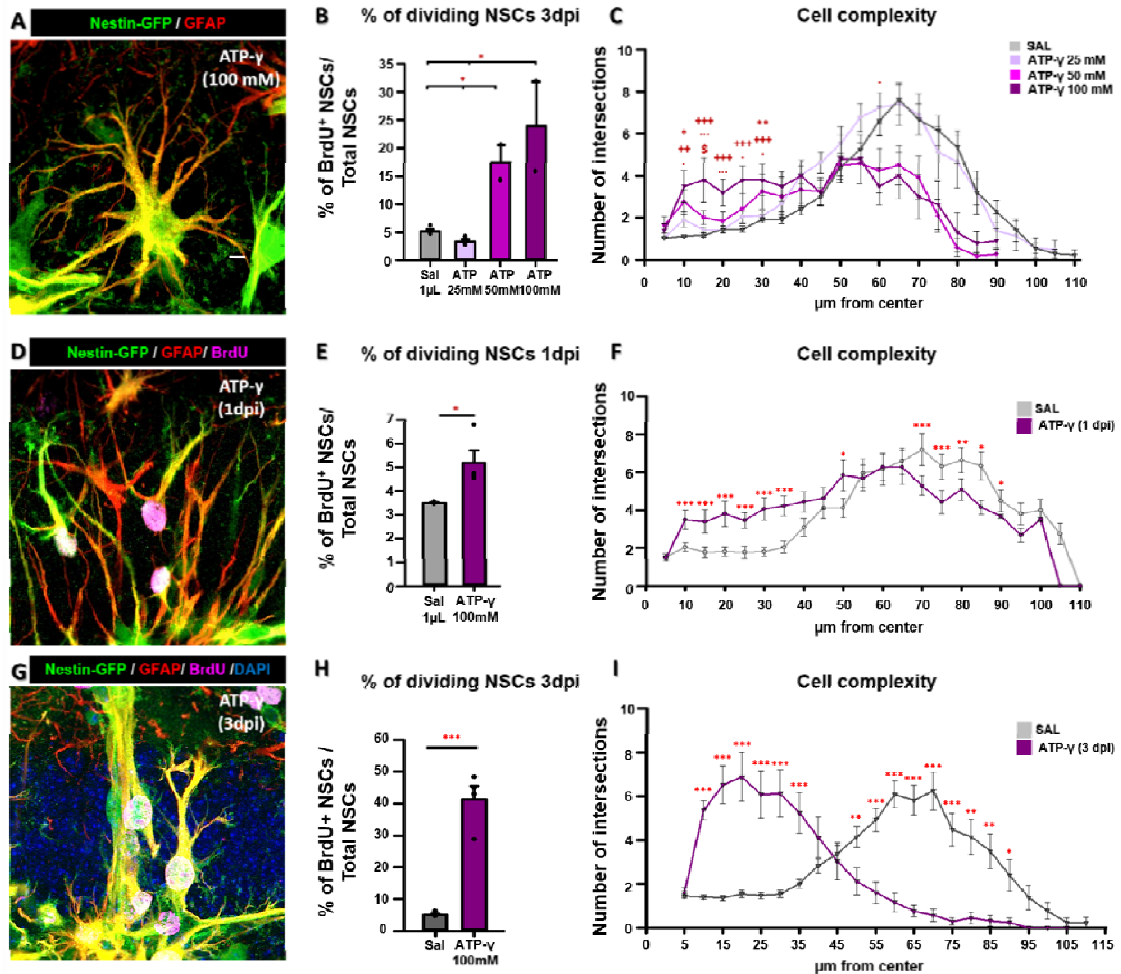
Figure 13. ATP induces React-NSCs in a dose-dependent manner. (A) Confocal microscopy images (projection from z-stacks) showing a React-NSCs after the injection of ATP-γ (100mM). (B) Quantification of the proportion of dividing NSCs, measured by the incorporation of BrdU after the injection of different dosis of ATP-γ (25, 50 and 100mM). (C) Quantification of the complexity of NSCs by 3D-Sholl analysis. (D) Confocal microscopy images showing dividing React-NSCs present in the SGZ of ATP-γ-injected mice at 3 dpi. (E) Quantification of the proportion of dividing NSCs, measured by the incorporation of BrdU, 1 day after the injection of ATP, showing a significant increase. (F) Quantification of the complexity of NSCs by 3D-Sholl analysis. As soon as 1 day after the injection NSCs start to modify their phenotype. (G) Confocal microscopy images (projection from z-stacks) showing a dividing Reac-NSC after the injection of ATP-γ (100mM) 3 days post injection. (H) Quantification of the proportion of dividing NSCs, 3 days after the injection showing a significant increase. (I) Quantification of the complexity of NSCs by 3D-Sholl analysis. *p<0.05, **p < 0.01, ***p <0.001 ANOVA repeated measured followed by Bonferroni post-hoc test in C, F, I. * p<0.05 One way ANOVA after all pairwise multiple comparisons by Holm-Sidak post hoc test in B. * p<0.05, ***p < 0.001 by Student's t test in E and H. Bars show mean ± SEM. Dots show individual data.

As a positive control and to investigate how selective or promiscuous is ATP in the DG we focused our study on other cell types, such us, microglia (data not shown) oligodendrocytes precursors (OPC), pericytes or astrocytes (Figure14A) in the molecular layer and in the hilus (Figure 14). A single dose of ATP is able to induce the proliferation of all these cell types in the hilus (Figure13B) and in the molecular layer (Figure 13C). Thus, for future studies focused on the specific effect on NSCs we will have to avoid the use of generic ATP receptors agonists or antagonists.
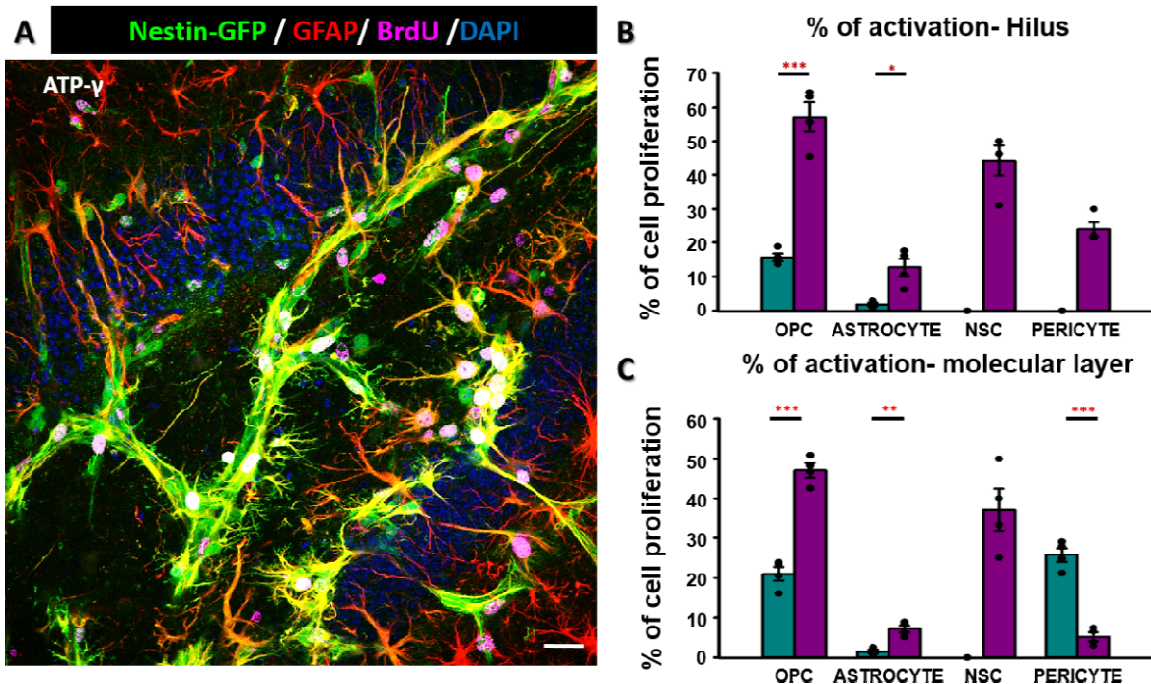
Figure 14. ATP induces the proliferation of different cell types. (A) Confocal microscopy images (projection from z-stacks) showing the DG of Nestin-GFP mice after the injection of ATP-γ (100mM, 3 days). (B-C) Quantification of the proportion of dividing OPCs, astrocytes, NSCs and pericytes in the hilus and in the molecular layer. *p<0.05, **p < 0.01, ***p <0.001 One way ANOVA after all pairwise multiple comparisons by Holm-Sidak post hoc test in B and C. Bars show mean ± SEM. Dots show individual data.

All together these results let us confirm that the ATP is able to trigger the conversion of NSCs into React-NSCs and therefore could be a potential main effector of this response in MTLE. Nevertheless, the effect of neuron-released ATP on NSCs could be still mediated through intermediate actors. As NSCs are surrounding by different types of cells such as microglia, astrocytes or neurons the interaction between them or the direct communication with NSCs could explain the conversion of NSCs into React-NSCs. To further characterize the individual response of NSCs to ATP and being able to investigate the signalling cascade we moved to *in vitro* studies.

6.3.5 ATP induces reactivity in adult neuprogenitors.

We obtained neurospheres from the DG of the adult hippocampus of Nestin-GFP mice, (formed by neural stem and progenitor cells, NPCs) keept in proliferative non-differentiating conditions) from adult DG of Nestin-GFP mice and exposed them to increasing doses of ATP from 25 mM to 500mM (Figure15A). ATP induced proliferation of NSPCs. The higher doses, from 200mM to 500mM triggered cell death and therefore we choose the low dose of 50mM and 200mM as the concentration to work with (Figure 15B). As morphological change is one of

our main readouts *in vivo* to characterize React-NSCs we tested whether ATP induced morphological alterations on NSPCs *in vitro* by measuring the area occupied by the cells in the different conditions. This quantification showed a significant increase in the area of the ATP-treated cells confirming that as it happens *in vivo* ATP *in vitro* induced changes the morphology of NSPCs and that we can use this readout to measure their reactive response (Figure15C) in NSPCs.
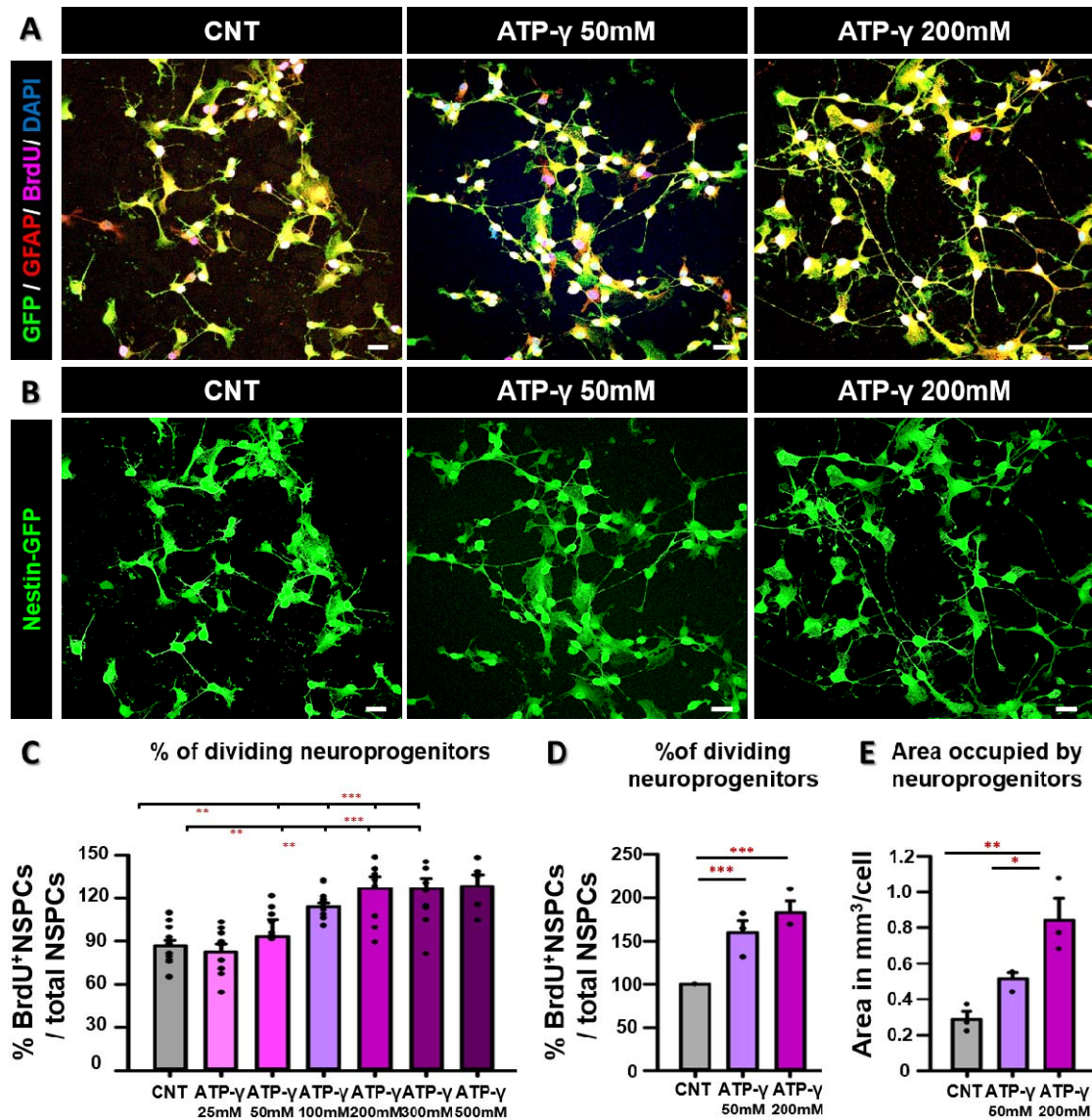
Figure 15. ATP induces cell proliferation and morphological alterations in NSPCs *in vitro*.(A-B) Confocal microscopy images showing Nestin-GFP adult DG-derived neurosphere cultures after staining for BrdU and GFAP. ATP affects the morphology of NSPCs inducing a cellular enlargement. (C) Quantification of the proportions of NSPCs measured by incorporation of BrdU (applied for 13h starting 2h after the addition of ATP at different doses up to 500mM. NSPCs were treated with ATP-γ for 15 hours). ATP increases significantly NSPCs proliferation in a dose-dependent manner compared to control (vehicle-treated) cells. (D) Quantification of the proliferation of NSPCs at 50 and 200 mM. (E) Quantification of the area occupied by each cell in mm^3. ATP increases the area occupied by NSPCs in a dose dependent manner.*$p < 0.05$, **$p < 0.01$, ***$p < 0.001$ one-way ANOVA by all pairwise multiple comparison by Holm-Sidak post hoc test. Bars show mean ± SEM. Dots show individual data.

We also analyzed the presence of purinergic receptors *in vitro* as we described before for NSCs *in vivo* (Figure 16A). For this purpose the RNA of the NSPCs was isolated and the levels mRNA expression of the P2 receptors was measured by RT-qPCR. *In vitro* NSPCs express 3 subtypes of P2X receptors, specifically, P2X3, P2X4 and P2X7 (Figure16 B-D) but do not express P2Y receptors. Thus, *in vitro* NSPCs respond directly to ATP via P2X receptors as their *in vivo* counterparts and can be used to perform detailed signalling studies in the near future. To further validate our system we used a P2X receptor antagonist.
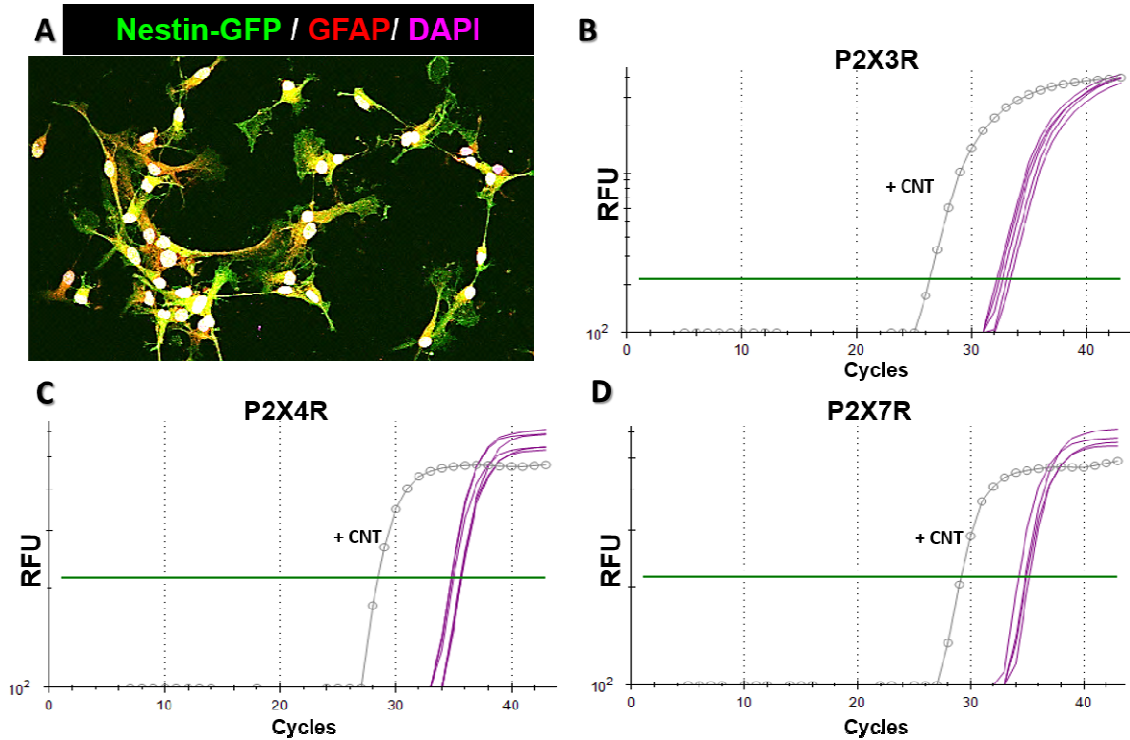
Figure 16. NSPCs express P2XR *in vitro*. (A) Confocal microscopy images showing NSPCs disaggregated from neurospheres derived from the DG of adult Nestin-GFP. (B-D) Amplification graphs of RT-qPCRs. NSPCs express 3 types of P2X receptor, P2X3R, P2X4R and P2X7R. Amplification graph shows the positive control (hippocampus) to validate the expression of the gene.

6.3.6 TNP-ATP antagonist of P2X receptors blocks reactivity in adult neuprogenitors.

We used the P2X receptor antagonist TNP-ATP and measured the effect on NSPCs measuring both cell proliferation and cell area as readouts. We first added the antagonist 2 hours later the ATP so that the P2X receptor were blocked when the ATP was added to the medium (Figure 17A). The addition of TNP-ATP blocked the ATP-induced increase of cell proliferation (Figure 17B) as well as the ATP-induced increase in cell growth.
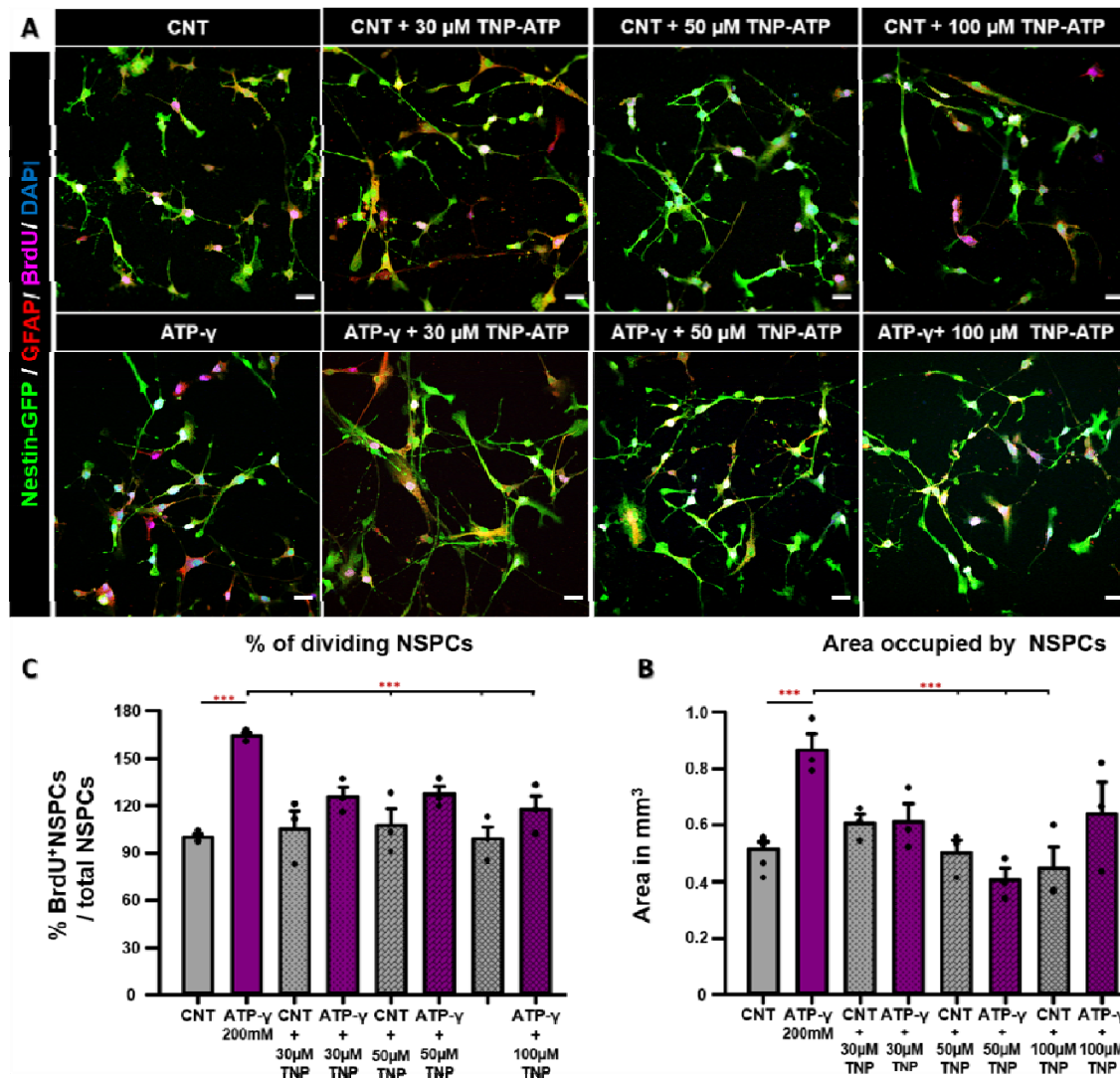
Figure 17. TNP-ATP, an antagonist of P2XR blocks the ATP-induced changes in NSPCs *in vitro*. (A) Confocal microscopy images showing the morphology of cultured Nestin-GFP NSPCs with the addition of ATP or. ATP+TNP-ATP. (B) Quantification of the proportion of dividing NSPCs, measured by incorporation of BrdU, after the addition of the antagonist of P2X receptors TNP-ATP (applied for 13h starting 2h after the addition of ATP and TNP-ATP at different doses up to 100μM). (C) The antagonist TNP-ATP blocks the increase in the area occupied by each cell***$p < 0.001$ one-way ANOVA by all pairwise multiple comparison by Holm-Sidak post hoc test. Bars show mean ± SEM. Dots show individual data.

### 6.3.7 miRNA can effectively blocking the expression of P2X receptors.

Once that we clearly stablished the effect of ATP on NSCs *in vivo* an on their *in vitro* correlate we decided to move on and delineate a way to block P2X receptor expression specifically in NSCs, *in vivo*. Under this premise we resorted to use interference RNA and elaborate in particular a miRNA to block specifically the P2X receptor, for this purpose we collaborated through a stay abroad with the group of Veerle Baekelandt , Principal Investigator of the group for Neurobiology and Gene Therapy in the department of Neuroscience of the

Katholieke Universiteit Leuven (Figure16A) . The construct was made to infect eukaryotic cells (Figure 16B and C). We used the Neuro2a cell line to test the effects of our constructs (immature neurons) analyzing the levels of P2X receptors mRNA expression as a readout. We found that two of the plasmids for P2X3 and P2X4 receptors were highly efficient and significantly reduced after the treatment with the lentiviral vectors (Figure 16D and E).

These results opened new perspective to work with in a future and measure the effect of the blockade of the purinergic receptors in the conversion of NSCs into React-NSCs as we can use especific promoters to drive the expression of the miRNA or use inducible Cre-Based transgenic mice to assure the specific effect on NSCs.
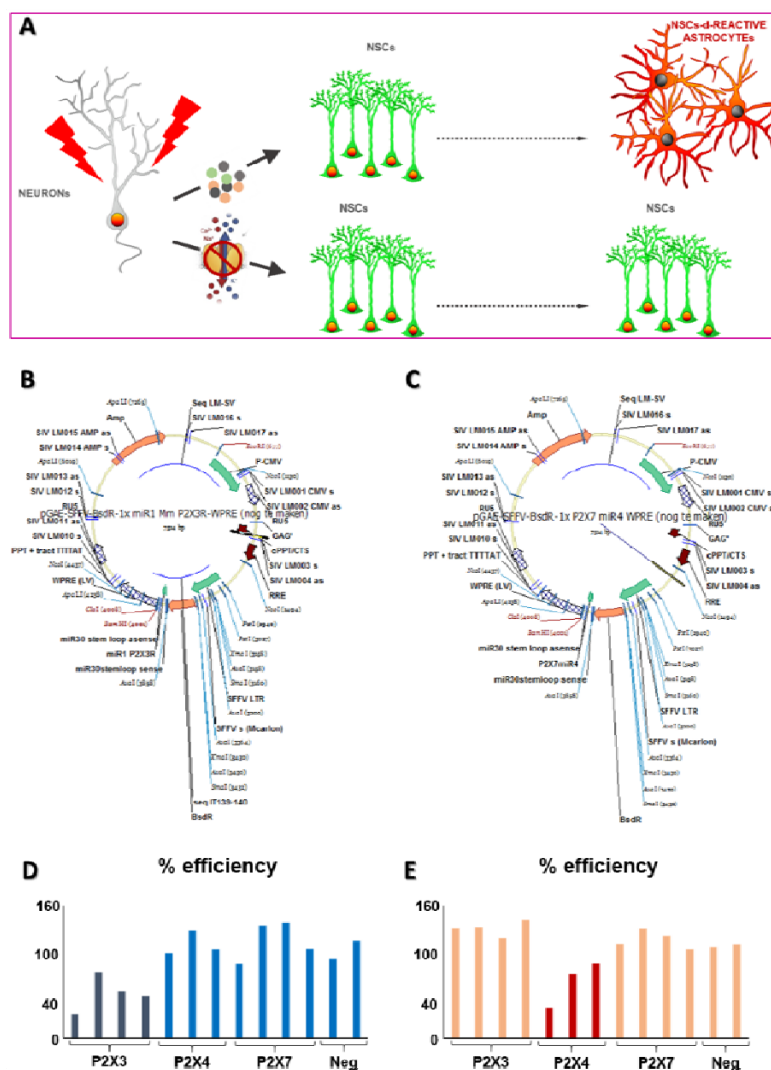
Figure 18. miRNA are effective blocking the expression of P2XRs. (A) We hypothesize that knocking down the expression of P2XR in NSCs will prevent them from becoming React-NSCs. We are developing RNA interference tools to test this idea. (B-C) Constructs for the expression of miRNA to block the expression of P2X3 and P2X7. (D-E) RT-qPCR showing the reduction of P2X3 (D) and P2X4 receptor (E) expression by the constructs in the Neuro2a cell line *in vitro*.

So far we have described the behaviour of NSCs and the generation of React-NSCs in the context of epilepsy as a neurological disorder. We wanted next to study NSCs in a very different pathophysiological context in which AHN is extensively known to be impaired. We then moved on to study NSCs in a naturally ocuring phenomenom that is widely considered as a pathophysiologcal condition, aging.

6.4 Phenotypical and Funtional Heterogeneity of NSCs in the Aged Hippocampus

Neurogenesis declines drastically with age directly affected by aging (Kunh *et al.*, 1996), with the depletion of NSCs population being the main driving force (Encinas *et al.*, 2011; Encinas and Sierra, 2012). Nevertheless, the properties of those NSCs remaining in the DG as it ages can be also altered and therefore can be contributing to the decline in neurogenesis. For this reason we sought to investigate in detail NSCs and their properties during aging.

6.4.1 NSCs population and total activation rate decrease drastically with aging, but the relative rate of NSC activation remains constant.

To describe how the age can affect NSCs, we analyzed the population of NSCs at different time points, in 1, 2, 6 and 12 month-old (mo) mice (Figure 19). Using C57BL/6 mice we analyzed the changes in the total number of NSCs, considering hippocampal NSCs as cells with the soma located in the subgranular zone (SGZ) which present a single radial process that crosses the granule cell layer (GCL) and arborizes in the molecular layer (ML) (Eckenhoff and Rakic, 1984; Encinas *et al.*, 2006; Kempermann *et al.*, 2004; Kosaka and Hama, 1986; Kronenberg *et al.*, 2003; Mignone *et al.*, 2004; Seri *et al.*, 2004; Seri *et al.*, 2001). These cells are positive for Nestin, GFAP, BLBP and vimentin. Based on these characteristics we quantified the total Nestin positive GFAP positive radial NSCs in all ages (Figure 19A). We observed that between one month and one year of age the population of NSCs decreases around 90% in older mice (12 mo.) in agreement with previous results (Encinas *et al.*, 2011) (Figure 19A). This reduction is reflected in the total number of dividing NSCs, measured by incorporation of BrdU. After a short pulse of BrdU (a semicumulative paradigm, 4 injections 2 hours apart) the animals were sacrificed, 2 hours after the last injection, in order to measure the proliferative capacity of NSCs (Figure 19B and C). The total number of dividing NSCs also decreases over time, with 90% fewer dividing NSCs in older mice (12 mo.) than in the younger animals (1 mo.) (Figure 19B). However the fraction of dividing NSCs within the total population of NSCs did not change at different ages. Only a small proportion of NSCs, between 2-4 % of the total population, are dividing at any given timepoint (Figure 19D). This is an interesting finding

because the total size of the population would allow for a more sustained rate of activation, and neurogenesis, as many NSCs remain unactivated, and because the mechanism by which the population of NSCs is able to keep the rate of activation constant remains unknown.

The correspondence between the decrease of dividing NSCs and the decrease in the total number of NSCs let us to hypothesized that the activation, understood as the division, of NSCs could explain the loss of NSCs along the time. Indeed the activation of NSCs predicted up to 99% the loss of NSCs in the next time point, using a linear regression analysis (p<0.001), providing further evidence that the depletion of NSCs is linked to their activation (Figure 19E). At this point we can conclude that the activation of NSCs is the main, but not the only, force driving the depletion of NSCs along the time.
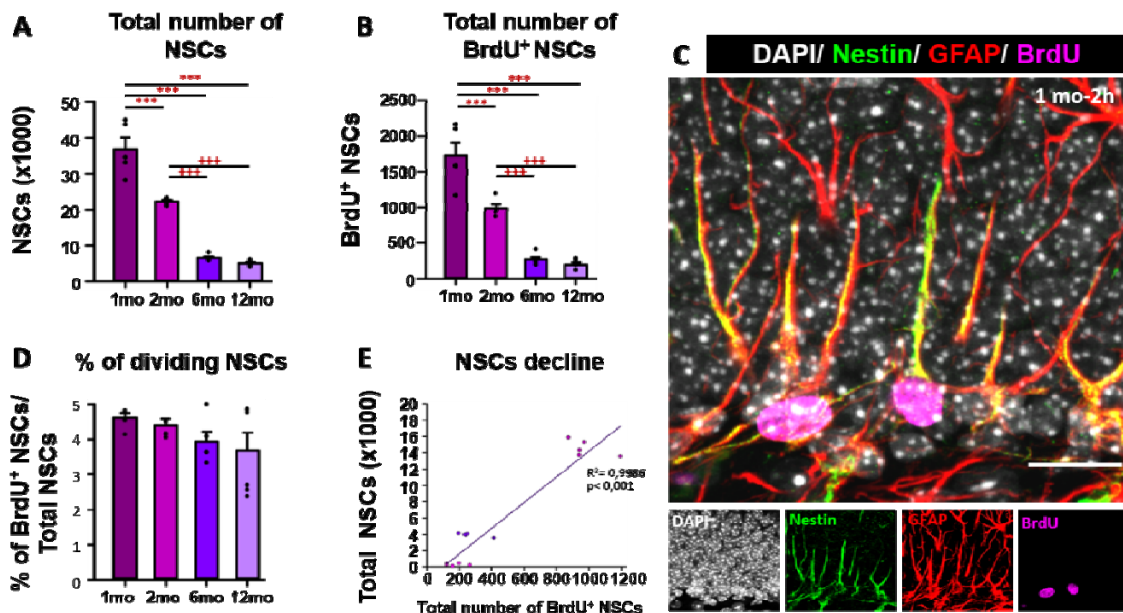
Figure 19. NSCs population decreases drastically with aging. (A) Quantification of the total number of NSCs in 1, 2, 6, and 12 mo. Wild type animals showing the depletion of NSCs population with age. (B) Quantification of the total dividing NSCs showing a significant decrease with age. (C) Quantification of the proliferative capacity measured by the incorporation of BrdU, in 1, 2, 6 and 12 mo. mice, the total number of BrdU cells decreases with aging. (D) Projections of confocal-microscopy z-stacks (8-µm thick) showing a dividing NSC in 1 mo. mice after staining for Nestin (green) and GFAP (red) and BrdU (Margenta). (E) Quantification of the proportion of dividing NSCs (BrdU$^+$NSCs) among the total population of NSCs, the proportion remains constant throughout the age. (F) Quantification of the proportion of dividing NSCs (BrdU$^+$NSCs) among the total number of dividing cells (BrdU$^+$), the proportion remains constant throughout the age.(G) Linear regression analysis of the relationship between the total number of activated NSCs and the total number of NSCs in the next time point. ***p < 0.001 by One way ANOVA Holm Sidak post hoc test. Bars show mean ± SEM. Scale bar is 20 µm-. Dots show individual data.

Previous studies have suggested that the population of NSCs is complex and heterogeneous (Gebara *et al.*, 2016; Lugert *et al.*, 2010). In fact, a subpopulation of NSCs, called beta NSCs, was described as a transitional step from NSCs into astrocytes. These beta-NSCs (β-cells) presents some astrocytic characteristic as the expression of S100-β. Moreover they bear a multibranched morphology distinct from that of astrocytes and that of classic radial glia-like type-1 NSCs (Kempermann *et al.*, 2004), referred to as alpha-NSCs (α-cells), and do not seem to divide in normal conditions (Gebara *et al.*, 2016) an dtherefore should not be termed NSCs. Focus on this heterogeneity we explore the properties of NSCs in aged mice.

6.5. NSCs DrasticallCchange Their Morphological Properties with Aging.

Besides the decrease in size and activation of the NSCs population, we observed a change in the morphology of NSCs along aging that we proceeded to characterize in detail using Nestin-GFP transgenic mice (Mignone *et al.* 2004). This tool allowed us to study the properties of NSCs enabling the assessment of the undergoing morphological changes in hippocampal NSCs with age. NSCs are identified as radial-glial-like cells located at the SGZ and with a long process crossing the granule cell layer (GCL) that ramifies into the molecular layer (ML, Figure 20 left image), these cells are positive for GFP (on the Nestin-GFP transgenic line), Nestin, GFAP and BLBP markers (Seri *et al.*, 2001; Kempermann *et al.*, 2004; Encinas *et al.*, 2006). We observed that in aged mice (12 mo. and 18 mo.) the majority of Nestin-GFP/GFAP cells remaining in the SGZ and the GCL presented a complex morphology with extensive branching and multipolar extensions similar to the reactive-like morphology of React-NSCs induced by hippocampal seizures (Sierra *et al.*, 2015) (Figure 20A right image) and in clear contrast to the typical morphology of type-1 radial glia-like NSCs (Figure 20A left image).

To further investigate and quantify these differences in cell morphology we analyzed the complexity of NSCs using 3D-sholl analysis. Nestin-GFP/GFAP NSCs within the SGZ and the GCL cells were randomly selected in order to measure morphological complexity of a given cell based on the quantification of the number of intersection between virtual spheres of increasing radio and the 3D-reconstruction of the cell. We employed confocal-imaging z-stack reconstructions of NSCs (Figure 20B). This test was performed at the population level by analyzing cells located in the SGZ+GCL, regardless of their morphology, to avoid any possible bias.

We observed a significant increase in the complexity of NSCs in aged mice (Figure 20C). Cells in 12 and 18 mo. mice presented a higher number of intersections within the 50 μm

nearest to the nucleus than those NSCs from 3 mo. mice, which in contrast presented more intersections in the distal portion of the cell, due to the profuse "broccoli"-like arborisation characteristic of radial NSCs.

We further analyzed morphological parameters such as length, volume or number of branches which can account for the increased morphological complexity associated with aging. NSCs in aged mice, 18 mo., are significantly shorter than in 3 mo., around 30 µm less in the oldest mice (Figure 20D). The volume occupied by the NSCs from 12 and 18 mo. mice was three-fold larger than the 3 month old mice (Figure 20E). The number of primary processes, defined as the cytoplasmic prolongations that emerge directly from the soma increased in aged mice was also significantly higher in the two aged groups (two fold higher in 18 mo. mice) (Figure 20F). In contrast to the typical single radial process that characterizes NSCs in normal conditions of young mice several primary processes emerged from the NSCs of aged mice (Figure 20A, B and F). Frequently, basal ramifications emerging from the hilus-oriented portion of the cell body were found in the NSCs of aged mice. In addition, the number of secondary branches that emerged from the primary process was 3 fold higher in NSCs than older mice (Figure 20G). Finally, we found also a difference in the location the cell body of NSCs which in older mice was located into the GCL and further from the hilus. (Figure 20H).
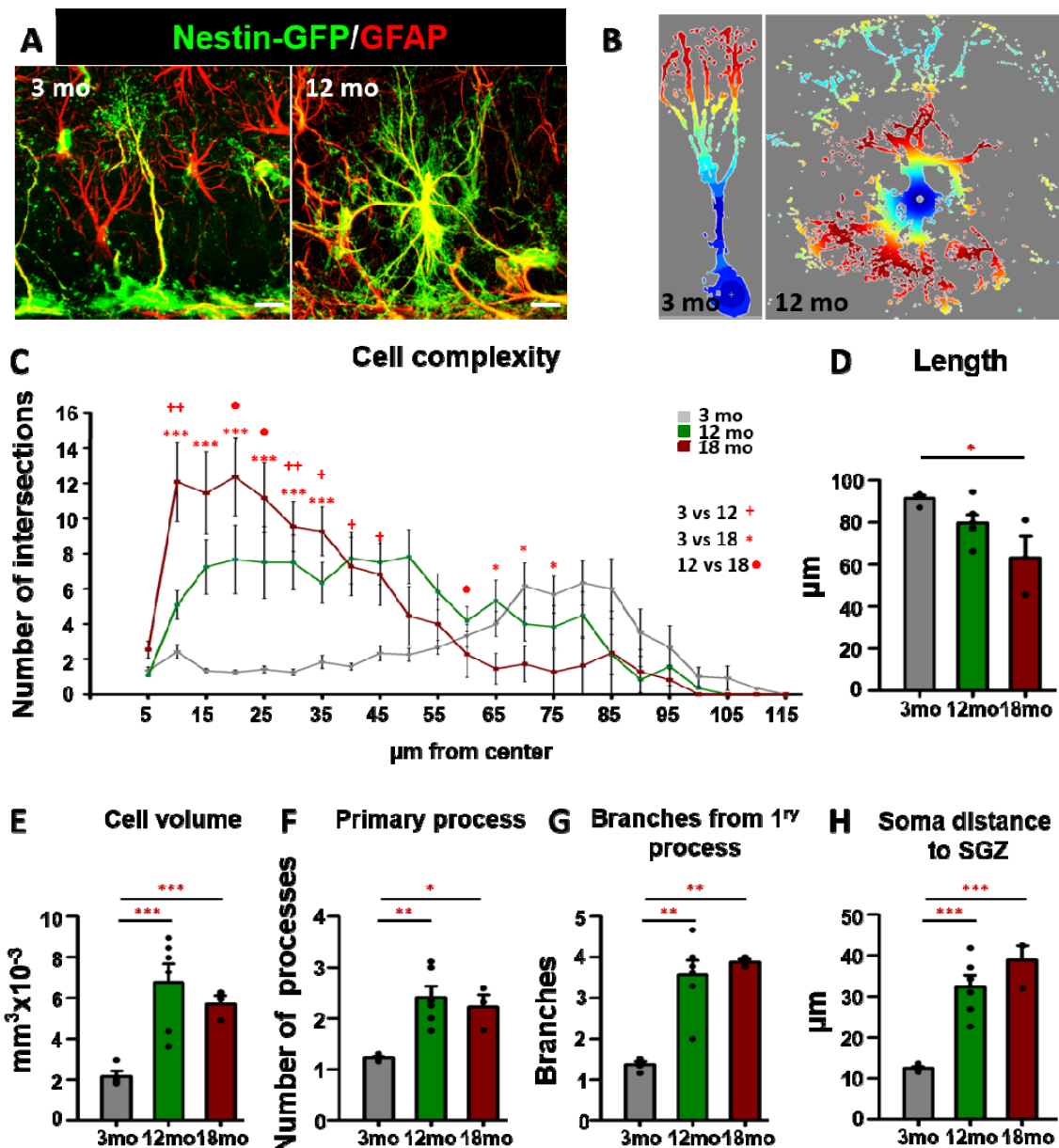
Figure 20. NSCs drastically change their morphological properties with aging.(A) Projections of confocal-microscopy z-stacks (8-μm thick) showing the differences between NSCs in 3 mo. (3mo, left image) and 12 mo. (12mo, right image) Nestin-GFP mice after staining for GFP (green) and GFAP (red). (B) Z-stack projections of Nestin-GFP+/GFAP+ cells prepared for 3D-Sholl analysis. (C) Complexity of NSCs was measured by quantification of the number of intersections between spheres of increasing radios and the 3D reconstruction of the Nestin-GFP+/GFAP+ cells. At least 25 randomly-chosen cells from 3m o. mice and 13 from 12 mo. and 18 mo. mice were analyzed. (D) Quantification of the length (center of soma to furthest tip of NSCs) showing a significant decrease in the 12 and 18 mo. mice. (E) Quantification of the cell volume showing the increase of the volume occupied by NSCs in older mice. (F) Quantification of the number of NSCs primary processes, defined as those emerging from the soma. (G) Number of NSCs secondary processes, defined as those branching from the primary process. (H) Quantification of the distance between the center of cell body and the SGZ. Scale bar is 10 μm in A and B. * $p<0.05$, **$p < 0.01$, ***$p <0.001$ ANOVA repeated measured followed by Bonferroni post-hoc test in C and one way ANOVA after all pairwise multiple comparisons by Holm-Sidak post hoc test (D-H) . Bars show mean ± SEM. Dots show individual data.

These results show that with aging NSCs not only are reduced in number but in addition they switch drastically their morphology to a more complex and reactive-like one. We noticed than rather than a generalized change in complexity in all NSCs, the population of NSCs is compound by a mix of different subpopulations of NSCs.

6.5.1. At least two populations of Nestin-GFP+/GFAP+ cells are found in aged DG.

At least two distinct subpopulations of Nestin-GFP/GFAP positive cells located in the SGZ and the GCL could be found. The first type correspond to the typical radial astrocyte, type-1, or radial NSCs whose morphological and functional properties have been extensively described (Seri *et al.*, 2001; Filippov *et al.*, 2003; Mignone *et al.*, 2004; Encinas *et al.*, 2011) Their soma is located in the SGZ and extend a single radial process that crosses the GCL and arborizes profusely in the molecular layer (ML) (Figure 21A). For the sake of distinction and following previous literature (Gebara *et al.*, 2016) we will refer to these cells as "alpha" (α-cells) from now onwards. The second phenotype corresponds to Nestin-GFP/GFAP positive cells that are located not only in the SGZ but also in the GCL. These cells are more ramified, presenting several prolongations emerging from the soma towards the SGZ and the hilus. All their prolongations are thicker than in their α-cell counterparts. We will refer to these cells as "omega" (Ω-cells). Following these morphological criteria these cells could be classified as "beta" (β-cells described recently by Gebara *et al.*, 2016). However, in clear contrast to β-cells, Ω-cells do not express S-100β (Figure 20A). In order to quantify the absolute cell numbers of the distinct populations of Nestin-GFP/GFAP cells (Figure 21A) and their relative proportions over aging we established the following criteria:

-α-cells: These cells present one single process emerging from the soma, of at least 40 μm in length and that crosses the GCL bifurcating in the ML. Their cell body is located in the SGZ without any or very short (5 μm or less) basal processes.

-β-cells: As previously characterized these cells present a multibranched morphology; the cell body can be located either in the SGZ or the GCL and importantly, they express the S-100β (Gebara *et al.* 2016).

-Ω-cells: These cells present a multibranched morphology with several primary processes emerging from the soma. The cell body can be located either in the GCL and they bear basal processes that extend form the soma towards the SGZ or hilar region. They do not express S-100β.

113

To facilitate the understanding of the distinction among the cell of interest and other that form part of the hippocampal neurogenic niche a scheme summarizing the differences in marker expression is shown (Figure 21B).Detailed quantification of the different Nestin-GFP/GFAP cell-type subpopulations considered along aging showed that the population of α-cells declined sharply, from several thousands to a few hundred cells (Figure 21C) in agreement with previous reports (Encinas *et al.*, 2011; Walter *et al.*, 2011). β-cells followed a similar trend but their absolute numbers were much lower already in the young mice (8 fold) (Figure 21C). In contrast Ω-cells increased the size of its population from 3 to 12 months of age, and then dropped again, although still remained higher at 18 than at 3 months (Figure 21C).

When considering the proportion of each cell type to the total population of Nestin-GFP/GFAP positive cells a fundamental change was observed. While in 3 mo. mice α-cells clearly comprised the majority of the NSCs population, it converted into the smallest subpopulation in the 12 and 18 mo. animals (79.88% in 3 mo., 9.73% in 12 mo., and 8.24% in 18 mo. mice)(Figure 21D). Conversely, Ω-cells represented the smallest relative proportion in the 3 mo. mice, but were the largest subpopulation in the animals of 12 and 18 months of age (4.97% in 3 mo., 74.44% in 12 mo. and 70.62% in 18 mo. mice) (Figure 21D). β-cells represented a more stable relative population over time (Figure 21D). We focused our study on α and Ω-cells, as β-cells have already been well characterized and because they lack cell division and their expression of S-100β suggest that they are a transitional step towards astrocytic differentiation (Gebara *et al.*, 2016). We moved on to analyze the complexity of α and Ω-cells separately by 3D-Sholl analysis in each age point. We found that the complexity of α-cells did not change regardless of the age of the animals, whereas the complexity of the Ω-cell population significantly increased over time (Figure 21E). A readier visualization of this change can be obtained by plotting the overall complexity index (what is it explain) at the different age points (Figure 21F). The complexity of Ω-cells was higher than that of α-cells at 3 mo., and it further increased at 12 mo., being even higher at the 18 mo. age point, whereas it stayed flat for α-cells. When considering the total population of Nestin-GFP/GFAP positive cells (and S-100β negative), the complexity index change parallels that of Ω-cells (-2.26 in 3mo., -1.68 in 12 mo. and -0.68 in 18 mo.) (Figure 21F). This can be attributed to the fact that with age the population of α- cells gets depleted and Ω-cells increase their number and their proportion. We performed Ward's hierarchical clustering to independently classify α-cells and Ω-cells, together and separately at each age point (Figure 21G). The analysis yielded three groups α-cells at 3, 12 and 18 months of age clustered together and with α-cells and Ω-cells at 3 mo., reflecting the fact that α-cells account for most of the NSCs in younger animals, and that

this population does not change its morphology over time. Ω-cells at 3 and 12 mo. clustered with α and Ω-cells at 12 mo., reflecting how their morphology is clearly different from that of α-cells and account for most of the NSCs population at 12 mo. of age. Finally, Ω-cells at 18 mo. clustered together with the sum of Ω-cells and α-cells, reflecting not only that Ω-cells are the most abundant cell type at this age point, but also that their complexity continues to increase with aging (Figure 21G). In addition the distance of the cell soma to the SGZ (Figure 21I) and the cell volume (0.002 in α-cells and 0.003 in Ω -cells) (Figure 21H) is larger for Ω-cells. These results are the same for all the age points analysed.
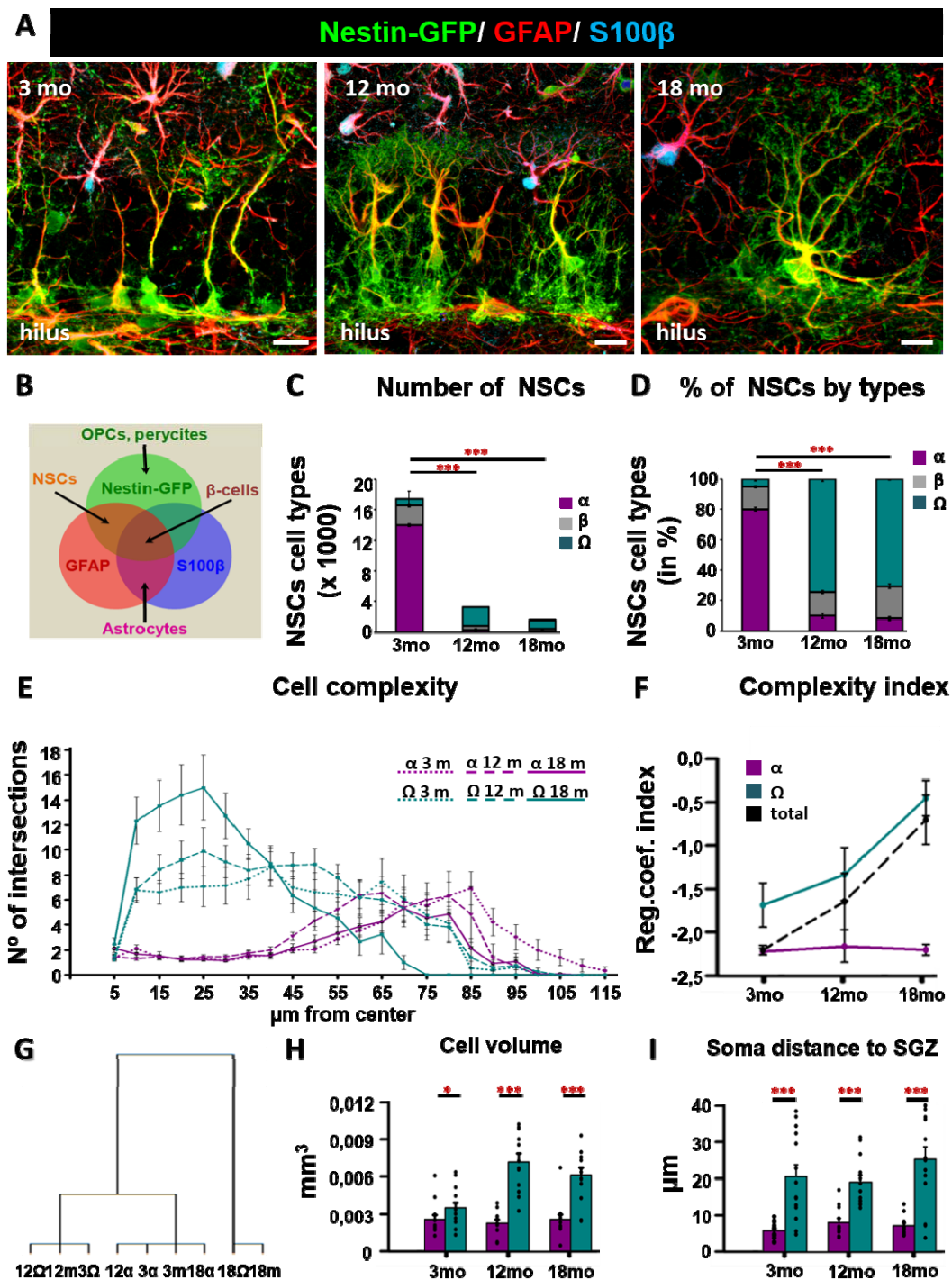
Figure 21. At least two populations of Nestin-GFP[+]/GFAP^{+} cells are found in aged DG. (A) Confocal microscopy images (projection from z-stacks) showing the increase in the complexity of NSCs over aging (3, 12 and 18 mo. mice). (B) Scheme showing the differential pattern of marker expression of cell types in the DG. (C) Quantification of the total number of the different NSCs-like populations (α, β, and Ω) in 3, 12 and 18 mo. mice. (D) Quantification of the different NSCs populations (α, β, and Ω) in percentage showing the significant decrease of α-cells and the concomitant increase in the proportion of Ω-cells. The β subpopulation remains relatively constant. (E) Quantification of the α and Ω-cells complexity by 3D-Sholl analysis in each time point showing a significant difference between α and Ω-cells regardless of the age. (F) Quantification of the complexity index showing a significant increase of the complexity in Ω-cells and in the total population of NSCs with age. (G) Ward's hierarchical clustering based on 3D-Sholl analysis to independently classify α and Ω-cells in each age point. (H) Quantification of the cell volume by cell type and age point showing a significant increase between α and Ω-cells and with age. (I) Quantification of the distance of the body cell to the SGZ showing the increase of the distance in Ω-cells. Scale bar is 20 µm in (A). (E)* $p<0.05$, **$p < 0.01$, ***$p < 0.001$ ANOVA repeated measured followed by Bonferroni post-hoc test. (C,D, F H,I) after all pairwise multiple comparisons by Holm-Sidak post hoc test. (G) Hierarchical clustering was performed using Ward's method and squared Euclidean distances as linkage metric. Bars show mean ± SEM. Dots show individual data.

These results show that there are two populations of Nestin-GFP/GFAP positive, S-100β negative cell in the aging DG, distinct from β-cells (Figure 22A). While the extensively described α-cells decline sharply in numbers the morphologically distinct population of Ω-cells increase their numbers with aging and comprise by large the most abundant population in aged mice. In addition, the Ω-cells population increases its morphological complexity overtime.

We then moved forward to measure several morphological parameters that could account for the observed changes in cell complexity. Ω-cells bear more processes emerging directly form the soma (2 fold higher in Ω-cells than in α-cells) (Figure 22B), and these primary processes bifurcate with higher frequency (2 fold higher in Ω-cells than in α-cells in all time point) (Figure 22C). The length of Ω -cells is also significantly shorter than that of α-cells (between 10 and 25µm shorter comparing to α-cells) (Figure 22D).
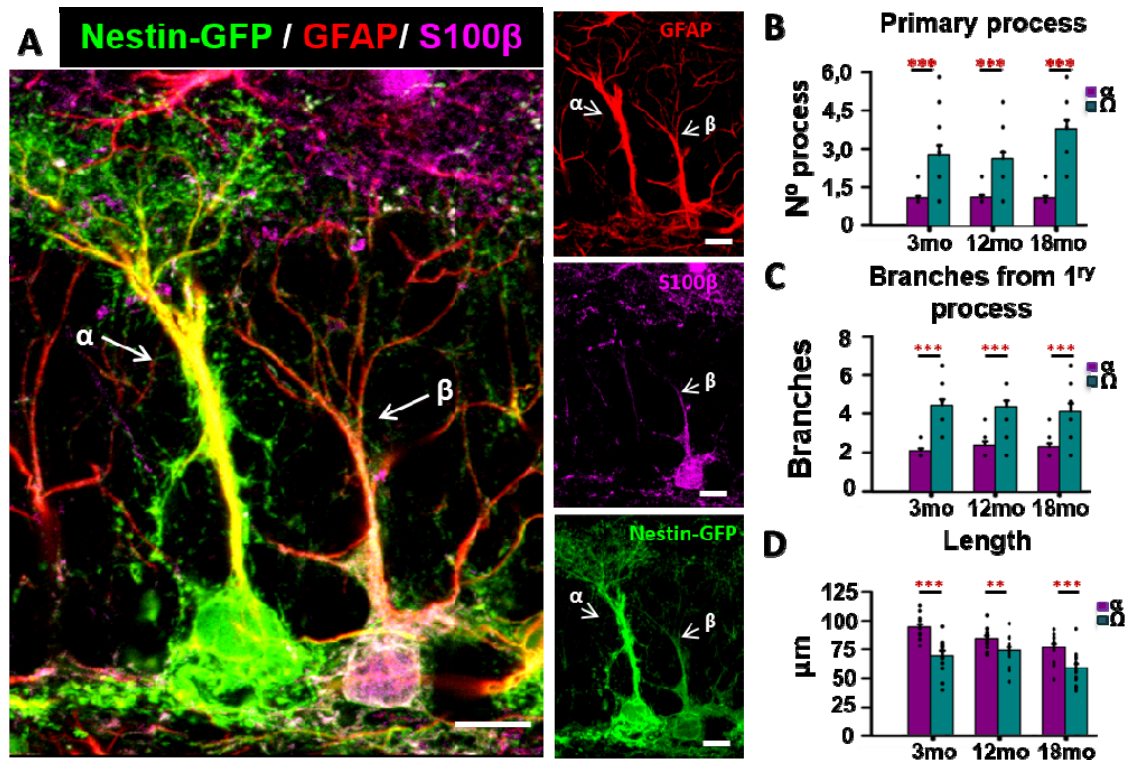
Figure 22. At least two populations of Nestin-GFP[+]/GFAP^{+} cells are found in aged DG. (A) Representative confocal microscopy image of a Nestin-GFP[+]/GFAP[+]/S100β[-] α-cells and a Nestin-GFP[+]/GFAP[+]/S100β[+] β-cells. (B) Quantification of the number of primary processes, in α-cells and a Ω-cells, defined as those emerging from the soma, in 3, 12 and 18 mo. mice, showing a significant increase in Ω-cells regardless the age. (C) Quantification of the number of secondary processes, defined as those branching from the primary processes, showing a significant increase in a Ω-NSCs in all timepoint. (D) Quantification of the length (center of soma to furthest tip of NSCs) showing a significant decrease in Ω-cells in all ages. **p < 0.01, ***p < 0.001 one way ANOVA after all pairwise multiple comparisons by Holm-Sidak post hoc test. Bars show mean ± SEM. Dots show individual data.

These results suggest that α-cells and Ω-cells are not two populations generated independently, but rather than α-cells could transform into Ω-cells with aging, and that the development of a reactive-like complex morphology is a progressive time-dependent process.

6.5.2 Ω-cells divide with lower probability.

To analyze the mitotic potential of NSCs we resorted to inject BrdU to 3, 12 and 18 mo. mice. The animals received 4 injection of BrdU 2 hour apart (Figure 23A) and were sacrificed 24 hours after the first injection. We measured the proportion of dividing cells of the total NSCs population as these NSCs which incorporated BrdU. The proportion of BrdU positive cells, remained constant between 3 mo. and 12 mo. between 3-4% of the total, confirming the results reported before in non-transgenic animals for the most part. The proportion of BrdU[+] NSCs, was slightly but significantly increased in 18 mo. animals (Figure 23B), but when put in

the context of actual numbers the difference is minimal as the proportion of dividing NSCs does not exceed the 5% of the total population in any case.

Next, we studied the capacity of NSCs to reenter in the cell cycle. For this purpose we used the cell cycle marker KI67. By determining the fraction of Ki67$^+$BrdU$^+$cells (Figure 23A) among the total dividing cells, (BrdU$^+$ cells) it was possible to obtain the proportion of NSCs that were reentering in the cell cycle (Figure 23C). There was no difference in any of the agepoints, the proportion of cell cycle reentering in NSCs remained constant over time, being the 4-6% of the dividing population. These results evidenced that the population of NSCs is mostly quiescent and only a small proportion of NSCs are able to divide and reenter in the cell cycle.

We next sought to investigate whether the two morphologically distinctive populations had also different functional properties (Figure 23D). First, we found that the capacity to incorporate BrdU is almost restricted to type α-cells which account for most of the dividing NSCs at any analyzed age point (the proportion of α-cells BrdU+ is 95.40% in 3 mo., 87.22% in 12 mo. and 83.33%in 18 mo. mice). However, Ω-cells retained some mitotic potential and incorporated BrdU although with very low frequency (Figure 23E). At all the different age points α-cells accounted for the vast majority of Nestin-GFP/GFAP cells that incorporated BrdU while the fraction of Ω-cells was much lower (Figure 23E). In both cases the majority of the cells comprising each population remained quiescent, but interestingly, α-cells were able to increase their activation over time as shown by the significantly higher proportion of BrdU labeled cells among the α-cells population in aged mice (from 0.66 in 3 mo., to 14.04% in 18 mo. mice). In contrast, the proportion of activated Ω-cells significantly decreased in aged mice (from 3.54 in 3 mo., 0.05 in 12 mo. to 0.07% in 18 mo.). While the remaining α-cells in the aged DG increase their activation rate, Ω-cells become even more quiescent with aging (Figure 23F). To further analyze α and Ω-cell mitotic activity, we next analyzed the capacity of NSCs to reenter in the cell cycle by measuring the proportion of BrdU-positive cells that expressed the mitotic marker Ki67 among the total number of BrdU positive cells of each type. Similarly to the results obtained for cell activation we found that Ω-cells re-entered the cell cycle with significantly lower probability than α-cells, regardless of the age point (86.95% α-cells and 13.05% Ω-cells in 3 mo., 75% α-cells and 25% Ω-cell in 12 mo. and 66.66% α-cells and 33.33% Ω-cells in 18 mo. mice) (Figure 23G). These results combined strongly suggest that Ω-cells have markedly reduced mitotic potential compared to α-cells and that not only they are activated with lower rate but also that the probability of undergoing another round of cell division within the next 24 hours after activation is substantially decremented.
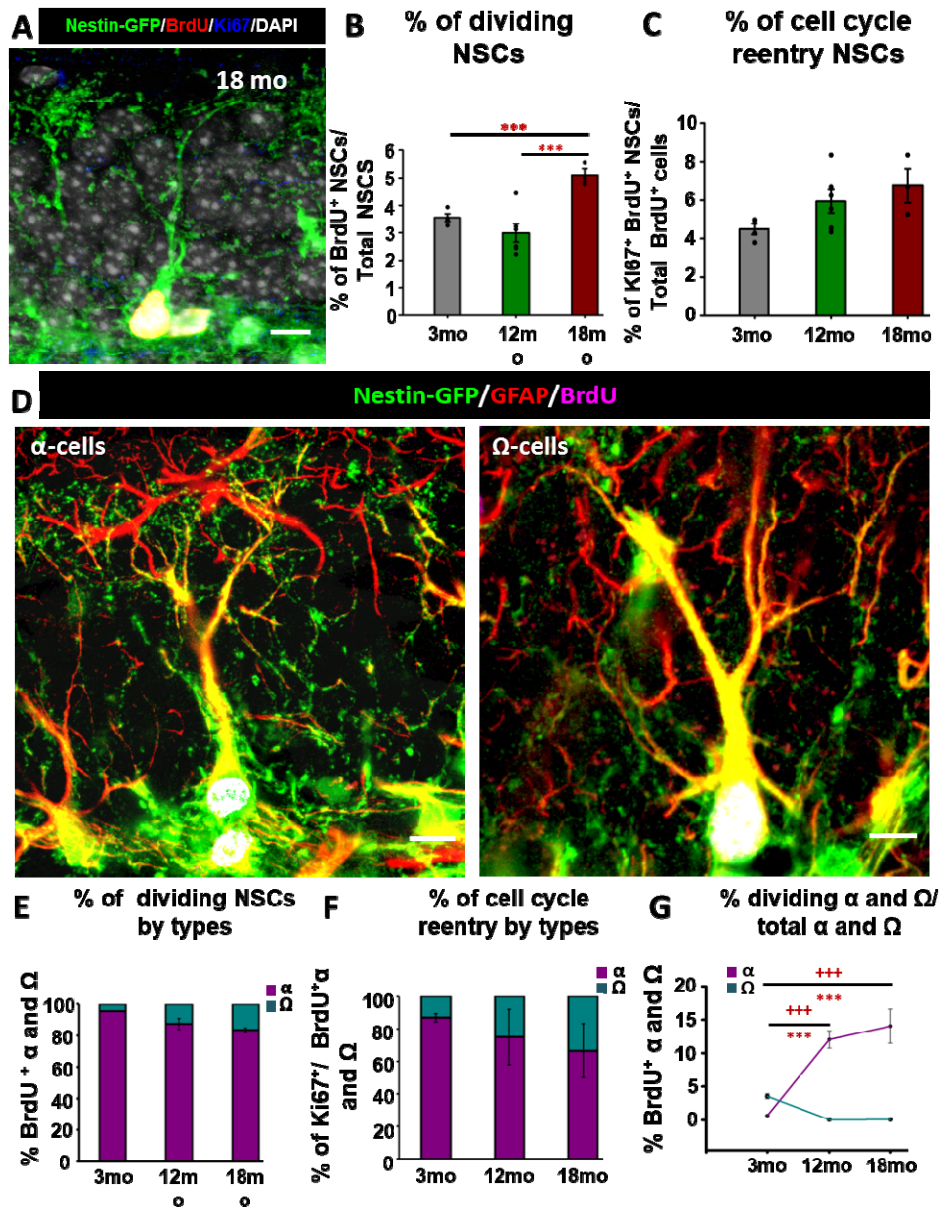
Figure 23.The proportion of dividing NSCs remains constant over time but Ω-cells divide with lower probability. (A) Confocal images of NSCs in 3, 12 and 18 mo. mice showing colabeling for BrdU and Ki67 in the DG of 18 mo. mice. (B) Quantification of the proportion of activated NSCs (BrdU[+] NSCs) among the total numbre of NSCs. (C) Quantification of the proportion of NSCs BrdU[+] and Ki67^{+} cells relative to total number of BrdU^{+} cells at 3, 12 and 18 mo., measured by the co-expression of Nestin-GFP, BrdU and the cell cycle marker Ki67 among the total number of BrdU^{+} cells.(D) Representative confocal microscopy images of a dividing Nestin-GFP[+]/GFAP[+] α-NSC after staining for GFP, BrdU, and GFAP at 3 mo. and 18 mo. (E) Quantification of cell division in the different subpopulation of NSCs. The capacity to incorporate BrdU is mostly restricted to the α-cells. (F) Quantification of the proliferative capacity of α and Ω-cells showing a significant increase in the proliferative capacity of α-cells with age. (G) Quantification of the mitotic activity of NSCs (Ki67 and BrdU positive NSCs) Ω-cells divide with much lower probability. Scale bar is 10 µm in A and D ***$p < 0.001$ after all pairwise multiple comparisons by One-way ANOVA Holm-Sidak post hoc test. Bars show mean ± SEM. Dots show individual data.

We next wondered whether Ω-cells retained at least plasticity to respond to pro-activation stimulus and adapt their rate of mitosis to neuronal activity as α-cells do (Sierra *et al.*, 2015).

6.5.3. Ω-cells remain quiescent even in pro-activation conditions

We subjected mice of 12 months of age to intrahippocampal injection of KA in a dose that triggers neuronal hyperactivation (without inducing seizures or cell death) and a subsequent increase in the number of NSCs that enter the cell cycle. To be even surer that this procedure did not trigger alterations in the niche such as the induction of React-NSCs we analyzed actually the contralateral hemisphere (Figure 24A). KA was injected in the right hippocampus and after two days the animals received BrdU (4 injections 2 hours apart). Twenty four after the last injection the animals were sacrificed and the left hemisphere was analyzed (Figure 24B and C). We chose the 12 month age point to have a sufficient number of Ω and α-cells to analyze and to avoid anaesthesia and surgery-related problems in older mice. The total number of NSCs was not changed between the control injected with saline and the experimental (12 mo. KA) group (Figure 24D). Further, analyzing separately the total number by subtypes, in both conditions the same number of α and Ω-cells was found (Figure 24H). We confirmed that intrahippocampal KA significantly activated more NSCs (almost 2 fold in KA) (Figure 24E), which was translated into a higher proportion of BrdU-incorporating NSCs (3.54 and 7.16± 0.26 in KA) (Figure 24F). α–cells accounted for the vast majority of dividing cells in both situations, but in KA the percentage of dividing α-cells was even higher (Figure 24G). While the total number of activated α–cells increased significantly in the KA-injected mice, the number of Ω-cell BrdU incorporating remained unchanged (Figure 24I). This change was also observed when considering the proportion of α and Ω-NSCs among the total BrdU positive cells (2.59% in saline and 4.36 in KA for dividing α-cells and 0.09 in saline vs 0.04 in KA in Ω-cells) (Figure 24J).
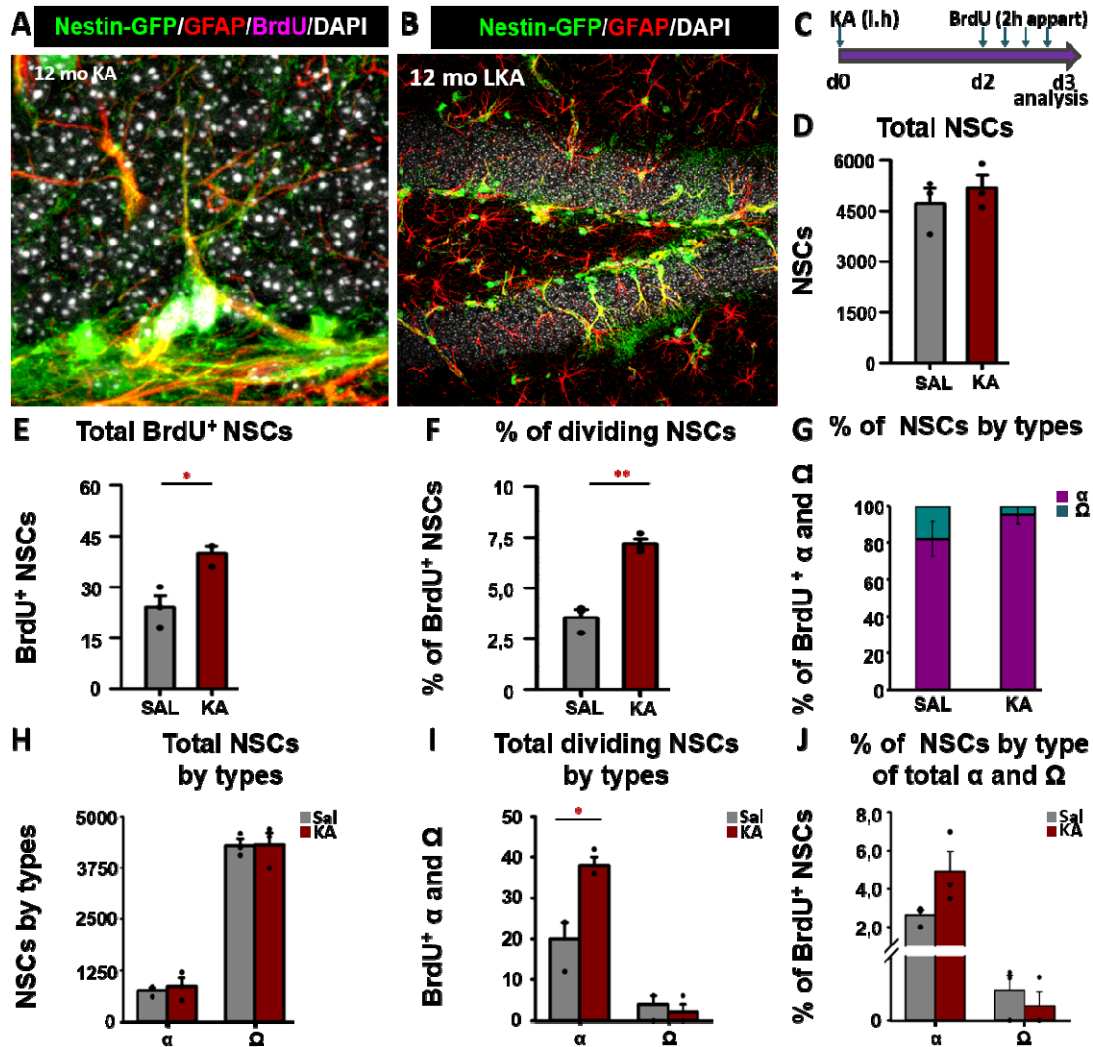
Figure 24. Ω-cells are more quiescent even in pro-activation conditions. (A) Confocal microscopy projections of z-stacks showing a dividing α-cells immunostaining for GFP, GFAP and BrdU. (B) Confocal microscopy projections of z-stacks (8-μm thick) showing the DG of a 12 mo. injected animal immunostaining for GFP, GFAP. (C) Experimental paradigm of Sal/KA and BrdU administration to 12 mo. animals. Mice were given 4 injections of BrdU, 2h part, starting 48h after the intrahippocampal injection of saline or KA and were sacrificed 24h after the first injection of BrdU. (D) Quantification of the total number of NSCs in both showing that KA does not alter the total number of NSCs. (E) Quantification of the total number of dividing NSCs showing a significant increase in the KA-injected mice .(F) Quantification of the proportion of dividing NSCs (BrdU+NSCs) showing the significant increase in the NSCs dividing in KA-injected mice. (G) Quantification of the total number of dividing NSCs by subtypes showing that only α-cells increase their proliferative capacity in the KA-injected mice. (H) Quantification of the total number of NSCs by subtypes showing that KA does not alter the total number of NSCs subtypes. (I) Quantification of the subpopulation of dividing NSCs showing that Ω-cells are the less proliferative subpopulation even in pro-activation (KA) conditions. (J) Quantification of the proliferative capacity (BrdU incorporation) of α and Ω- cells of the total α and Ω-cells showing that even in pro-activation condition Ω-cells are more quiescent. Scale bar is 10 μm in B. * p<0.05, **p < 0.01 by Student's t test. Bars show mean ± SEM. Dots show individual data.

These results confirm that Ω-cells are more quiescent than α-cells and are unable to increase their rate of mitosis even in pro-activation condition such as KA-induced neuronal hyperactivation and that thus they are a different population not only morphologically but also functionally.

Next we wanted to confirm whether-,_as suggested by the previous results, α–cells trasform into Ω-cells overtime, rather than α–cells and Ω-cells comprising two different populations established early on.

6.5.4. Chronic inflammation converts α-cells into Ω.

We hypothesized that chronic neuroinflammation, a hallmark of the aged brain (Lynch, 2010) might be playing a role in the accumulation of Ω-cells as neuroinflamation is anti-neurogenic and reduces the activation of NSCs (Ekdahl *et al.*, 2003; Sierra *et al.*, 2015) (Figure 25A). To test this hypothesis we injected 3 mo. mice intraperitoneally with a low dose of Interferon-α (IFN-α, 4×10^5 IU/Kg) during 20 days in order to mimic the chronic inflammation of the aged brain or "inflammaging"(Franceschi *et al.*, 2006). 24 hour after the last injection of IFN-α, the mice received 4 injections of BrdU (2 hours apart) and were analyzed 24 hour after the last one (Figure 25B) . We chose the 3 mo. time point because at this age the α-cell population is largely predominant. The total number of NSCs was not changed by the IFN-α compared to the control (Figure 25C). The proportion of α-cells was significantly reduced in animals injected with IFN-α (around 25% fewer in IFN-α) whereas the proportion of Ω-cells was significantly increased (around 20% more in IFN-α). β-cells represented a more stable relative population (Figure 25D). We analyzed whether IFN-α promoted functional changes by analyzing BrdU incorporation as a measure of mitotic activity. IFN-α reduced the overall activation of NSCs both in absolute numbers (Figure 25E) and in relative proportion (25% reduced in IFN-α) (Figure 25F).

We next focused on α and Ω-cells, using the criteria defined above, and found that the total number of α-cells was significantly diminished in the IFN-α mice whereas the number of Ω-cells was significantly increased (3 fold) (Figure 25G). Interestingly, the proportion of activated α-cells (among the total of α-cells) did not change but that the proportion of dividing Ω-cells (among the total of Ω-cells) was significantly decremented, thus accounting for the overall reduction of Nestin-GFP/GFAP cell activation the proportion of activated Ω-cells are less proliferative than the α-cells in IFN-α mice (Figure 25H).

We then analyzed overall Nestin-GFP/GFAP cell complexity by 3D-Sholl analysis in a random manner, i.e. without making any selection by cell types. Complexity was found to be significantly higher in IFN-α injected mice than in the control (saline-injected) mice (Figure 25I).
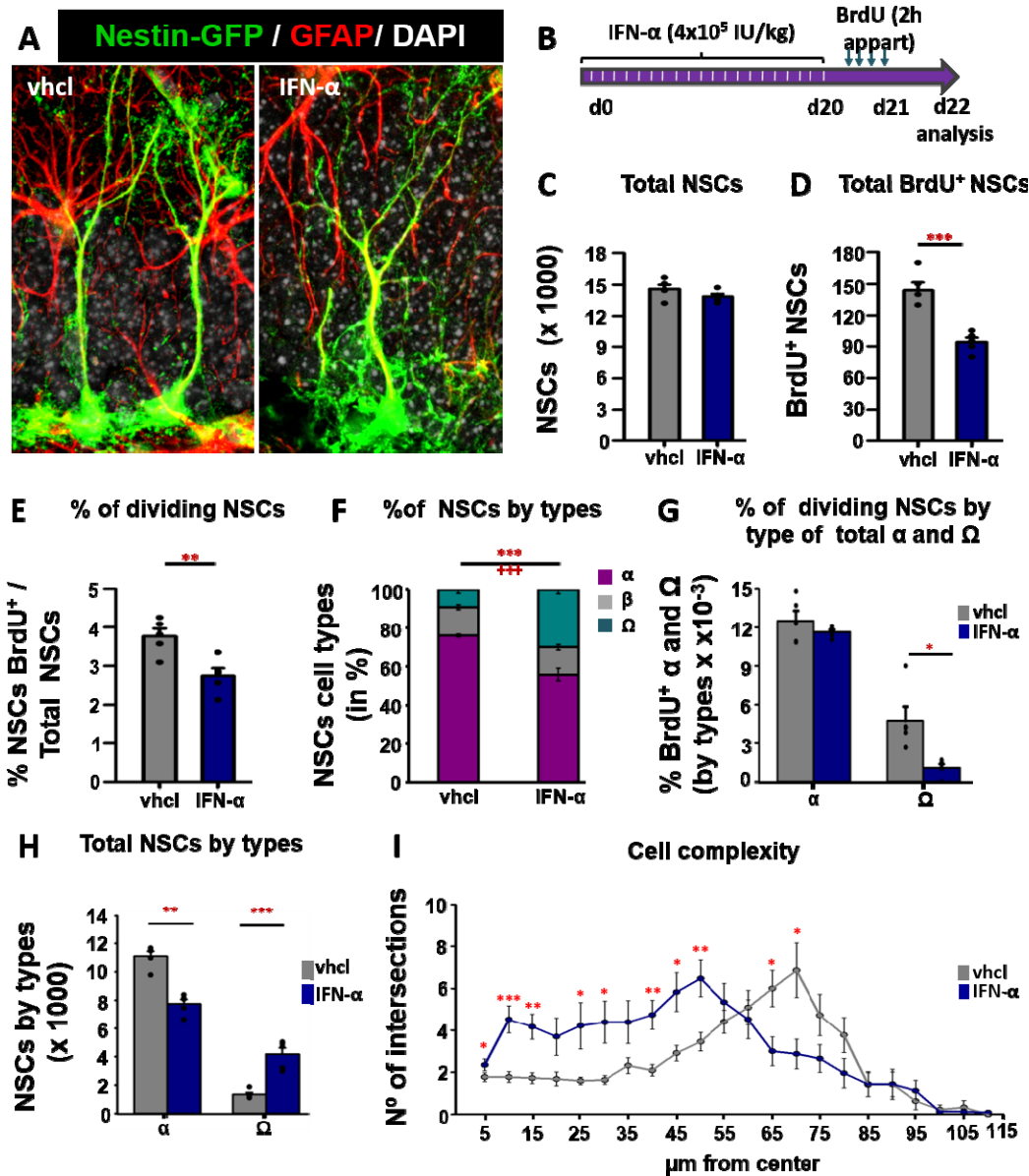
Figure 25. Chronic inflammation converts α-cells into Ω. Confocal microscopy projections of z-stacks showing Nestin-GFP/GFAP positive NSCs and the increase in the complexity of IFN-α injected NSCs. (B) Experimental paradigm of Sal/IFN-α and BrdU administration. (C) Quantification of the total number of NSCs, the number of NSCs is not affected by the IFN-α. (D) Quantification of the dividing NSCs showing the significant decrease in the absolute number of dividing NSCs in IFN-α mice. (E) Quantification of the proportion of dividing NSCs showing the decrease in the treatment mice. (F) Quantification of the different subtypes of NSCs showing the significant decrease of α-cells and the increase of Ω-cells, the β-cells population remains constant. (G) Quantification of the dividing NSCs by subtypes, the IFN-α mice show less proliferative capacity in Ω-cells. (H) Quantification of the total number of α and Ω-cells showing the decrease of the α-cells and the increase of the Ω-cells in IFN-α injected mice. (I) Quantification of the number of intersections between spheres of different radios and the 3-D reconstruction of the Nestin-GFP/GFAP NSCs showing a significant increase in the complexity in IFN-α injected mice. Scale bar is 10 μm in A. * p<0.05, **p < 0.01, ***p < 0.001. ANOVA repeted measured followed by Bonferroni post-hoc test in I. **p < 0.01, ***p < 0.001 by Student's t test. Bars show mean ± SEM. Dots show individual data.

As we showed in Fig. 25, IFN-α affects directly the complexity of NSCs (Figure 26A) sowe moved nextto analyze morphological parameters that could account for the change in complexity. First, the length of NSCs did not change between both conditions, although there is a tendency to decrease the length in IFN-α treated mice (Figure 26B). In addition, NSCs from the IFN-α mice had increased cell volume (from 0.006 mm^3 in saline to 0.008 mm^3 IFN-α (Figure 26C). Furthermore, the number of primary processes (45% more in IFN-α (Figure 26D) and the number of branches emerging from the primary processes was significantly increased in IFN-treated mice (40% more in IFN-α) (Figure 26E); and their soma was localized into the GCL further from the SGZ (Figure 26F) repeating the same pattern observed in aged mice (Figure 21).

Thus, IFN-α is not only triggering the morphological and anatomical changes in α-cells but is also inducing quiescence, a main characteristic of Ω-cells (Figure 23). These results support our hypothesis that the suggestion extracted from the results described that Ω-cells are derived from those α-cells that do not get depleted over time and remain in the DG. In addition they suggest that chronic inflammation could be playing a role in the conversion of α-cells into Ω-cells (using both the morphological and the functional criteria) and therefore in the reduction of neurogenesis associated with aging.
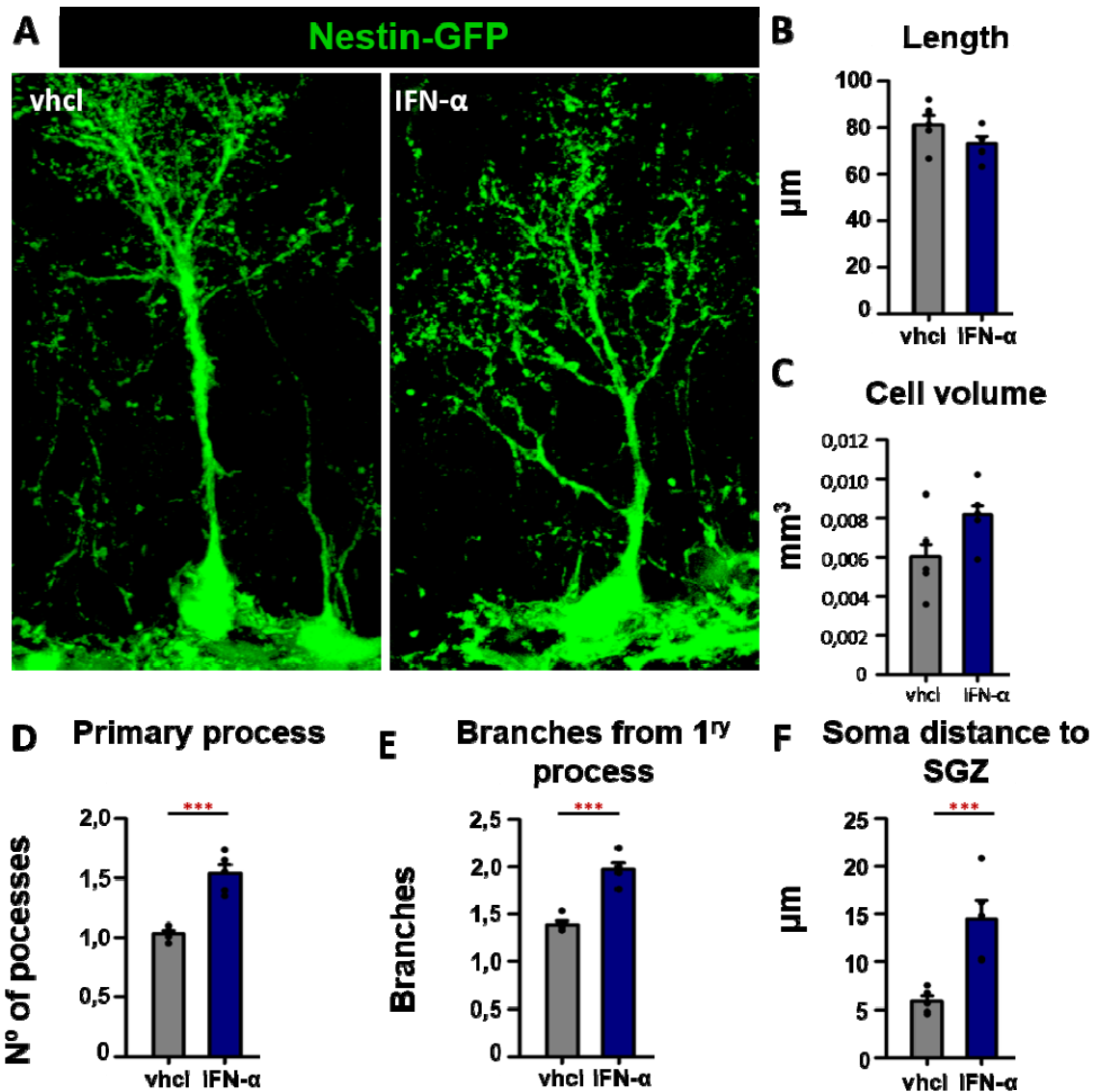
Figure 26. Chronic inflammation increase the complexity of NSCs. (A) Confocal microscopy projections of z-stacks showing Nestin-GFP positive NSCs and the increase in the complexity of IFN-α injected NSCs. (B) Quantification of the length (center of soma to furthest tip of NSCs showing a significant decrease in the IFN-α. (C) Quantification of the cell volume showing the increase of the volume occupied by NSCs in treated mice. (D) Quantification of the number of NSCs primary processes, defined as those emerging from the soma. (E) Number of NSCs secondary processes, defined as those branching from the primary process. (F) Quantification of the distance between the center of cell body and the SGZ. Scale bar is 10 μm in A. ***p < 0.001 by Student's t test. Bars show mean ± SEM. Dots show individual data.

So far we have described that aging modify the behaviour of NSCs. Aged NSCs not only alter their phenotype but also they became functionally impaired. We associate these changes to the increased senescence that hippocampal niche suffer during the aging process. In order to analyzed the effect of the lack of division in NSCs we resorted to use a transgenic mouse model in which the lack of cyclin D2 abolishes the proliferation of precursors.

Taken together these results suggest that α-cells transform into Ω-cells progressivelly, becoming more quiescent, even senescent, and that inflammation might promote this transformation. We hypotehsize that those α-cells that remain unactivated or unused over time in the DG transform into Ω-cells, becoming more and more quiescent. Thus increased quiescence itself would promote the senescent-like Ω-cells phenotype. We are currently looking for a model in which to test this hypothesis.

6. 6 Lack of Cell Divission associates with Omega-Phenotype

6.6.1 NSC population gets depleted in Ciclyne D2 cko mice.

Cyclins D are cell cycle regulatory proteins that control specific cyclin-dependent kinases. Three cyclins D have been described, D1, D2, and D3. In most of the cells, there is an expression of more than one cyclin D. It was described that cyclin D2 completely abolishes proliferation of neuronal precursors in the adult brain, thus indicating the role of cyclin D2 in adult neurogenesis. It was describes that mice with cyclin D2 gene disrupted through homologous recombination (D2 KO; Sicinski *et al.*, 1996) were virtually deprived of BrdU incorporation in the hippocampus and OB. First, we analyzed the percentage of each subtype of NSCs, α-cells, β-cells or Ω-cells and found that in contrast with wild type mice, where α-cells are the main subtype, the NSCs population cD2 KO mice was comprised mostly by Ω-NSC. In both cases the percentage of β-cells remained constant (Figure 27B). We next moved to confirm whether this impaired capacity to divide in cD2 KO mice could affect equally the mitotic capacity of the different subtypes of NSCs. In both animals, wild type and cD2 KO, the only cells that proliferated (measured by Ki67 staining) were the α-cells (Figure 27C and D).
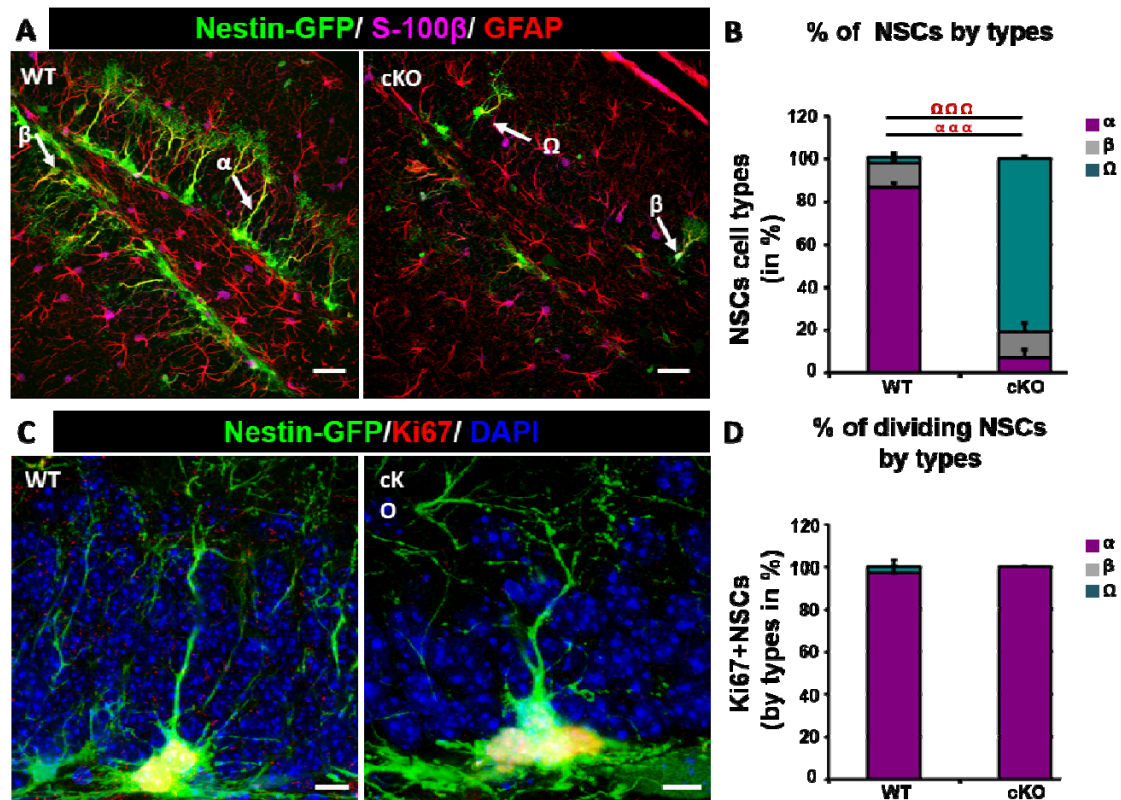
Figure 27. NSCs population gets depleted in Ciclyne D2 cko mice.(A) Confocal microscopy images (projection from z-stacks) showing the depletion of NSCs population in cKO mice, the remaining cells present an increase in the complexity of NSCs. (B) Quantification of the proportion of the different subtypes of NSCs showing a significant decrease of α-cells and the increase of Ω-cells, the β-cells population remains constant (C) Quantification of the total number of dividing NSCs by subtypes showing that only α-cells are able to divide in both conditions. ***p < 0.001 by Student's t test. Bars show mean ± SEM. Dots show individual data

6.6.2 The complexity of remaining NSCs is increased in cD2 KO mice

We describe that Ω-cells were the predominant subtype in cD2 KO mice and then we focused our analysis on the morphology of the remaining NSCs (Figure 28A). The first morphological feature that we measured was the length of NSCs and we observed that NSCs from cD2 KO mice were significantly shorter than NSCs from wild type mice (around 20 μm shorter in cKO mice (Figure 28B). Next, we moved on to analyze the complexity of NSCs. For this purpose we performed a 3D-Sholl analysis on Nestin-GFP/GFAP positive but S-100β negative NSCs was measured, in a random manner, without make any selection by subtype. In cD2 KO mice the complexity was higher than in wild type mice (Figure 28C).
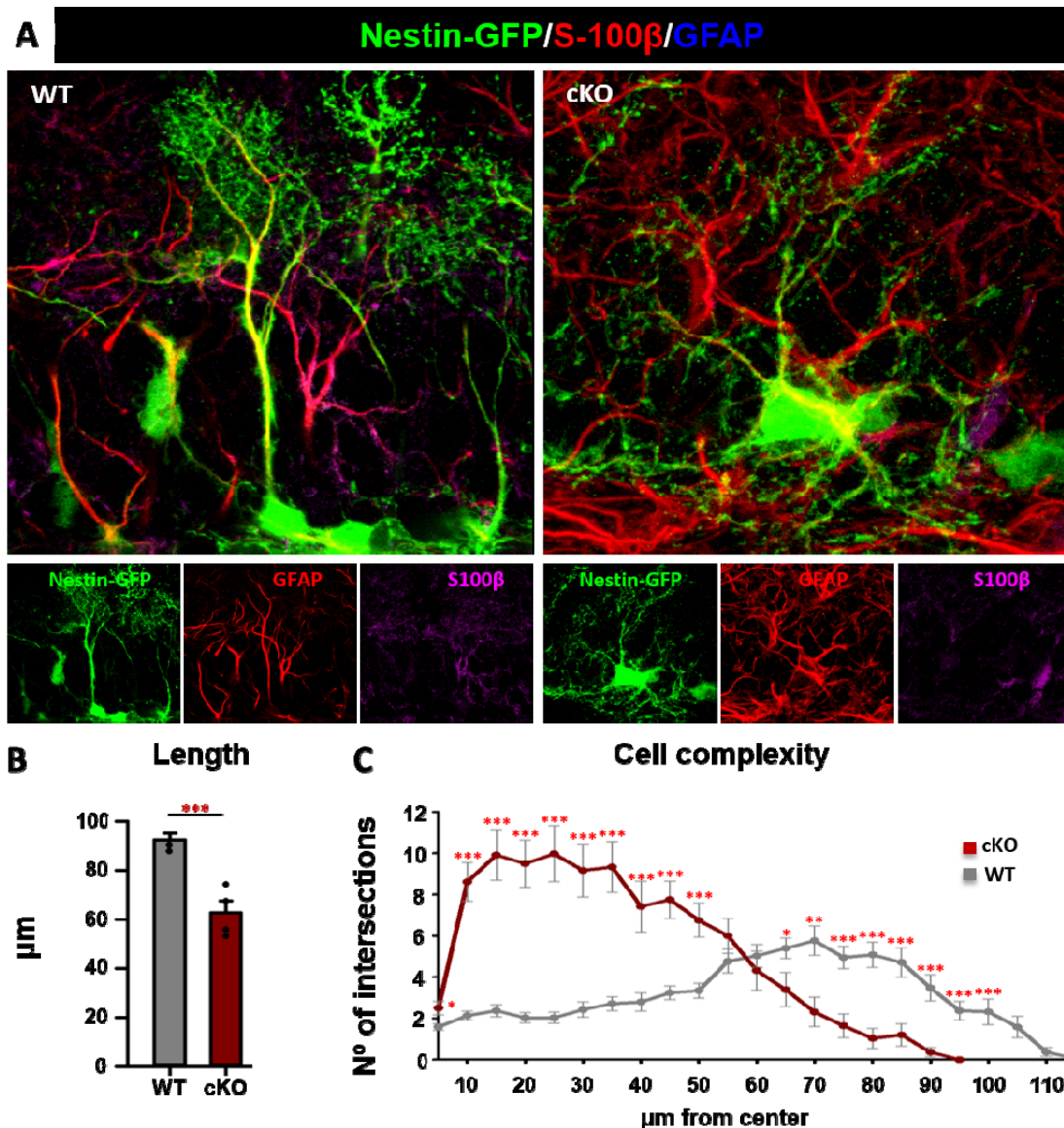
Figure 28. The complexity of remaining NSCs is increased in cKO mice (A) Confocal microscopy projections of z-stacks showing a Nestin-GFP[+] /GAFP[+]/ S100β[-] NSCs and the increase in the complexity of cKO NSCs. (B) Quantification of the length (center of soma to furthest tip) of NSCs showing a significant decrease in the cKO mice. (C) Quantification of the number of intersections between spheres of different radios and the 3-D reconstruction of the Nestin-GFP/GFAP NSCs showing a significant increase in the complexity in cKO mice. Scale bar is 10 µm in A. * $p<0.05$, **$p < 0.01$, ***$p < 0.001$. ANOVA repeated measured followed by Bonferroni post-hoc test(C). ***$p < 0.001$ by Student's t test. Bars show mean ± SEM. Dots show individual data.

Thus, cD2KO mice not only had increased quiescence in NSCs, but alsopresented morphological changes in NSCs that closely resemble those associated with aging. These results are preliminary but they support our hypothesis that quiescence promotes or derives in senescence with an altered (omega, reactive-like) phenotype.

6.7 AHN Depends on the Activation of Neural Stem Cells

6.7.1 The rate of reentry in the cell cycle is maintained with age in NSCs and in neuronal precursors.

The number of dividing cells, measured by the incorporation of BrdU, in the granule cell layer (GCL) and subgranular zone (SGZ) decline with age in all studied time points (3,12 and 18 mo.) (Figure 29A). The remaining proliferative cells in 18 mo. mice was 95% fewer than in 3 mo. (Figure 28B). To further analyze the mitotic activity in aging, we next focused our study in the capacity of the cells to reenter in the cell cycle, by measuring the proportion of BrdU positive cells that expressed the mitotic marker Ki67 (Figure 29C) of the total dividing cells. Interestingly the capacity to reenter in the cell cycle, in the same fashion as activation, remains constant over time. This means that once a cell divides it is very likely that it divides again in the next 24 hours, independently of the age of the mouse (Figure 29C).

We also analyzed proliferation in DCX-positive cells, or neuroblasts (Figure 29D). The proportion of proliferating neuroblasts, (BrdU-positive) of the total population of neuroblasts, was 3-4-% in 3 mo. animals but in 12 mo. old and 18 mo. mice was mostly absent (Figure 29E). The results were similar when we analyzed the proportion of dividing neuroblasts among the total of proliferative cells (Figure 29C).
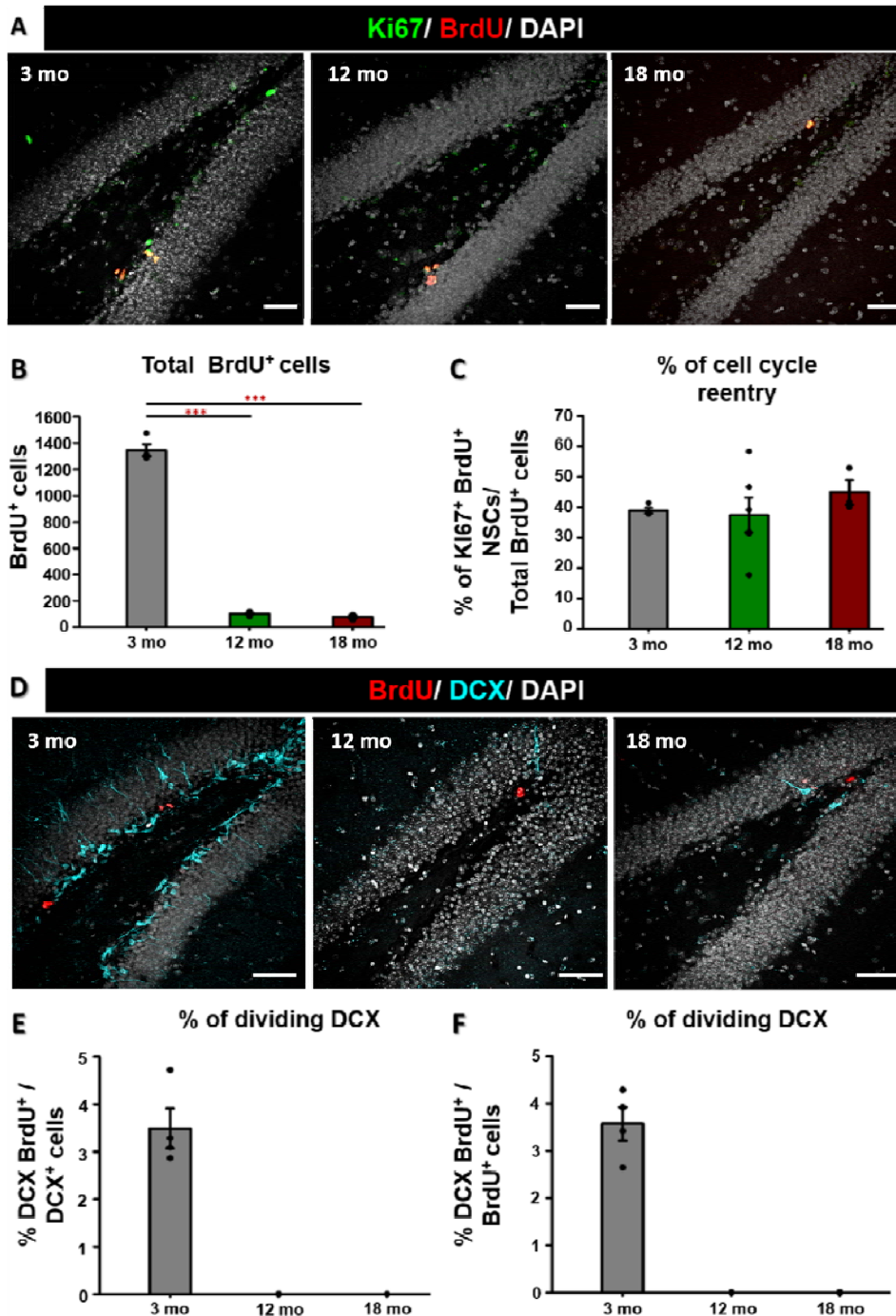
Figure 29. The rate of reentry in the cell cycle is maintained with age although neurogenesis declines over time measured as cells coexpressing BrdU and DCX–. Confocal images showing the capacity to reenter in the cell cycle at 3 (left), 12 (middle) and 18 (right) mo. measured by the incorporation of BrdU (B) Quantification of the proliferative capacity measured by the incorporation of BrdU, in 3, 12 and mo. mice, the total number of BrdU cells decreases with aging. (C) Quantification of the proportion of cells re-entering in the cell cycle at 3, 12 and 18 mo., measured by the co-expression of BrdU and the cell cycle marker Ki67 among the total number of BrdU^{+} cells. (D) Confocal microscopy images showing DCX[+] neuroblast at 3(left), 12(middle) and 18 (right) mo.(E) Quantification of BrdU[+] neuroblast that express doublecortin among the absolute number of DCX^{+} cells at 3, 12 and 18 moth old mice. (F) Quantification of BrdU[+] neuroblast that express DCX among the absolute number of BrdU^{+} cells at 3, 12 and 18 mo. mice . ***$p < 0.001$. One way ANOVA Holm Sidak post hoc test. Bars show mean ± SEM. Scale bar is 20 μm in A and D. Dots show individual data.

These result point at a reduction of the proliferative capacity also of neuroblasts (NBs) with age. Nevertheless, because of the low proportion of dividing NBs even in young animals, this result cannot be functionally relevant. We finally analyzed the astrocytic population during aging, as the NSCs ultimate differentiation should translate into an increased number of this cell type over time.

6.8 The Numbers of Astrocytes Increases Significantly in the Dentate Gyrus of Aged Mice

Astrocytes are by far the most numerous glial cells in the hippocampus. Several studies have described that during aging there is an age-related increases in astrocytes (Pilegaard and Ladefoged, 1996; Long *et al.*, 1998; Mouton *et al.*, 2002). Recent mathematical models demonstrated that at least 50% of NSCs depletion could be attributed to direct transformation into astrocytes (Ziebell *et al.*, 2018).

To analyze whether aging could affect hippocampal astrocytes (Figure 30A) we quantified the total number of $GFAP^+$ $S\text{-}100\beta^+$ astrocytes in the DG. We observed that in 18 mo. mice the total number of astrocytes was significantly higher than in younger animals (around 30% more in oldest mice) (Figure 30B). Next, we analyzed the number of astrocytes by regions. First we quantified the number of astrocytes in GCL, although there were not significant changes there was a tendency to increase in 18 mo. mice (Figure 30C). However, the number of astrocytes in the hilus was increased 40% in older animals (18 mo.) comparing to younger ones (Figure 30D). Finally, the number of astrocytes in the molecular layer was increased but only in 18 mo. mice (Figure 30E). These variations by DG region could be attributed to the proposed migration that NSCs undergo as they differentiate into astrocytes (Encinas *et al.*, 2011) but could also be defned by other paramaeters and reflect heterogeneity of the astrocytic population, as astrocyte-derived gliogenesis can occur in the hippocampus.
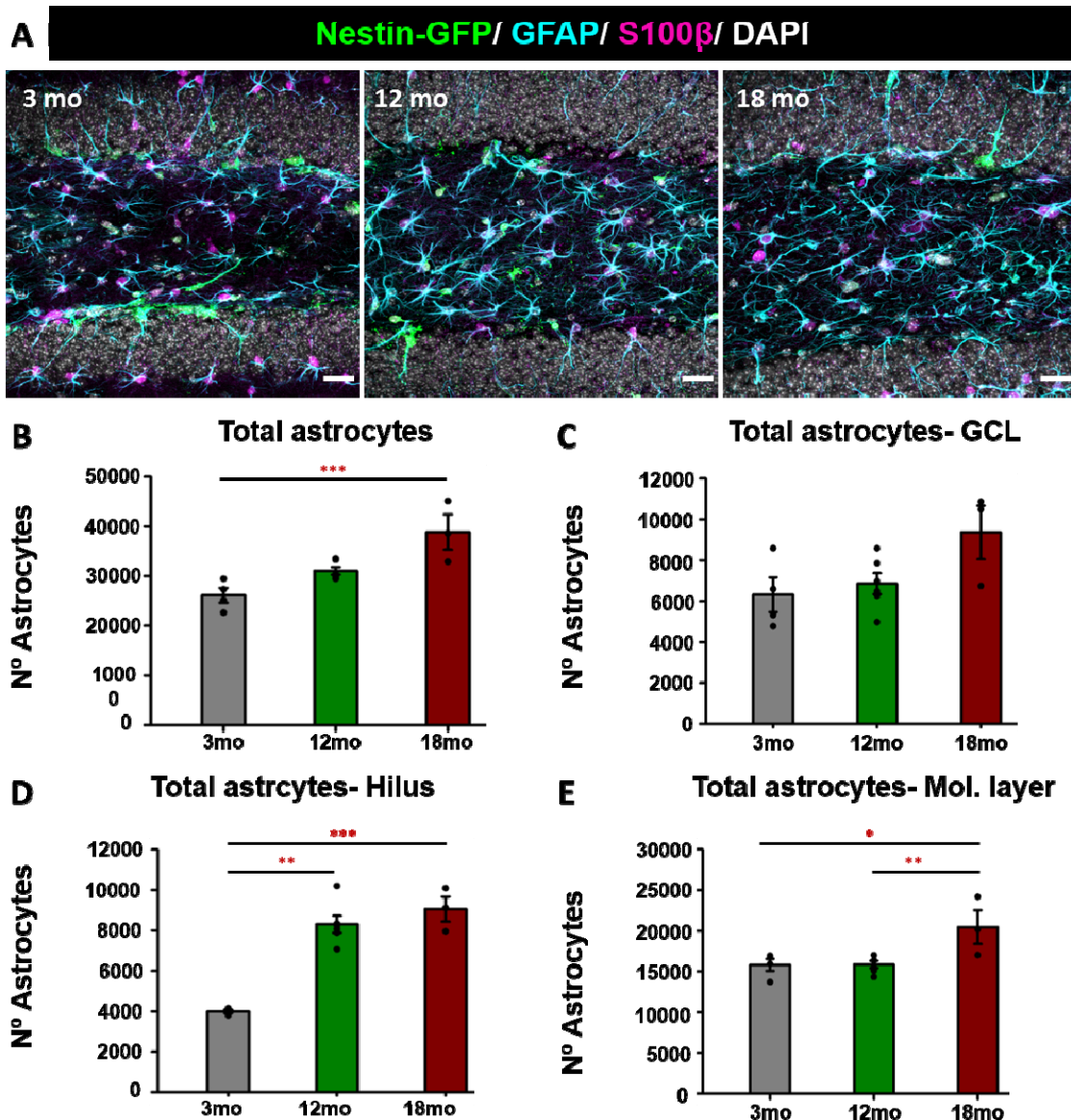
Figure 30. The number of astrocytes increases significantly in the dentate gyrus of aged mice. (A) Projections of confocal-microscopy z-stacks showing astrocytes in 3(left), 12(middle) and 18 (right) mo. after staining for and GFAP (cyan) and S100β (margenta). (B) Quantification of the total number of astrocytes in the dentate gyrus, the number of astrocytes increases with time. (C) Quantification of the total number of astrocytes in the granule cell layer, there is a tendency to increase the number of astrocytes. (D) Quantification hilus-, the number of astrocytes present in the hilus increases in the older animals. (E) Quantification molecular layer (ML), the number of astrocytes present in the ML increases in 18 mo. animals. **p < 0.01, ***p < 0.001 by One way ANOVA Holm Sidak post hoc test. Bars show mean ± SEM. Scale bar is 20 μm in A-. Dots show individual data.

6.9 The Depletion of NSCs Population is Not Due to an Alteration in the Expression in the Nestin-GFP Transgen

As described before, the transgenic Nestin- GFP mice allows the rapidly identification of hippocampal NSCs, in these animals Nestin gene regulatory element drives the expression of the fluorescent proteins (Encinas and Enikolopov, 2008; Encinas *et al.*, 2006; Encinas *et al.*,2011; Enikolopov and Overstreet-Wadiche, 2008; Mignone *et al.*, 2004). In Nestin-based reporter lines, NSCs can be identified as radial-glia-like cells positive for GFP, GFAP, BLBP, Nestin, and vimentin with a long process crossing the GCL and ramifying in the ML. In addition to NSCs, another cell types as ANP (type II progenitor cells), while are still in contact with NSCs, oligodendrocyte precursor cells (OPCs) or pericytes express the transgene.

In spite of the extensive use of this transgenic tool, we investigated whether the expression of Nestin-GFP transgene could change along aging (Figure 31). For this purpose the co-expression of GFP and Nestin immunostaining by antibody was analyzed. We observed that almost the totality of hippocampal NSCs (more than 98%) expressed both markers (Figure 31A) indicating there is not age-related reduction in transgene expression (Figure 31B) (Encinas *et al.*, 2011). Based on this event we can confirm that the observed changes in the NSCs population are not due to an alteration in the expression of the Nestin-GFP transgene. The results mentioned above about the depletion of NSCs with age in wild type C57BL/6 mice (Figure 19) and the confirmation that the Nestin-GFP transgene do not change along the time (Figure 31B) let us to hypothesized that in Nestin-GFP mice the population of NSCs should behave as in C57BL/6 mice. We used Nestin-GFP mice to determine the age-related changes because in these mice NSCs could be specifically analyzed not only in a population level but also individually. The quantification of total number of NSCs at 3, 12 and 18 mo. showed that as it happened in wild type C57BL/6 mice (Figure 31D) the population of Nestin-GFP NSCs decreases with age losing the 90% of the NSCs population between 3 mo. and 18 mo. (Figure 31 C and D) (Encinas *et al.*, 2011). The number of dividing NSCs, as expected, also decreases with the depletion of NSCs population. The loss of NSCs reduced also the number of dividing cells with age following the same tendency (Figure 31E) (Encinas *et al.*, 2011).

These results matched previous data showing the dramatic loss of NSCs population over time, becoming almost depleted with age.
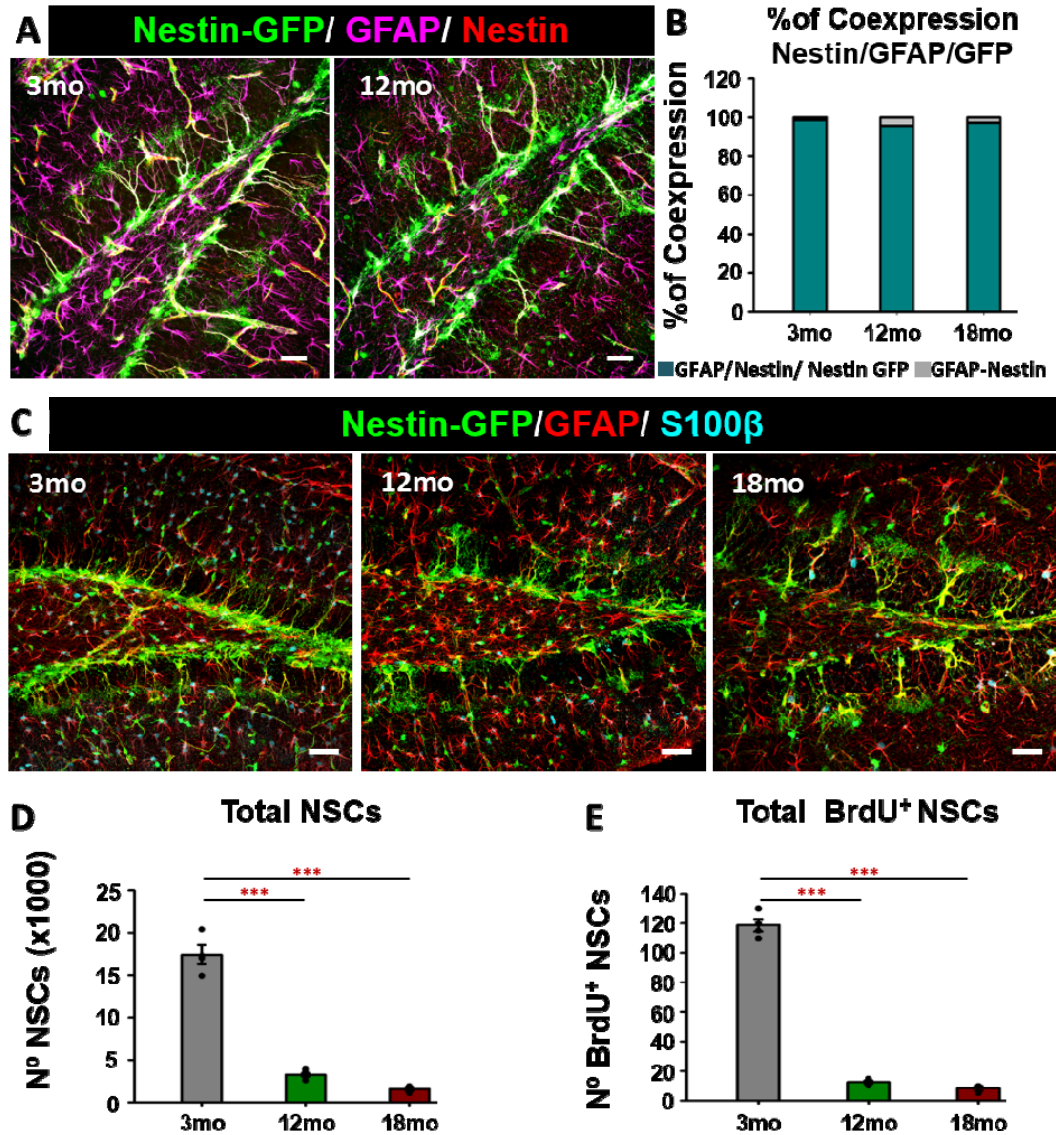
Figure 31. The population of NSCs decreases with age and the depletion is not due to an alteration in the expression of the Nestin-GFP transgen. (A) Projections of confocal-microscopy z-stacks showing the colocalization with Nestin antibody (red), Nestin-GFP (green) and GFAP (magenta) in the NSCs of the dentate gyrus. (B) Quantification of the percentage of colocalization with nestin antibody and Nestin-GFP transgen in 3, 12 and mo. Nestin-GFP animals. (C) Confocal microscopy images showing total population of NSCs (Nestin-GFP and GFAP positive but S-100β -negative cells) located in the SGZ at 3 (left), 12 (middle) and 18 (right) mo. (D) Quantification of total number of NSCs (Nestin-GFP-positive, GFAP-immunopositive cells with radial morphology located in the SGZ) showing the significant decrease of the NSCs population with age. (E) Quantification of absolute number of BrdU[+] NSCs, the total number of dividing NSCs also decreases with age. ***p < 0.001 One way ANOVA Holm Sidak post hoc test. Bars show mean ± SEM. Scale bar is 20 μm in A and C. Dots show individual data.

7. DISCUSSION

7. DISCUSION

7.1 Different levels of neuronal hyperexcitation affect Neural Stem Cells distinctly

Hippocampal Neural stem cells (NSCs) give raise to neurons in a process called neurogenesis (Altman and Das, 1965).This process is tightly controlled by intrinsic and extrinsic factors. The vast majority of external stimulus which affects neurogenesis (increasing or decreasing it) do not affect directly NSCs and only strong stimulus involving electrical activity (such as ECS or KA) can alter the population of NSCs (Sierra *et al.*, 2015 Segi-Nishida *et al.*, 2008). In physiologycal conditions neurogenesis decreases with age (Kuhn *et al.*, 1996), and the main driving force is the depletion of NSCs actually provoked by their activation (entry into cell cycle)(Encinas *et al.*, 2011; Sierra *et al.*, 2015). Thus we hypothesized that neuronal hyperexcitation would accelrate the depletion of NSCs because is promoting NSCs activation. We used a context of pathophysiological relevance, epilepsy (MTLE specifically) to test this hypothesis. We found our hypothesis to be true. Neuronal hyperexcitation in the form EA (discharges with more frequent and larger spikes but no seizures) increased NSCs activation, neurogeneis in the short term and provoked NSCs depletion and decreased neurogenesis in the long term. We found however new properties of NSCs unveiled by higher levels of neuronal hyperactivity. Seizures induce NSCs to drastically change their morphology and to become functionally proinflammatory (thus termed React-NSCs); to get massively activated; to switch to a symmetric mode of cells division and to ultimately differentiate into reactive astrocytes abandoning their neurogenic program. Our data show that this reponse could be common to other types of epilepsy (such as DS) and even to TBI (Wang *et al.*, 2015). We investigated what was the link between neuronal hyperactivity and the induction of React-NSCs, in other words, what cell type and how was communicating with NSCs after seizures and instruct them to reprogram. We found that ATP induces the same response in NSCs as seizures, and because ATP is released by neurons to the extracellular medium upon seizures (Wieraszko and Seyfried, 1989, Dale and Frenguelli, 2009; Santiago *et al.*, 2011), we hypothesize that ATP can be a main mediator between neurons and NSCs in epilepsy. Accordingly we have established an experimental set up to further investigate this hypothesis.

DISCUSSION

7.1.1 Intrahippocampal injection of KA mimics MTLE in mouse

We chose MTLE as the framework to test our hypothesis about the possibility of increased NSCs activation accelerating NSCs depletion because it affects directly the hippocampus, which is normally the focus of seizures; it is one of the most common epilepsies (Crespel *et al.,* 2002); it is resistant to drug treatment in high proportion of cases (35%) (Duveau *et al.*, 2016) and it has one of the worse prognosis (Quirico-Santos *et al.*, 2013). Thus, our study could not only answer fundamental questions about NSCs and AHN, but also shed light about MTLE. To induce seizures adult mice were injected with KA and they developed convulsive seizures (*status epilepticus*) as soon as 30 minutes after the injection which repeated up to 6 hours post injection (Bouilleret *et al.*, 1999; Sierra *et al.*, 2015). In addition, mice developed unprovoked spontaneous chronic seizures after a few days thus becoming epileptic. These spontaneous seizures were registered up to 150 days post injection, our last time point of analysis (Sierra *et al.*, 2015).

KA injection is able to induce recurrent focal seizures, hippocampal sclerosis, cell death, inflammation and GCD (Eyo *et al.*, 2017; Bouilleret *et al.*, 1999; Sierra *et al.*, 2015; Abiega *et al.*, 2016). Although there are other, widely used, models of epilepsy such as pilocarpine we discarded this option due to their high mortality rate and the difficulty to replicate (Curia *et al.*, 2008; Levesque and Avoli 2013). In contrast to KA pilocarpine is a systemic injection with a high spectrum of action being uncontrollable in terms of the area of the brain which is going to be affected. However the intrahippocampal injection of KA is directly delivered in the molecular layer in a very small volume, restricting the area of action and without systemic alterations as those induced by the intraperitoneal alternative.

7.1.2 NSCs became reactive as they divide impairing the neurogenesis.

Even though EA confirm our hypothesis derived based on the "disposable stem cell" "activation-coupled astrocytic differentiation" model (Encinas *et al.*, 2011), the novel finding of the reactive-glia potential of NSCs deserves detailed explanation, as it open new venues of research and potential therapeutic strategies. In the mouse model of MTLE, neuronal hyperexcitation induces NSCs to develop a hypertrophic cytoplasm and a multibranched phenotype with overexpression of Nestin and GFAP. At the same time they get activated in much higher proportion than in normal conditions or even EA. Strikingly, in MTLE NSCs change their mode of division from the typical asymmetric, ANP-generating, neurogenic mitosis to a symmetric React-NSCs duplicating mode (Sierra *et al.*, 2015). We cannot here separate both

phenomena, as both take place simultaneously short-time (1-3 days) after KA injection. However other lines of research in the laboratory, focused in the role of lysophosphatydic acid receptor 1 (LPA$_1$) show us that cell division seems to, or at least can be, regulated separately from the induction of the reactive phenotype. In any case, it is remarkable that just the initial episode of seizures trigger the induction of React-NSCs and their massive activation. Whether NSCs and the neurogenic niche could recover if further seizures were prevented is still unknown.

The conversion of NSCs into React-NSCs and their final differentiation into reactive astrocytes depletes the pool of NSCs (Sierra *et al.*, 2015) but not because of their exhaustion due to astroglial differentiation after neurogenic cell division, but because of a drastic and swift switch in cell differentiation. Nevertheless, in MTLE the number of apoptotic cells (programmed cell death) ,mostly in the SGZ, significantly increased starting as soon as 6 hours post injection, in part due to accumulation of cell corpses because of microglial function (phagocytosis) impairment (Abiega *et al.*, 2016). We therefore evaluated the possibility of NSCs death contributing to the depletion of the pool. NSCs death is absent in normal conditions, or at least has never been observed or reported. Even though in MTLE it can be found, the percentage of death in NSCs cannot contribute significantly to their exhaustion and confirms our hypothesis that NSCs depletion is due to the direct conversion into React-NSCs in MTLE.

The precise mechanism underlying the seizure-induced increase in NSCs activation is unclear, but several potential mechanisms could be playing a role. First, it has been described in normal conditions and using intraperitoneal KA administration that the expression of Ascl1 is required for the activation of NSCs as its conditional (in NSCs) knock down prevents NSCs activation, and by the way, NSCs depletion in normal conditions (Andersen *et al.*, 2014). Second, the role of GABA could be of special importance during the early post-seizure period (Shaoyu *et al.*, 2006), as it has been established that GABA plays a crucial role in various steps of adult neurogenesis, including the activation of NSCs (Song *et al.*, 2012; Giachino *et al.*, 2014). Although we did not explore these mechanisms herein, we, as we will explain later, found a potential signalling pathway that could be crucial for seizure-induced activation of NSCs.

7.1.3 NSCs contribute directly to the MTLE.

Traditionally, the study of glial cells is focused mainly on astrocytes or microglia. The role of these cells in the development of inflammatory process or epilepsy is widely described (Pernhorst *et al.*, 2013; Crunelli *et al.*, 2015). We have focused much of the initial aspects of the NSCs in MTLE project in cell division and morphological changes, namely the acquisition or development of a reactive-like morphology similar to that of reactive astrocytes derived from parenchymal astroglia. We therefore sought to investigate whether React-NSCs were really reactive also functionally. Although it has been proposed that NSCs are able to generate and release different molecules into the extracellular medium which can influence and modulate the response the neurogenic niche NSCs have been considered just a source of new neurons. Under inflammatory conditions (such as LPS, Poly I:C or IL-6) NSCs release molecules such as trophic factors (Ourednik *et al.*, 2002), ameliorate chronic inflammation (Einstein *et al.*, 2003; Pluchino *et al.*, 2005), inhibiting T-cell activation (Einstein *et al.*, 2007) or inflammatory cytokines (Covacu *et al.*, 2009).

Here we demonstrate that React-NSCs increase drastically the expression of IL1β after seizures. This cytokine has been extensively studied as it is one of the major effectors in neuroinflammation (Brocker *et al.*, 2010; Fensterl and Sen, 2009). Interestingly, reactive astrocytes-derived IL-1β has been shown to participate in the chronification of seizures and thus has been proposed to be epileptogenic (Devinsky *et al.*, 2013). Thus React-NSCs and React-derived astrocytes (Sierra *et al.*, 2015) could be playing a similar role as parenchymal reactive astrocytes in MTLE and epileptogenesis. Furthermore the conversion of NSCs into React-NSCs and their posterior differentiation into reactive astrocytes contribute to the development of hippocampal sclerosis in the DG, a hallmark of MTLE which correlates with bad prognosis and resistance to antiepileptic drugs (Duveau *et al.*, 2016; Quirico-Santos *et al.*, 2013; Sierra *et al.*, 2015).

7.1.4 Neurogenesis is absent in MTLE human patients.

MTLE is a pharmaco-resistant focal epilepsy, therefore many patients require resection of the epileptic hippocampus (Quirico-Santos *et al.*, 2013). The study of samples from MTLE patients confirms that our mouse model of MTLE is a perfect tool to understand the progression of the epilepsy. The samples were obtained from patients who have suffered MTLE for years and finally surgical resection of the hippocampus, as the focus of seizures, is the last therapeutic resort. The value of these samples resides in that they were obtained immediately during the surgery and then washed and fixed immediately, thus preserving antigenicity. The drawback of

course is the lack of an appropriate control. We refrained from using post-mortem samples as controls as our experience in the past has been very negative. Freshly-ressected control, or at least pseudocontrol, samples exist, as sometimes the hippocampus although not being directly affected is removed preventively due to gliomas or seizures being generated in neighbouring regions. We are in the process of obtaining such samples. In the past the samples presented an extensive gliosis which do not allowed us to distinguish between React-NSCs and reactive astrocytes (Blümcke *et al.*, 2001) so we cannot conclude by any means that MTLE induces React-NSCs in the human hippocampus, specially because the presence of NSCs and AHN in older humans is still object of debate (this topic will be discussed further in the aging section). We however were no able to found any proliferative cell or neuroblasts in the DG, in agreement with our mice data in the long term (Sierra *et al.* 2015). Our observation in mice, the conversion of NSCs into React-NSCs abolishing their neurogenic capacity of NSCs, could explain the data obtained with the human samples, but causality cannot be assumed.

7.1.5 Dravet syndrome mice induce Reactive NSCs.

DS is severe infantile multifocal epilepsy and intractable childhood epilepsy characterized by frequent prolonged seizures, developmental delays, speech impairment, and motor/ orthopaedic issues (Dravet 1978; Dravet 2011) including dysautonomia, nutrition issues, characteristics of autism, and a high rate of sudden unexpected death in epilepsy (SUDEP) approximately 10–20% of the afflicted children do not survive (Genton *et al.*, 2011; Sakauchi *et al.*, 2011)

Here we analysed samples of SCN1A knockout animal model of DS kindly provided by Dr. Onintza Sagredo from the UCM. These animals manifest spontaneous seizures, motor deficits, ataxia and premature death (Yu *et al.*, 2006; Kalume *et al.*, 2007; Ogiwara *et al.*, 2007; Tang *et al.*, 2009; Martin *et al.*, 2010). Here we describe that DS mice presented reactive gliosis and sclerosis in the hippocampus as soon as at P25 and we report for the first time an increase of the number of proliferative GFAP-positive radial cells of the SGZ. These putative NSCs present a reactive phenotype compared to WT and similar to that described in the MTLE model, and thus we also consider them React-NSCs. Moreover, the neurons of the GCL present nuclear dystrophy, characterized by the loss of circularity. These two analyses are pioneer in the field as study of the effect of DS in the hippocampus and more specifically in NSCs and the neurogenic niche have not been carried out before and open new research and therapeutic possibilities that we will pursue in the near future.

7.2 Inflammation alone is not enough to induce Reactive Neural Stem Cells.

Seizures involve very high levels of neuronal activity, and excitotoxicity followed by neuronal damage and cell death. As a result, neuroinflammation, protagonized by astrocytes and microglia ensues (Monje *et al.*, 2003; Ekdahl *et al.*, 2003; Borsini *et al.*, 2014). We then wondered whether the induction of React-NSCs could be a by-product derived of seizure-generated inflammation, rather than being directly triggered by neuronal hyperexcitation. Exploring this question would also provide cues for addressing the mechanisms by which NSCs turn into React-NSCs. Inflammation can be triggered by a variety of stimuli including pathogens, such as bacteria, fungi, parasites, and viruses (Nayak *et al.*, 2014), therefore we resorted to used different models of inflammation, from bacterial- (LPS) and viral- (Poly I:C) like infections to the direct delivery of cytokines (IFN-α or IL-6) in the brain. These factors are frequently administrated intraperitoneally but, this mode of administration involves a wide-range of systemic actions that we wanted to avoid. We therefore resorted to inject these factors directly into the hippocampus, also allowing for more direct comparison with the results obtained with the MTLE model. We used several models to cover as much of the range of processes included under the inflammation umbrella. For instance to mimic a bacterial infection we used LPS, which induces a widespread microglial and astroglial activation and strongly suppresses neurogenesis in the adult rodent hippocampus (Ekdahl *et al.*, 2003; Monje *et al.*, 2003). It has been described that NSCs express mRNA that encodes to TLR family (Rolls *et al.*, 2007) thus NSCs could react directly to LPS. On the contrary, Poly I:C, used to mimic a viral-infection-derived inflammation we used has not been reported to act directly on NSCs. We also injected directly cytokines such as IL-6 or IFN-α, effective mediators of the inflammatory process itself. We observed that either NSCs activation was not altered or was even diminished as it was the case for IFN-α in agreement with previous studies (Kaneko *et al.*, 2006; Zheng *et al.*, 2014). This was expected as several previous studies had demonstrated the antineurogenic effect of different models of inflammation, although without dwelling in detail on the effect of NSCs (Widera *et al.*, 2006; Sun *et al.*, 2004; Nakanishi *et al.*, 2007; Barkho *et al.*, 2006; Ben-Hur 2008). None of the inflammation-like stimuli induced a reactive phenotype in NSCs. Our results confirmed that NSCs proliferation decreases in inflammation accordingly to previous studies

DISCUSSION

We used two models of neuronal hyperactivity to test the effect on NSCs, our known model of intrahippocampal injection of KA, and controlled cortical impact as a model of TBI that we are also using and investigating in the laboratory. In both case we found increased activation of NSCs as well as induction of the reactive phenotype. It can be argued that neitherKA or TBI can be considered as clean models of neuronal hyperexcitation. Excitotoxicity with neuronal damage and death will be inevitably accompanied by inflammation and thus the claim that we can make is that inflammation alone, characterized by the presence of reactive astroglia and microglia is not enough to induce React-NSCs.
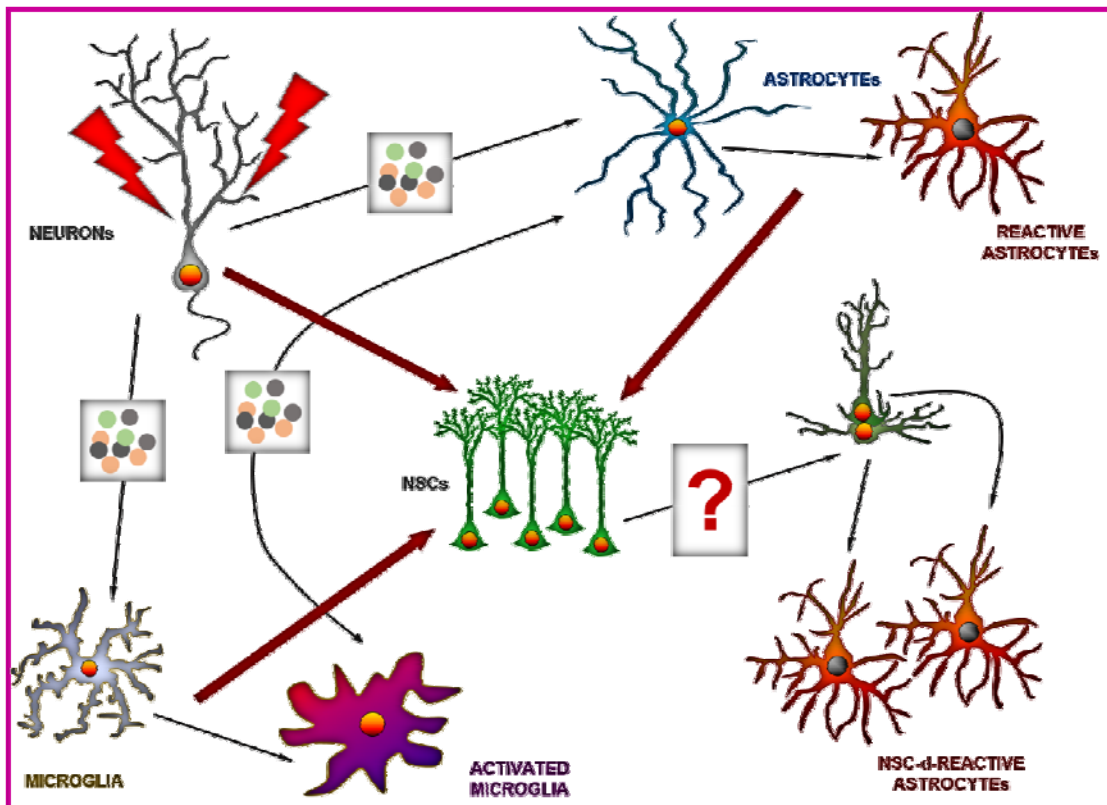
Figure 32. Potential ways of interaction between neurons, astricytes and microglia to trigger React-NSCs. MTLE induces React-NSCs but what cell type is responsible of instructing NSCs to reprogram remains unknown. Neurons release factors which act on astro and microglia, who in turn release factors that mediating reciprocal interaction

We reasoned then, that if reactive and activate astrocytes and microglia do not instruct NSCs to become reactive, it has to be neurons the cell type that triggers such response. Therefore we sought to find candidates that would convey that message from hyperactive neurons to NSCs.

7. 3 ATP induces Reactive Neural Stem Cells.

We hypothesized that extracellular ATP could be the mediator of the conversion of NSCs into React-NSCs because although under normal conditions ATP is released by neurons and astrocytes as neurotransmitter/neuromodulator (Burnstock 2006), during seizures ATP is released in much large amounts (Wieraszko and Seyfried, 1989, Dale and Frenguelli, 2009; Santiago *et al.*, 2011). Also, several studied have demonstrated the presence of purinergic receptors in several types of NSCs (Tang and Illes 2017) and ATP is known to mediate cell proliferation and reactive responses in the astrocytes (Abbracchio *et al.*, 1996), to whom NSCs as we know are very closely related. To assess whether ATP is able to induce or at least acts as a mediator in the conversion of NSCs into React-NSCs we injected ATP intrahipocampally. ATP is degraded *in vivo* to ADP and AMP (Zimmermann, 1999) rapidly, so in order to solve this problem we used a non-degradable form of ATP, the synthetic ATP-γ. Although the dose of ATP-γ is relatively high compared to standard doses used *in vivo* or *in vitro* we wanted to mimic the amount of ATP (of mM concentrations of ATP) released during the insults by damaged cells (Trautmann, 2009). Thus, the dose used for the study of the effect of ATP is within the range of ATP released during pathological conditions. Importantly, as we used a non-degradable ATP we assured the effect only in ATP-specific receptors which could extend its effects to surrounding cells (Robson *et al.*, 2006).

Strikingly, intrahippocampal ATP induces a very similar response on NSCs than intrahippocampal KA: Massive activation and switch to a reactive phenotype, meaning that indeed ATP could be a mediator between hyperactive neurons and NSCs.

7.3.1 Purinergic receptors are present in adult NSCs *in vivo*.

We demonstrated by RT-qPCR that NSCs (isolated from the adult mouse hippocampus) express purinergic receptors, specifically they express P2X3, P2X4 and P2X7 some of them had already been detected by single-cell sequencing before (Hogg *et al.*, 2004; Shin *et al.*, 2015). P2X7 receptor is of special interest as it has been described to play an ambiguous role controlling necrosis/apoptosis and also proliferation (Adinolfi *et al.*, 2010; Sperlagh and Illes, 2014). Furthermore, this receptor precludes the evolution of a one-time *status epilepticus* into chronic epilepsy. P2X7 receptor is activated at highest concentrations of ATP (Pankratov *et al.*, 2008) in contrast to the other six receptors which require lower concentrations of ATP which could represent a bias for activation under abnormal conditions such as seizures. Also, the selective modulation of P2X receptors could be an option to modulate the response of NSCs in epilepsy.

we cultured adult hippocampal neuroprogenitors (NSPCs) as an *in vitro* model of NSCs and afterwards we analyzed the expression of P2X receptors and we showed that *in vitro* NSPCs expressed the receptors P2X3, P2X4 and P2X7 as it happens *in vivo*

7.3.2 ATP signalling is present in NSCs *in vitro*.

In order to investigate in detail our hypothesis that ATP could be a main effector in the conversion of NSCs into React-NSCs we need to establish a good model to quickly and efficiently manipulate this signalling pathway. ATP-induced activation of P2X receptor, especially P2X4 and P2X7, differentially induces receptor-operate calcium entry (Gilbert *et al.*, 2016). The oscillation in the intracellular calcium regulates numerous basic process including proliferation, differentiation and cellular motility, thus changes in the balance of intracellular calcium could explain at least in part the conversion of NSCs into React-NSCs.

Neurospheres, NSPCs derived from the adult neurogenic niches and maintained in proliferative non-differentiating conditions are an extensively used model to study NSCs. In our case they offer the advantage of isolating NSCs form the other cell types mainly astrocytes that express P2X receptors in the brain.

It had been previously demonstrated that the administration of Bz-ATP (agonist of PX7) accelerated the entry into the cell cycle (Glaser *et al.*, 2014) a result that we can replicate using ATP-γ. We also found that *in vitro* NSPCs altered their morphology and grew larger after ATP addition. As mentioned before ATP via P2X receptors can promote either cell death or cell proliferation. In our hands, the highest doses of ATP indeed killed the cultured NSPCs. We confirmed the expression of P2X receptors in *in vitro* NSPCs and using a selective antagonist (TNP-ATP) could block the ATP-induced increase in cell proliferation and morphological change.

These *in vivo* and *in vitro* experiments convinced us that indeed hyperactivated neuron-released ATP can play an important role in inducing React-NSCs. A key experiment to address this hypothesis would be to specifically knock out or down P2X receptor expression only in NSCs in the hippocampus. This is a future goal towards which we have already started to work. We have elaborated short-hairpin miRNA to block the P2X receptors. Later the successful constructs will be specifically targeted or expressed using specific promoters for NSCs (LPA$_1$ or Nestin) via viral vectors or inducible transgenic lines of mice (Osório *et al.*, 2014).
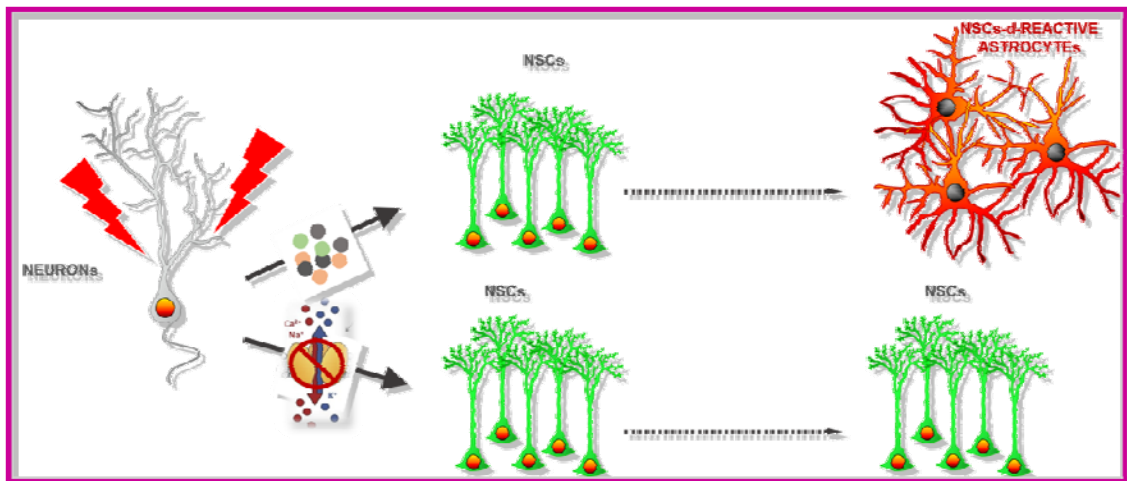
Figure 33. ATP mediates the conversion of NSCs intro React.-NSCs, Block P2X receptors could maintain the population of NSCs in normal conditions.

7.4 Neural Stem Cells in Aging

The age-related decrease of neurogenesis has been extensively documented (Cameron and McKay, 1999; Hattiangady and Shetty, 2008; Kuhn *et al.*, 1996; Leuner *et al.*, 2007; Olariu *et al.*, 2007; Seki and Arai, 1995), however, the mechanisms underlying this reduction cannot yet completely justify this decline.

7.4.1 Activation of NSCs predicts their depletion.

Recent data obtained using mathematical modeling shows that the activation-coupled astrocytic differentiation alone might not account for all the depletion of the NSCs pool and that other mechanisms, might be apoptosis, could play an important role (Ziebell *et al.*, 2018). In-vivo two-photon imaging of neurogenesis in the hippocampus has confirmed most of these observations with unprecedented resolution and has yielded new findings: hippocampal NSCs might comprise several subpopulations with different behaviors regarding asymmetric versus symmetric division, neurogenic versus astrocytic differentiation, and difference in the period of quiescence between mitosis (Pilz *et al.*, 2018). Noteworthy, depletion of NSCs alone cannot explain the loss of generation of neuronal progenitors that eventually give rise to newborn neurons. As the number of activated NSCs is very small compared to the total size of the population, the number of activated NSCs (and subsequently the number of neuronal progenitors) could remain constant for longer periods of time even if the total size of the NSCs population declines. The amount of neurogenesis in the human hippocampus is currently subject of intense debate with data supporting the generation of newborn neurons through

aging in a more or less continuous fashion (Eriksson *et al.*, 1998; Spalding *et al.*, 2013; Boldrini *et al.*, 2018) or with a dramatic decline similar to rodents (Knoth *et al.*, 2010). Reduction of neurogenesis to undetectable levels in the human hippocampus after infancy has also been reported (Sorrells *et al.*, 2018; Dennis *et al.*, 2016; Cipriani *et al.*, 2018). In any case the key to explain these results altogether resides in how sharp is the loss of neurogenesis.

Here we confirm that the age-related decline of neurogenesis (Encinas *et al.*, 2011; Sierra *et al.*, 2015) is coupled to their activation of NSCs. We discovered that the activation of NSCs explain almost in a 100% the depletion of the total population. Although NSCs can undergo symmetric division to generate more copies of themselves this process is not frequent enough to counterbalance in normal conditions the age-associated decline of NSCs (Bonaguidi *et al*, 2011). We can confirm that the main, but not the only, force driving the decrease of neurogenesis is the depletion of NSCs population and interestingly the depletion of NSCs population can be explain by the activation of the NSCs.
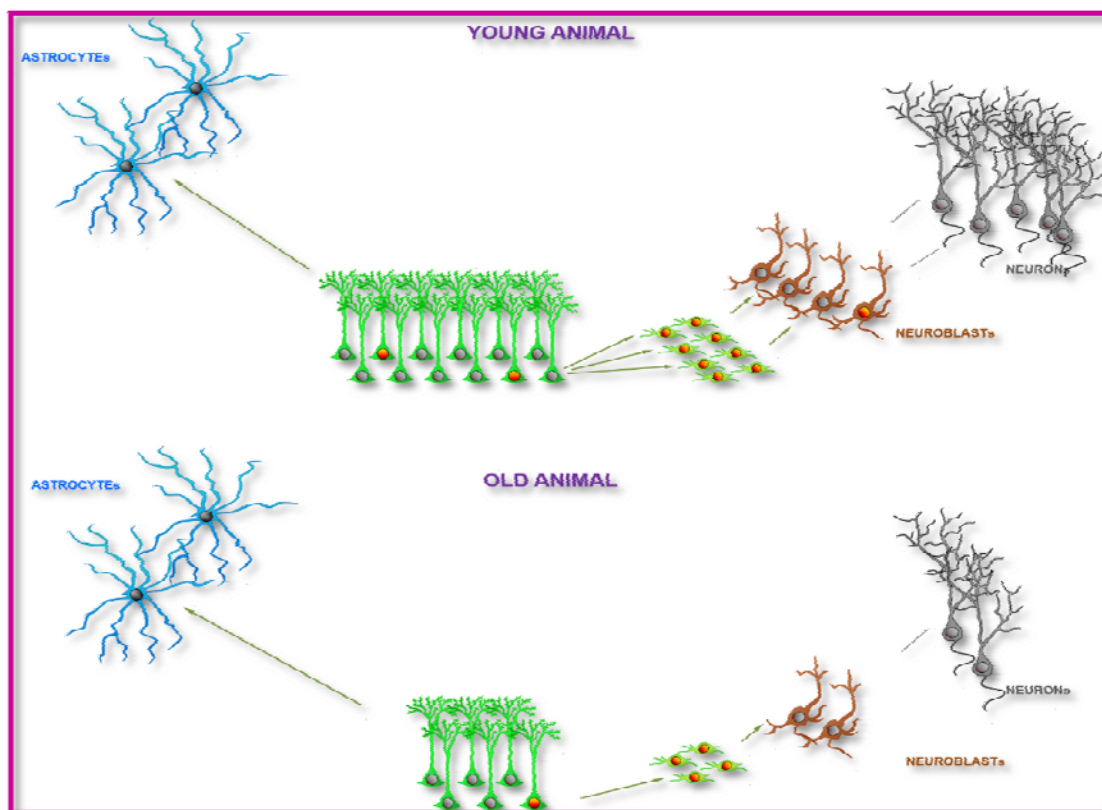
Figure 34. Depletion of NSC explains the age-associated decline of AHN as long as the proportion of activated (and therefore "exhausted") NSCs remains constant over time.

7.4.2 Phenotypical and functional heterogeneity of NSCs in the aged hippocampus.

When analyzing the DG of mice at different ages we observed that Nestin-GFP/GFAP positive cells in the SGZ and GCL were different morphologically in the older animals. After a tridimensional analysis of NSCs, we found a new phenotype of NSC coexisting with the described typical α-cells and β-cells (Gebara *et al.*, 2016). This new subtype, that we called herein Ω-cells as they are the last one standing in the aged DG and for the sake of clarity, present a significant increase in the complexity characterized by a multibranched morphology with several primary processes, a decrease of the length and the cell body located in the SGZ+GCL. Ω-cells divide with much lower probability as measured by the incorporation of BrdU. The lack of S-100β expression in Ω-cells differentiates them from the β-cells. Furthermore, even in pro-activation conditions as KA injections (Sierra *et al.*, 2015) Ω-cells are the less proliferative sub-population.

Our description of a new subtype of NSCs shed light on the behavior of NSCs in aged DG, because as we described, whereas the α-cells decline sharply in numbers from several thousands to a few hundred cells, in agreement with previous reports (Encinas *et al.*, 2011, Walter *et al.*, 2011), but in contrast Ω-cells increase their numbers and comprise, by large, the most abundant population in aged mice.
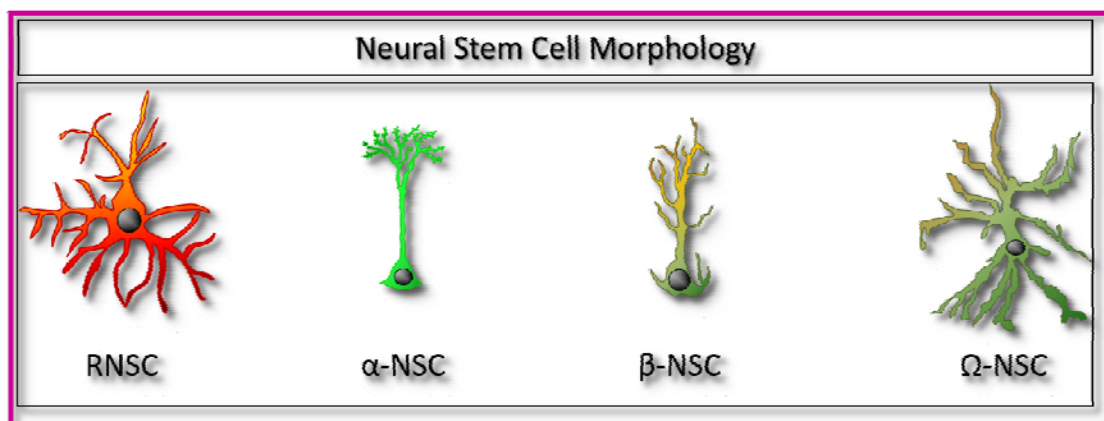
Figure 35. **Types of NSC-like cells in the epileptic and aged hippocampus.** NSCs, defined by their expression of Nestin-GFP and GFP plus location in the SGZ+GCL present distinct morphologies in normal conditions (α andβ), aging (Ω) and epilepsy (React, R). Altered mitotic potential and differentiation associate with these morphological classes.

This morphological change is directly related to aging, as it was showed in the population profile changes. While in young animals the proportion of α-cells comprised the majority of the NSCs population, in old animals α-cells represented the smallest relative proportion, being Ω-cells the main subtype in older mice. We hypothesize that rather than two

different populations generated independently, a subpopulation of α-cells senesces into Ω-cells. Our data from IFN-α treated mice strongly support this idea. Mice injected with IFN-α showed a very similar total number of NSCs compared to saline injected mice. IFN-α induced, however, a reduction in the number of α-cells and a proportional increase in Ω-cells, thus suggesting a conversion from α- to Ω-cells. Indeed our analysis showed a high level of correlation between the α-cells that disappear and the Ω-cells that are generated. Therefore, α-cells could transform into Ω-cells with aging, developing a more complex morphology progressively in a time-dependent process, diminishing their proliferative capacity at the same time. Recently, mathematical models described that the age-related depletion of the NSCs might be explained because NSCs spend longer time in quiescence during aging (Ziebell *et al.*, 2018). This model also predicts that the probability of exiting the quiescent stage through activation versus depletion increases during aging, which fits with our results.

The molecular changes that occur in NSCs population during aging remain to be elucidated but this work provides a framework for future research. It is known that in aged mice the genes associated with inflammation and oxidative stress are upregulated compared to young mice (Lynch *et al.*, 2010) and one of the main effects of the neuroinflammation is the reduction of neurogenesis (Gebara *et al.*, 2016; Sierra *et al.*, 2015; Ekdahl *et al.*, 2003). We demonstrated that the chronic administration of IFN-α mimics the chronic inflammation related to aging, IFN-α increases the quiescence of NSCs and induce or at least contributes significantly to the conversion of α-cells into Ω-cells. These findings give us reasons to hypothesize that chronic inflammation could mediate the acquisition of Ω phenotype and increase the quiescence in NSCs. According to several studies the lengthy treatment with IFN-α affects directly cell proliferation in the SGZ thus reducing hippocampal neurogenesis (Kaneko *et al.*, 2006). In fact, the direct administration of this molecule diminishes specifically the neurogenic function of NSCs in the DG (Zheng *et al.*, 2014), confirming our data.
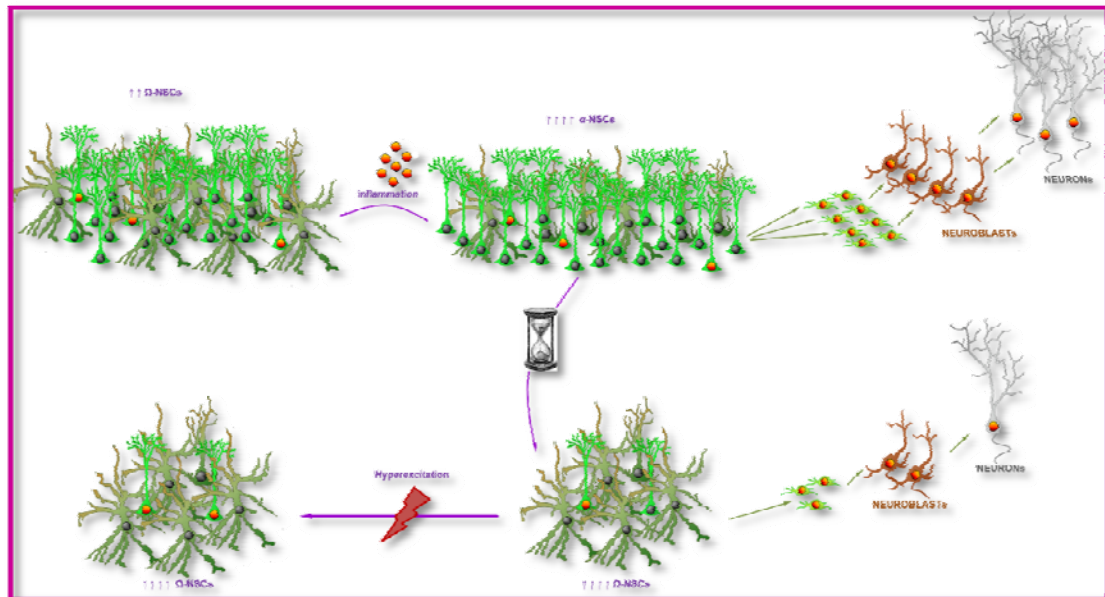
Figure 36. Besides declining in population NSCs convert into a "senescent-like" phenotype (Ω-NSCs) with aging. These Ω-NSCs enter cell division with much lower probability than their typical α-NSCs counterparts. Even when promoting NSC activation through increased neuronal excitation Ω-NSCs remain mostly quiescent while α-NSCs increase their activatin rate. A proinflammatory stimulus pushes the conversion of α-NSCs into Ω-NSCs.

We were curious about the relationship between increased quiescence and morphological changes and therefore made use of a transgenic line of mice in which NSC cell division is blocked due to knocking out CD1. The cyclin family are important regulators of cell cycle progression and the lack of proliferation abolishes AHN. Interestingly we found the Ω-phenotype in the NSCs of the cKO mice at young age. This result is only preliminary but supports the notion that quiescence/senescence and morphological alterations are closely related in hippocampal NSCs.

All together our results shed light about how aging affects DG neurogenesis and in particular how NSCs may be affected by aged-related inflammation ("inflammaging") because it is not only the "deforestation" of NSCs but also their conversion into a senescent phenotype associated to chronic inflammation that explains the decrease of neurogenesis with aging.

8. CONCLUSIONS

8. CONCLUSIONS

1. **Seizures induce the conversion of NSCs into React-NSCs in the hippocampal neurogenic niche.**

    V.   Neuronal hyperexcitation in the form of EA promote NSC activation and subsequent depletion without changes in differentiation.

    VI.   In a mouse model of MTLE seizures provoke the massive activation of NSCs and their transformation into a functionally and morphologically reactive phenotype (React-NSCs).

    VII. MTLE seizures-induced React-NSCs divide symmetrically and generate reactive astrocytes.

    VIII. MTLE induces in the human hippocampal neurogenic niche alterations comparable with the disruptions found in the neurogenic niche of the MTLE mice.

2. **Reactive Neural Stem Cells are present in the Dravet syndrome mouse model**

    IV.   Cell proliferation and NSCs activation are increased in the mouse model of DS.

    V.   React-NSCs are present in the hippocampal neurogenic niche of DS mice.

    VI.   The nuclei of neurons of the GCL present a distorted shape in DS mice.

3. **Inflammation does not induce the conversion of NSCs into React-NSCs**

    III. Proinflammatory stimuli or mediators maintain or even reduce NSCs activation.

    IV.   Insults that involve neuronal hyperexcitation such as seizures or traumatic brain injury induce NSCs activation and React-NSCs.

4. **ATP acts as a mediator in the induction of React-NSCs.**

    V.   P2X purinergic receptors are present in the hippocampal NSCs *in vivo* and *in vitro.*

    VI.   ATP induces the conversion of NSCs into React-NSCs and their massive activation *in vivo*.

VII.   ATP promotes proliferation and morphological alteration of *in vitro* hippocampus-derived NSPCs and these effects are blocked by the P2X receptor antagonist TNP-ATP.

VIII.   Interference RNA (shRNA) can be used to knock down P2X receptor expression *in vitro.*

5.   Aging induces profound functional and morphological changes in hippocampal NSCs.

IX.   The total number of NSCs and activated NSCs decreases with aging but the relative proportion of activated NSCs remains constant over time.

X.   The activation of NSCs predicts the depletion of the NSCs population over time.

XI.   At least two different populations of NSCs with particular morphology and mitotic capacity coexist in the aging DG.

XII.   α-cells represent the most morphologically simple NSCs and account for most of the dividing NSCs over time and after a pro-activation stimulus.

XIII.   Ω-cells are morphologically more complex, and become more quiescent over time even after a proactivation stimulus. α-cells disappear with aging and Ω-cells accumulate (in relative proportion) in the aged DG.

XIV.   A proinflammatory stimulus can induce, or accelerate, the transformation of α-NSCs into Ω-NSCs in younger mice.

XV.   The reactive-like (Ω-like) morphology associates with increased quiescence in a cyclin D2 knock out mouse.

XVI.   The number of astrocytes increases differentially with aging in the distinct areas of the DG.

CONCLUSIONS

9. BIBLIOGRAPHY

9. BIBLIOGRAPHY

- Abiega, O., Beccari, S., Diaz-Aparicio, I., Nadjar, A., Laye, S., Leyrolle, Q., Gomez-Nicola, D., Domercq, M., Perez-Samartin, A., Sanchez-Zafra, V., *et al.* (2016). Neuronal Hyperactivity Disturbs ATP Microgradients, Impairs Microglial Motility, and Reduces Phagocytic Receptor Expression Triggering Apoptosis/Microglial .

- Aguzzi, A., Barres, B.A., and Bennett, M.L. (2013). Microglia: scapegoat, saboteur, or something else? Science 339, 156-161.

- Ahl, M., Avdic, U., Skoug, C., Ali, I., Chugh, D., Johansson, U.E., and Ekdahl, C.T. (2016). Immune response in the eye following epileptic seizures. Journal of neuroinflammation 13, 155. Phagocytosis Uncoupling. PLoS Biol 14, e1002466.

- Ahn S, Joyner AL. *In vivo* analysis of quiescent adult neural stem cells responding to Sonic hedgehog. Nature. 2005;437:894–897.

- Aimone, J.B., Li, Y., Lee, S.W., Clemenson, G.D., Deng, W., and Gage, F.H. (2014). Regulation and function of adult neurogenesis: from genes to cognition. Physiol Rev 94, 991-1026.

- Akiyama M, Kobayashi K, Yoshinaga H, Ohtsuka Y. A long-term follow-up study of Dravet syndrome up to adulthood. Epilepsia. 2010;51:1043–52.

- Altman J, Das GD. Autoradiographic and histological evidence of postnatal hippocampal neurogenesis in rats. J. Comp. Neurol. 1965;124:319–335.

- Altman, J. (1969). Autoradiographic and histological studies of postnatal neurogenesis. IV. Cell proliferation and migration in the anterior forebrain, with special reference to persisting neurogenesis in the olfactory bulb. J Comp Neurol 137, 433-457.

- Amor, S., Puentes, F., Baker, D., and van der Valk, P. (2010). Inflammation in neurodegenerative diseases. Immunology 129, 154-169.

- Andersen J, Urbán N, Achimastou A, Ito A, Simic M, Ullom K, Martynoga B, Lebel M, Göritz C, Frisén J, Nakafuku M, Guillemot F. (2014) A Transcriptional Mechanism Integrating Inputs from Extracellular Signals to Activate Hippocampal Stem Cells. Neuron 83(5):1085-1097.

- Artegiani B1, Lyubimova A1, Muraro M1, van Es JH1, van Oudenaarden A1, Clevers H2. A Single-Cell RNA Sequencing Study Reveals Cellular and Molecular Dynamics of the Hippocampal Neurogenic Niche. Cell Rep. 2017 Dec 12;21(11):3271-3284. doi: 10.1016/j.celrep.2017.11.050.

- Babb, T .L., Pereira-Leite, J., Mathern, G.W., and Pretorius, J.K. (1995). Kainic acid induced hippocampal seizures in rats: comparisons of acute and chronic seizures using intrahippocampal versus systemic injections. Ital J Neurol Sci 16, 39-44.

- Bachstetter AD, Xing B, de Almeida L, Dimayuga ER, Watterson DM, Van Eldik LJ. Microglial p38alpha MAPK is a key regulator of proinflammatory cytokine up-regulation induced by toll-like receptor (TLR) ligands or beta-amyloid (Abeta). J Neuroinflammation. 2011;8:79.

- Bao H, Asrican B, Li W, Gu B, Wen Z, Lim SA, Haniff I, Ramakrishnan C, Deisseroth K, Philpot B, Song J Long-Range GABAergic Inputs Regulate Neural Stem Cell Quiescence and Control Adult Hippocampal Neurogenesis.C ell Stem Cell. 2017 Nov 2;21(5):604-617.e5. doi: Knobloch 10.1016/j.stem.2017.10.003.

- Barkho, B.Z., *et al.*, Endogenous matrix metalloproteinase (MMP)-3 and MMP-9 promote the differentiation and migration of adult neural progenitor cells in response to chemokines. Stem Cells, 2008. 26(12): p. 3139-49.

- Barkhoudarian, G., Hovda, D.A., Giza, C.C., 2011.The molecular pathophysiology of con-cussive brain injury. Clin. Sports Med. 30, 33–48 (vii–iii).

- Ben Abdallah NM, Slomianka L, Vyssotski AL, & Lipp HP (2010) Early age-related changes in adult hippocampal neurogenesis in C57 mice. Neurobiol Aging 31(1):151-161.

- Ben-Ari, Y., and Cossart, R. (2000). Kainate, a double agent that generates seizures: two decades of progress. Trends Neurosci 23, 580-587.

- Ben-Ari, Y., and Lagowska, J. (1978). [Epileptogenic action of intra-amygdaloid injection of kainic acid]. CR Acad Sci Hebd Seances Acad Sci D 287, 813-816.

- Ben-Ari, Y., and Lagowska, J. (1978). [Epileptogenic action of intra-amygdaloid injection of kainic acid]. C R cad Sci Hebd Seances Acad Sci D 287, 813-816.

- Ben-Hur T, Ben-Menachem O, Furer V, Einstein O, Mizrachi-Kol R, Grigoriadis N. Effects of proinflammatory cytokines on the growth, fate, and motility of multipotential neural precursor cells. Mol Cell Neurosci. 2003;24(3):623–631.

- Bergami M, Rimondini R, Santi S, Blum R, Götz M, Canossa M. (2008) Deletion of TrkB in adult progenitors alters newborn neuron integration into hippocampal circuits and increases anxiety-like behavior. Proc Natl Acad Sci U S A 105(40):15570-15575.

- Bernal GM, Peterson DA. Phenotypic and gene expression modification with normal brain aging in GFAP-positive astrocytes and neural stem cells. Aging Cell. 2011;10:466–482. doi: 10.1111/j.1474-9726.2011.00694.
- Block, M.L., and Hong, J.S. (2005). Microglia and inflammation-mediated neurodegeneration: multiple triggers with a common mechanism. Prog Neurobiol 76, 77-98.

- Blumcke I., Schewe J.C., Normann S., Brustle O., Schramm J., Elger C.E., Wiestler O.D. Increase of nestin-immunoreactive neural precursor cells in the dentate gyrus of

pediatric patients with early-onset temporal lobe epilepsy. Hippocampus. 2001;11:311–321.

▪ Boldrini M, *et al.* (2018) Human Hippocampal Neurogenesis Persists throughout Aging. Cell Stem Cell 22(4):589-599 e585.

▪ Bonaguidi MA, *et al.* (2011) *In vivo* clonal analysis reveals self-renewing and multipotent adult neural stem cell characteristics. Cell 145(7):1142-1155.

▪ Bonfoco, E., Krainc, D., Ankarcrona, M., Nicotera, P., and Lipton, S.A. (1995). Apoptosis and necrosis: two distinct events induced, respectively, by mild and intens e insults with N-methyl-D-aspartate or nitric oxide/superoxide in cortical cell cultures. Proc Natl Acad Sci U S A 92, 7162-7166.

▪ Borsini A, Zunszain PA, Thuret S, Pariante CM. The role of inflammatory cytokines as key modulators of neurogenesis. Trends Neurosci. 2015;38:145–157.

▪ Bouilleret, V., Ridoux, V., Depaulis, A., Marescaux, C., Nehlig, A., and Le Gal La Salle, G. (1999). Recurrent seizures and hippocampal sclerosis following intrahippocampal kainate injection in adult mice: electroencephalography, histopathology and synaptic reorganization similar to mesial temporal lobe epilepsy. Neuroscience 89, 717-729.

▪ Bracko O., Singer T., Aigner S., Knobloch M., Winner B., Ray J. *et al.* (2012). Gene expression profiling of neural stem cells and their neuronal progeny reveals IGF2 as a regulator of adult hippocampal neurogenesis. J. Neurosci. 32 3376–3387.

▪ Braun, and Jessberger. Adult neurogenesis: mechanisms and functional significance Development, 141 (2014), pp. 1983-1986.

▪ Breunig JJ, Silbereis J, Vaccarino FM, Sestan N, Rakic P. Notch regulates cell fate and dendrite morphology of newborn neurons in the postnatal dentate gyrus. Proc Natl Acad Sci U S A. 2007;104(51):20558–63.

▪ Brunklaus, R. Ellis, E. Reavey, G.H. Forbes, S.M. ZuberiPrognostic, clinical and demographic features in SCN1A mutation-positive Dravet syndrome Brain, 135 (2012), pp. 2329-2336.

▪ Bustin, S.A., Benes, V., Garson, J.A., Hellemans, J., Huggett, J., Kubista, M., Mueller, R., Nolan, T., Pfaffl, M.W., S hipley, G.L. , *et al.* (2009). The MIQE guidelines: minimum information for publication of quantitative real -time PCR experiments. Clinical chemistry 55, 611-622.

▪ Cameron HA & McKay RD (1999) Restoring production of hippocampal neurons in old age. Nat Neurosci 2(10):894-897.

▪ Cameron HA, Gould E(1994) Adult neurogenesis is regulated by adrenal steroids in the dentate gyrus. Neuroscience 61:203–209.

▪ Campbell IL, Abraham CR, Masliah E, Kemper P, Inglis JD, Oldstone MB, Mucke L (1993) Neurologic disease induced in transgenic mice by the cerebral overexpression of interleukin 6. Proc Natl Acad Sci U S A 90:10061–10065,

- Carpentier PA, Palmer TD. Immune influence on adult neural stem cell regulation and function. Neuron. 2009;64:79–92.

- Catterall WA, Dib-Hajj S, Meisler MH, Pietrobon D. Inherited neuronal ion channelopathies: new windows on complex neurological diseases. J Neurosci. 2008;28:11768–11777.

- Cendes, F. (2005). Mesial temporal lobe epilepsy syndrome: an updated overview. Journal of Epilepsy and Clinical Neurophysiology 11, 141-144.

- Chabardes S., Kahane P., Minotti L., Tassi L., Grand S., Hoffmann D., Benabid A. L. (2005). The temporopolar cortex plays a pivotal role in temporal lobe seizures. Brain 128, 1818–183110.1093/brain/awh512.

- Cheah CS, Yu FH, Westenbroek RE, Kalume FK, Oakley JC, Potter GB *et al.* Specific deletion of NaV1.1 sodium channels in inhibitory interneurons causes seizures and premature death in a mouse model of Dravet syndrome. Proc Natl Acad Sci USA 2012; 109: 14646–51.

- Cipriani S, *et al.* (2018) Hippocampal Radial Glial Subtypes and Their Neurogenic Potential in Human Fetuses and Healthy and Alzheimer's Disease Adults. Cerebral cortex (New York, N Y: 1991).

- Clelland CD, Choi M, Romberg C, Clemenson GD, Jr, Fragniere A, Tyers P, Jessberger S, Saksida LM, Barker RA, Gage FH, Bussey TJ. A functional role for adult hippocampal neurogenesis in spatial pattern separation. Science. 2009;325:210–213.

- Crunelli, V., Carmignoto, G., and Steinhauser, C. (2015). Novel astrocyte targets: new avenues for the therapeutic treatment of epilepsy. Neuroscientist 21, 62-83.

- Curia, G., Longo, D ., Biagini, G., Jones, R.S., and Avoli, M. (2008). The pilocarpine model of temporal lobe epilepsy. Journal of neuroscience methods 172, 143-157.

- D.W. Choi, M. Maulucci-Gedde, A.R. KriegsteinGlutamate neurotoxicity in cortical cell cultura J. Neurosci., 7 (1987), pp. 357-368.

- Dantzer R. Cytokine, sickness behavior, and depression. Immunol Allergy Clin North Am. 2009 May;29(2):247-64. doi: 10.1016/j.iac.2009.02.002.

- Deisseroth K, Singla S, Toda H, Monje M, Palmer TD, Malenka RC. 2004. Excitation-neurogenesis coupling in adult neural stem/progenitor cells. Neuron 42: 535–552.

- Del Bigio MR. (1999) Proliferative status of cells in adult human dentate gyrus. Microsc Res Tech 45:353–358.

- Deng W, Saxe MD, Gallina IS, Gage FH. Adult-born hippocampal dentate granule cells undergoing maturation modulate learning and memory in the brain. J. Neurosci. 2009;29:13532–13542.

- Dennis CV, Suh LS, Rodriguez ML, Kril JJ, & Sutherland GT (2016) Human adult neurogenesis across the ages: An immunohistochemical study. Neuropathology and applied neurobiology 42(7):621-638.

- Depienne C, Trouillard O, Saint-Martin C, Gourfinkel-An I, Bouteiller D, Carpentier W, *et al.* Spectrum of SCN1A gene mutations associated with Dravet syndrome: analysis of 333 patients. J Med Genet. 2009b;46:183–91.

- Dravet C. (1978) Les épilepsies graves de l'enfant. Vie Médicale 8:543–548.

- Dupret D, Revest JM, Koehl M, Ichas F, De Giorgi F, Costet P, Abrous DN, Piazza PV. Spatial relational memory requires hippocampal adult neurogenesis. PLoS One. 2008;3:e1959.

- Dutton SB, Makinson CD, Papale LA, Shankar A, Balakrishnan B, Nakazawa K, *et al.* Preferential inactivation of Scn1a in parvalbumin interneurons increases seizure susceptibility. Neurobiol Dis 2012; 49C: 211–20.

- Duveau, V., Pouyatos, B., Bressand, K., Bouyssieres, C., Chabrol, T., Roche, Y., Depaulis, A., and Roucard,C. (2016). Differential Effects of Antiepileptic Drugs on Focal Seizures in the Intrahippocampal Kainate Mouse Model of Mesial Temporal Lobe Epilepsy. CNS Neurosci Ther 22, 497-506.

- E. Sahin, R.A. DepinhoLinking functional decline of telomeres: mitochondria and stem cells during ageing Nature, 464 (7288) (2010), pp. 520-52.

- Eckenhoff MMF, Rakic PP. Radial organization of the hippocampal dentate gyrus: a Golgi, ultrastructural, and immunocytochemical analysis in the developing rhesus monkey. Journal of comparative neurology. 1984;223:1–21.

- Edwards FA, Gibb AJ, Colquhoun D. ATP receptor-mediated synaptic currents in the central nervous system. Nature. 1992;359:144–147.

- Ekdahl CT, Claasen JH, Bonde S, Kokaia Z, & Lindvall O (2003) Inflammation is detrimental for neurogenesis in adult brain. Proc Natl Acad Sci U S A 100(23):13632-13637.

- Ekdahl, C.T., Mohapel, P., Elmer, E., and Lindvall, O. (2001). Caspase inhibitors increase short-term survival of progenitor -cell progeny in the adult rat dentate gyrus following status epilepticus. Eur J Neurosci 14, 937-945.

- Ekdahl, C.T., Zhu, C., Bonde, S., Bahr, B.A., Blomgren, K., and Lindvall, O. (2003b). Death mechanisms in status epilepticus-generated neurons and effects of additional seizures on their survival. Neurobiol Dis 14, 513-523.

- Encinas JM & Sierra A (2012) Neural stem cell deforestation as the main force driving the age-related decline in adult hippocampal neurogenesis. Behavioural brain research 227(2):433-439.

- Encinas JM, Enikolopov G. Identifying and quantitating neural stem and progenitor cells in the adult brain. Methods Cell Biol. 2008;85:243–272.

- Encinas JM, Michurina TV, Peunova N, Park JH, Tordo J, Peterson DA, Fishell G, Koulakov A, Enikolopov G. (2011) Division-coupled astrocytic differentiation and age-related depletion of neural stem cells in the adult hippocampus. Cell Stem Cell 8(5):566-579.

- Encinas JM, Hamani C, Lozano AM, Enikolopov G. Neurogenic hippocampal targets of deep brain stimulation. J. Comp. Neurol. 2011a;519:6–20.

- Encinas JM, Vaahtokari A, & Enikolopov G (2006) Fluoxetine targets early progenitor cells in the adult brain. Proc Natl Acad Sci U S A 103(21):8233-8238.

- Encinas, J.M., and Enikolopov, G. (2008). Identifying and quantitating neural stem and progenitor cells in the adult brain. Methods Cell Biol 85, 243-272.

- Encinas, J.M., Michurina, T.V., Peunova, N., Park, J.H., Tordo, J., Peterson, D.A., Fishell, G., Koulakov, A., and Enikolopov, G. (2011). Division-coupled astrocytic differentiation and age-related depletion of neural stem Cells in the adult hippocampus. Cell Stem Cell 8, 566-579.

- Enikolopov G, Overstreet-Wadiche L. Transgenic reporter lines for studying adult neurogenesis. In: Gage GKF, Song H, editors. Adult Neurogenesis. CSHL Press; 2008. Hayes NL, Nowakowski RS. Dynamics of cell proliferation in the adult dentate gyrus of two inbred strains of mice. Brain Res Dev Brain Res. 2002;134:77–85.

- Eriksson PS, *et al.* (1998) Neurogenesis in the adult human hippocampus. Nat Med 4(11):1313-1317.

- Evans RJ, Derkach V, Surprenant A. 1992. ATP mediates fast synaptic transmission in mammalian neurons. Nature 357:503–505.

- Eyo, U.B., Murugan, M., and Wu, L.J. (2017). Microglia-Neuron Communication in Epilepsy. Glia 65, 5-18.

- Farioli-Vecchioli S, *et al.* (2008) The timing of differentiation of adult hippocampal neurons is crucial for spatial memory. PLoS Biol 6(10):e246.

- Fensterl, V. and G.C. Sen, Interferons and viral infections. Biofactors, 2009. 35(1): p. 14-20.

- Ferraro, T.N., Dlugos, D.J., Hakonarson, H., and Buono, R.J. (2012). Strategies for studying the epilepsy genome. In Jasper's basic mechanisms of the epilepsies, J.L. Noebels, M. Avoli, M.A. Rogawski, R.W. Olsen, and A.V. Delgado-Escueta, eds. (Oxford university press).

- Ferreira TA *et al.*(2014) Neuronal morphometry directly from bitmap images. Nat Methods 11(10):982-984.

- Ferrero -Miliani, L., Nielsen, O.H., Andersen, P.S., and Girardin, S.E. (2007). Chronic inflammation: importance of NOD2 and NALP3 in interleukin -1beta generation. Clin Exp Immunol 147, 227-235.

- Filippov V, *et al.* (2003) Subpopulation of nestin-expressing progenitor cells in the adult murine hippocampus shows electrophysiological and morphological characteristics of astrocytes. Molecular and cellular neurosciences 23(3):373-382.

- Fisher, R.S., Cross, J.H., French, J.A., Higurashi, N., Hirsch, E., Jansen, F.E., Lagae, L., Moshe, S.L., Peltola, J., Roulet Perez, E., *et al.* (2017). Operational classification of seizure types by the International League Against Epilepsy: Position Paper of the ILAE Commission for Classification and Terminology. Epilepsia 58, 522-530.

- Fisher, R.S., van Emde Boas, W., Blume, W., Elger, C., Genton, P., Lee, P., and Engel, J., Jr. (2005). Epileptic seizures and epilepsy: definitions proposed by the International League Against Epilepsy (ILAE) and the International Bureau for Epilepsy (IBE). Epilepsia 46, 470-472.

- Flores, M.A. BlascoThe role of telomeres and telomerase in stem cell aging FEBS Lett, 584 (17) (2010), pp. 3826-3830.

- Fukuda S, Kato F, Tozuka Y, Yamaguchi M, Miyamoto Y, Hisatsune T. Two distinct subpopulations of nestin-positive cells in adult mouse dentate gyrus. J. Neurosci. 2003;23:9357–9366.

- G. Li, S.J. PleasureMorphogenesis of the dentate gyrus: what we are learning from mouse mutants. Developmental Neuroscience, 27 (2005), pp. 93-99.

- Gaitatzis, A., Johnson, A.L., Chadwick, D.W., Shorvon, S.D., and Sander, J.W. (2004). Life expectancy in people with newly diagnosed epilepsy. Brain 127, 2427-2432.

- Gall C. M. (1993) Seizure-induced changes in neurotrophin expression: implications for epilepsy. Exp. Neurol.124, 150–166.

- Gargaro AC, Sakamoto AC, Bianchin MM, Geraldi C de VL, Scorsi-Rosset S, Coimbra ER, *et al.* Atypical neuropsychological profiles and cognitive Outcome in mesial temporal lobe epilepsy. Epi- lepsy Behav. 2013;27:461— 9.

- Gebara E, *et al.* (2016) Heterogeneity of Radial Glia-Like Cells in the Adult Hippocampus. Stem Cells 34(4):997-1010.

- Gebara E, Sultan S, Kocher-Braissant J, & Toni N (2013) Adult hippocampal neurogenesis inversely correlates with microglia in conditions of voluntary running and aging. Frontiers in neuroscience 7:145.

- Gemma C, Bachstetter AD, Cole MJ, Fister M, Hudson C, Bickford PC. Blockade of caspase-1 increases neurogenesis in the aged hippocampus. Eur J Neurosci. 2007;26:2795–2803.

- Genton P, Velizarova R, Dravet C. Dravet syndrome: the long-term outcome. Epilepsia 2011;52(Suppl 2):44-49.

- Giachino C, Barz M, Tchorz JS, Tome M, Gassmann M, Bischofberger J, Bettler B, Taylor V. (2014) GABA suppresses neurogenesis in the adult hippocampus through GABAB receptors. Development 141(1):83-90.

- Gong, S., Zheng, C., Doughty, M.L., Losos, K., Didkovsky, N., Schambra, U.B., Nowak, N.J., Joyner, A., Leblanc, G., Hatten, M.E., *et al.* (2003). A gene expression atlas of the central nervous system based on bacterial artificial chromosomes. Nature 425, 917-925.

- Greve MW and Zink BJ, 2009, 'Pathophysiology of traumatic brain injury', Mount Sinai Journal of Medicine, vol. 76, pp. 97-104.

- Guangnan Li, Li Fang, Gloria Fernández, and Samuel J. Pleasure . The ventral hippocampus is the embryonic origin for adult neural stem cells in the dentate gyrus Neuron. 2013 May 22; 78(4): 658–672.

- Guentchev M, McKay RD. Notch controls proliferation and differentiation of stem cells in a dose-dependent manner. Eur J Neurosci. 2006;23:2289–2296.

- Harkin LA, Bowser DN, Dibbens LM, Singh R, Phillips F, Wallace RH, Richards MC, Williams DA, Mulley JC, Berkovic SF, Scheffer IE, Petrou S. Truncation of the GABA(A)-receptor gamma2 subunit in a family with generalized epilepsy with febrile seizures plus. Am J Hum Genet. 2002;70:530–536.

- Hattiangady B, Rao MS, Shetty AK. Chronic temporal lobe epilepsy is associated with severely declined dentate neurogenesis in the adult hippocampus. Neurobiol. Dis. 2004;17:473–490.

- Heinrich C, Lahteinen S, Suzuki F, Anne-Marie L, Huber S, Haussler U, Haas C, Larmet Y, Castren E, Depaulis A. (2011) Increase in BDNF- mediated TrkB signaling promotes epileptogenesis in a mouse model of mesial temporal lobe epilepsy.Neurobiol Dis 42:35–47.

- Heinrich C, Nitta N, Flubacher A, Müller M, Fahrner A, Kirsch M, Freiman T, Suzuki F, Depaulis A, Frotscher M, Haas CA. Reelin deficiency and displacement of mature neurons, but not neurogenesis, underlie the formation of granule cell dispersion in the epileptic hippocampus. J. Neurosci. 2006;26:4701–4713.

- Heuser K1, Taubøll E, Nagelhus EA, Cvancarova M, Petter Ottersen O, Gjerstad L. Phenotypic characteristics of temporal lobe epilepsy: the impact of hippocampal sclerosis. Acta Neurol Scand Suppl. 2009;(189):8-13.

BIBLIOGRAPHY

- Hickey WF. Leukocyte traf fic in the central nervous system: the participants and their roles. Semin Immunol 1999; 11: 125–37.

- Hodge RD, Kowalczyk TD, Wolf SA, Encinas JM, Rippey C, Enikolopov G, Kempermann G, Hevner RF. Intermediate progenitors in adult hippocampal neurogenesis: Tbr2 expression and coordinate regulation of neuronal output. J Neurosci. 2008;28:3707–3717.

- Huttmann K, Sadgrove M, Wallraff A, Hinterkeuser S, Kirchhoff F, Steinhäuser C, Gray WP. (2003) Seizures preferentially stimulate proliferation of radial glia-like astrocytes in the adult dentate gyrus: functional and immunocytochemical analysis. Eur J Neurosci 18(10):2769-2778.

- Imayoshi, I., Sakamoto, M., Ohtsuka, T., Takao, K., Miyakawa, T., Yamaguchi, M., Mori, K., Ikeda, T., Itohara, S., and Kageyama, R. (2008). Roles of continuous neurogenesis in the structural and functional integrity of the adult forebrain. Nat Neurosci 11, 1153-1161.

- Isackson P. J., Huntsman M. M., Murray K. D. and Gall C. M. (1991) BDNF mRNA expression is increased in adult rat forebrain after limbic seizures: temporal patterns of induction distinct from NGF. Neuron 6 , 937–948.

- Altman, S.A. BayerDevelopment of the diencephalon in the rat. IV. Quantitative study of the time of origin of neurons and the internuclear chronological gradients in the thalamus. J. Comp. Neurol., 188 (1979), pp. 455-472.

- J. B. Aimone, W. Deng, and F. H. Gage. Resolving new memories: a critical look at the dentate gyrus, adult neurogenesis, and pattern separation. Neuron , 70(4):589–96, 2011.

- J.M. Long, A.N. Kalehua, N.J. Muth, M.E. Calhoun, M. Jucker, J.M. Hengemihle, *et al.*Stereological analysis of astrocyte and microglia in aging mouse hippocampus Neurobiol Aging, 19 (5) (1998), pp. 497-503.

- Jaiswal, M. K., and Keller, B. U. (2009). Cu/Zn superoxide dismutase typical for familial amyotrophic lateral sclerosis increases the vulnerability of mitocondria and perturbs Ca2+ homeostasis in SOD1G93A mice.Mol. Pharmacol. 75, 478–489. doi: 10.1124/mol.108.05083.

- Jessberger S., Clark R. E., Broadbent N. J., Clemenson G. D., Jr., Consiglio A., Lie D. C., *et al.* (2009). Dentate gyrus-specific knockdown of adult neurogenesis impairs spatial and object recognition memory in adult rats. Learn. Mem. 16, 147–154 10.1101/lm.1172609.

- Kalume F, Westenbroek RE, Cheah CS, Yu FH, Oakley JC, Scheuer T, *et al.* Sudden unexpected death in a mouse model of Dravet syndrome. J Clin Invest 2013; 123: 1798–808.

- kamoto M, Inoue K, Iwamura H, Terashima K, Soya H, Asashima M, Kuwabara T. Reduction in paracrine Wnt3 factors during aging causes impaired adult neurogenesis. FASEB J. 2011;25:3570–3582.

▪ Kan, A.A., van Erp, S., Derijck, A.A., de Wit, M., Hessel, E.V., O'Duibhir, E., de Jager, W., Van Rijen, P.C., Gosselaar, P.H., de Graan, P.N., *et al.* (2012b). Genome-wide microRNA profiling of human temporal lobe epilepsy identifies modulators of the immune response. Cellular and molecular life sciences: CMLS 69, 3127-3145.

▪ Kaneko N, *et al.* (2006) Suppression of cell proliferation by interferon-alpha through interleukin-1 production in adult rat dentate gyrus. Neuropsychopharmacology: official publication of the American College of Neuropsychopharmacology 31(12):2619-2626.

▪ Kempermann G, Gage FH, Aigner L, Song H, Curtis MA, Thuret S, Kuhn HG, Jessberger S, Frankland PW, Cameron HA, Gould E, Hen R, Abrous DN, Toni N, Schinder AF, Zhao X, Lucassen PJ, Frisén J (2018) Human adult neurogenesis: evidence and remaining questions. Cell Stem Cell doi:10.1016/j.stem.2018.04.004.

▪ Kempermann G, Jessberger S, Steiner B, & Kronenberg G (2004) Milestones of neuronal development in the adult hippocampus. Trends Neurosci 27(8):447-452.

▪ Kempermann G, Kuhn HG, & Gage FH (1998) Experience-induced neurogenesis in the senescent dentate gyrus. The Journal of neuroscience: the official journal of the Society for Neuroscience 18(9):3206-3212.

▪ Kettenmann, H., F. Kirchhoff, and A. Verkhratsky, Microglia: new roles for the synaptic stripper. Neuron, 2013. 77(1): p. 10-8.

▪ Kim KY, Hysolli E, Park IH. 2011. Neuronal maturation defect in induced pluripotent stem cells from patients with Rett syndrome. Proc Natl Acad Sci U S A 108:14169–14174.

▪ Knobloch M., Braun S.M.G., Zurkirchen L., von Schoultz C., Zamboni N., Araúzo-Bravo M.J., Kovacs W.J., Karalay O., Suter U., Machado R.A. Metabolic control of adult neural stem cell activity by Fasn-dependent lipogenesis. Nature. 2013;493:226–230.

▪ Knoth R, *et al.* (2010) Murine features of neurogenesis in the human hippocampus across the lifespan from 0 to 100 years. PloS one 5(1):e8809.

▪ Knuesel, M.T., Meyer, K.D., Donner, A.J., Espinosa, J.M., Taatjes, D.J.(2009) The human CDK8 subcomplex is a histone kinase that requires Med12 for activity and can function independently of Mediator. Mol. Cell. Biol. 29:650–661.

▪ Korff CM, Nordli DR., Jr. Epilepsy syndromes in infancy. Pediatr Neurol. 2006;34:253–263.

▪ Kornack, D.R., and Rakic, P. (1999). Continuation of neurogenesis in the hippocampus of the adult macaque monkey. Proc Natl Acad Sci U S A 96, 5768-5773.

▪ Kosaka, T., and Hama, K. (1986). Three-dimensional structure of astrocytes in the rat dentate gyrus. J Comp Neurol 249, 242-260.

- Kralic JE, Ledergerber DA, Fritschy JM. Disruption of the neurogenic potential of the dentate gyrus in a mouse model of temporal lobe epilepsy with focal seizures. Eur. J. Neurosci. 2005;22:1916–1927.

- Kronenberg G, Reuter K, Steiner B, Brandt MD, Jessberger S, Yamaguchi M, Kempermann G. Subpopulations of proliferating cells of the adult hippocampus respond differently to physiologic neurogenic stimuli. J. Comp. Neurol. 2003;467:455–463.

- Kuhn HG, Dickinson-Anson H, & Gage FH (1996) Neurogenesis in the dentate gyrus of the adult rat: age-related decrease of neuronal progenitor proliferation. J Neurosci 16(6):2027-2033.

- Kwon, M.J., Oh, E., Lee, S., Roh, M.R., Kim, S.E., Lee, Y., Choi, Y.L., In, Y.H., Park, T., Koh, S.S., *et al.* (2009). Identification of novel reference genes using multiplatform expression data and their validation for quantitative gene expression analysis. PLoS One 4, e6162.

- L.C. PlataniasMechanisms of type-I- and type-II-interferon-mediated signalling Nat. Rev. Immunol., 5 (2005), pp. 375-386.

- Lagace DC, Whitman MC, Noonan MA, Ables JL, DeCarolis NA, Arguello AA, Donovan MH, Fischer SJ, Farnbauch LA, Beech RD, *et al.* Dynamic contribution of nestin-expressing stem cells to adult neurogenesis. J. Neurosci. 2007;27:12623–12629.
- Legido, A., and Katsetos, C.D. (2014). Experimental studies in epilepsy: immunologic and inflammatory mechanisms. Semin Pediatr Neurol 21, 197-206.

- Lendahl, U., Zimmerman, L.B., and McKay, R.D. (1990). CNS stem cells express a new class of intermediate filament protein. Cell 60, 585-595.

- Leuner B, Kozorovitskiy Y, Gross CG, Gould E. Diminished adult neurogenesis in the marmoset brain precedes old age. Proc Natl Acad Sci U S A. 2007;104:17169–17173.

- Levesque, M., and Avoli, M. (2013). The kainic acid model of temporal lobe epilepsy. Neurosci Biobehav Rev 37, 2887-2899.

- Li L & Clevers H (2010) Coexistence of quiescent and active adult stem cells in mammals. Science 327(5965):542-545.

- Licht T, Rothe G, Kreisel T, Wolf B, Benny O, Rooney AG French-Constant C, Enikolopov G, Keshet E. VEGF preconditioning leads to stem cell remodeling and attenuates age-related decay of adult hippocampal neurogenesis. Proc Natl Acad Sci U S A. 2016 Nov 29;113(48):E7828-E7836. Epub 2016 Nov 14.

- Lichtenwalner RJ, Forbes ME, Bennett SA, Lynch CD, Sonntag WE, Riddle DR. Intracerebro ventricular infusion of insulin-like growth factor-I ameliorates the age-related decline in hippocampal neurogenesis. Neuroscience. 2001;107(4):603–613.

BIBLIOGRAPHY

▪ Loftis, J.M., M. Huckans, and B.J. Morasco, Neuroimmune mechanisms of cytokine-induced depression: current theories and novel treatment strategies. Neurobiol Dis, 2010. 37(3): p. 519-33.

▪ Lois, C., and Alvarez-Buylla, A. (1993). Proliferating subventricular zone cells in the adult mammalian forebrain can differentiate into neurons and glia. Proc Natl Acad Sci U S A 90, 2074-2077.

▪ Lucas, S.M., Rothwell, N.J., and Gibson, R.M. (2006). The role of inflammation in CNS injury and disease. British journal of pharmacology 147 Suppl 1, S232-240.

▪ Lugert S, Basak O, Knuckles P, Haussler U, Fabel K, Götz M, Haas CA, Kempermann G, Taylor V, Giachino C. Quiescent and active hippocampal neural stem cells with distinct morphologies respond selectively to physiological and pathological stimuli and aging. Cell Stem Cell. 2010;6:445–456.

▪ Lurton D, El Bahh B, Sundstrom L, Rougier A. Granule cell dispersion is correlated with early epileptic events in human temporal lobe epilepsy. Journal of Neurological Science. 1998;154:133–136.

▪ Lynch MA (2010) Age-related neuroinflammatory changes negatively impact on neuronal function. Front Aging Neurosci 1:6.

▪ Lynch, M.A., 1998. Age-related impairment in long-term potentiation in hippocampus: a role for the cytokine, interleukin-1 beta? Prog Neurobiol. 56,571-89.

▪ Marini C, Scheffer IE, Nabbout R, Mei D, Cox K, Dibbens LM, *et al.* SCN1A duplications and deletions detected in Dravet syndrome: implications for molecular diagnosis. Epilepsia. 2009;50:1670–8.

▪ Martynoga B., Mateo J. L., Zhou B., Andersen J., Achimastou A., Urbán N., *et al.* . (2013). Epigenomic enhancer annotation reveals a key role for NFIX in neural stem cell quiescence. Genes Dev. 27, 1769–1786. 10.1101/gad.216804.113.

▪ Mathern GW, Leiphart JL, De Vera A, Adelson PD, Seki T, Neder L, Leite JP. (2002) Seizures decrease postnatal neurogenesis and granule cell development in the human fascia dentata. Epilepsia 43(Suppl 5):68–73.

▪ McKhann, G.M., 2nd, Wenzel, H.J., Robbins, C.A., Sosunov, A.A., and Schwartzkroin, P.A. (2003). Mouse strain differences in kainic acid sensitivity, seizure behavior, mortality, and hippocampal pathology. Neuroscience 122, 551-561.

▪ Mignone, J.L., Kukekov, V., Chiang, A.S., Steindler, D., and Enikolopov, G. (2004). Neural stem and progenitor cells in nestin-GFP transgenic mice. J Comp Neurol 469, 311-324.

▪ Mikkonen M, Soininen H, Kalvianen R, Tapiola T, Ylinen A, Vapalahti M, Paljarvi L, Pitkanen A. Remodeling of neuronal circuitries in human temporal lobe epilepsy: increased expression of highly polysialylated neural cell adhesion molecule in the hippocampus and the entorhinal cortex. Ann Neurol. 1998;44:923–934.

- Mira H, *et al.* (2010) Signaling through BMPR-IA regulates quiescence and long-term activity of neural stem cells in the adult hippocampus. Cell Stem Cell 7(1):78-89.

- Miranda CJ, Braun L, Jiang Y, Hester ME, Zhang L, Riolo M, Wang H, Rao M, Altura RA, Kaspar BK. Aging brain microenvironment decreases hippocampal neurogenesis through Wnt-mediated survivin signaling. Aging Cell. 2012;11:542–552.

- Monje ML, Mizumatsu S, Fike JR, Palmer TD. Irradiation induces neural precursor-cell dysfunction. Nat Med. 2002;8:955–962.

- Monje, M.L., H. Toda, and T.D. Palmer, Inflammatory blockade restores adult hippocampal neurogenesis. Science, 2003. 302(5651): p. 1760-5.

- Morrison, S. J., and Spradling, A. C. (2008). Stem cells and niches: mechanisms that promote stem cell maintenance throughout life. Cell 132, 598–611. doi: 10.1016/j.cell.2008.01.038.
- Mullen SA, Scheffer IE. Translational research in epilepsy genetics – sodium channels in man to interneuronopathy in mouse. Arch Neurol. 2009;66:21–6.

- Munoz-Fernandez MA, Fresno M (1998). The role of tumour necrosis factor, interleukin 6, interferon-gamma and inducible nitric oxide synthase in the development and pathology of the nervous system. Prog Neurobiol 56: 307–340.

- Nakahira E, Yuasa S. Neuronal generation, migration, and differentiation in the mouse hippocampal primoridium as revealed by enhanced green fluorescent protein gene transfer by means of in utero electroporation. J Comp Neurol. 2005;483:329–340.

- Nakanishi M., Niidome T., Matsuda S., Akaike A., Kihara T. and Sugimoto H. (2007) Microglia-derived interleukin-6 and leukaemia inhibitory factor promote astrocytic differentiation of neural stem/progenitor cells. Eur. J. Neurosci. 25, 649–658.

- Nakashiba, T., *et al.*, Young dentate granule cells mediate pattern separation, whereas old granule cells facilitate pattern completion. Cell, 2012. 149(1): p. 188-201.

- Nayak, D., Roth, T.L., and McGavern, D.B. (2014). Microglia development and function. Annu Rev Immunol 32, 367-402.

- Ngwenya LB, Heyworth NC, Shwe Y, Moore TL, & Rosene DL (2015) Age-related changes in dentate gyrus cell numbers, neurogenesis, and associations with cognitive impairments in the rhesus monkey. Front Syst Neurosci 9:102.

- Nitta N, Heinrich C, Hirai H, Suzuki F. Granule cell dispersion develops without neurogenesis and does not fully depend on astroglial cell generation in a mouse model of temporal lobe epilepsy. Epilepsia. 2008;49:1711–1722.

- Njie E. G., Boelen E., Stassen F. R., Steinbusch H. W., Borchelt D. R., Streit W. J. (2012). Ex vivo cultures of microglia from young and aged rodent brain reveal age-related changes in microglial function. Neurobiol. Aging 33 195 e191–e112 10.1016/j.neurobiolaging.2010.05.008.

BIBLIOGRAPHY

- O'Callaghan JP, Miller DB, Reinhard JF., Jr Characterization of the origins of astrocyte response to injury using the dopaminergic neurotoxicant, 1-methyl-4-phenyl-1,2,3,6-tetrahydropyridine. Brain Res. 1990;521:73–80.

- Oguni H, Hayashi K, Osawa M, Awaya Y, Fukuyama Y, Fukuma G, Hirose S, Mitsudome A, Kaneko S. Severe myoclonic epilepsy in infancy: clinical analysis and relation to SCN1A mutations in a Japanese cohort. Adv Neurol. 2005;95:103–117.

- Olariu A, Cleaver KM, Cameron HA. Decreased neurogenesis in aged rats results from loss of granule cell precursors without lengthening of the cell cycle. J Comp Neurol. 2007;501:659–667.

- Opal, S.M. and DePalo, V.A. (2000) Anti-inflammatory cytokines. Chest, 117, 1162-1172. doi10.1378/chest.117.4.1162.

- Orrenius, S., Zhivotovsky, B., and Nicotera, P. (2003). Regulation of cell death: the calcium-apoptosis link. Nat Rev Mol Cell Biol 4, 552-565.

- Ortega-Martínez, S., Trejo, J.L., 2015. The postnatal origin of adult neural stem cells and the effects of glucocorticoids during their genesis. Behav. Brain. Res., 279, 166-176.

- Ourednik J, Ourednik V, Lynch WP, *et al.* Neural stem cells display an inherent mechanism for rescuing dysfunctional neurons. Nat Biotechnol. 2002;20:1103–10.

- P.R. Mouton, J.M. Long, D.L. Lei, V. Howard, M. Jucker, M.E. Calhoun, *et al.*Age and gender effects on microglia and astrocyte numbers in brains of mice Brain Res, 956 (1) (2002), pp. 30-35.

- Pantarelli L, Saxe M, Gross C, Surget A, Battaglia F, Dulawa S, Weisstaub N, Lee J, Duman R, Arancio O, *et al.* Requirement of hippocampal neurogenesis for the behavioral effects of antidepressants. Science. 2003;301:805–809.

- Parent JM, Elliott RC, Pleasure SJ, Barbaro NM, Lowenstein DH. Aberrant seizure-induced neurogenesis in experimental temporal lobe epilepsy. Ann. Neurol. 2006;59:81–91.

- Patino GA, Claes LR, Lopez-Santiago LF, Slat EA, Dondeti RS, Chen C, O'Malley HA, Gray CB, Miyazaki H, Nukina N, Oyama F, De Jonghe P, Isom LL. A functional null mutation of SCN1B in a patient with DS. J Neurosci. 2009;29:10764–10778.

- Pechnick, S. Zonis, K. Wawrowsky, J. Pourmorady, V. Chesnokovap21Cip1 restricts neuronal proliferation in the subgranular zone of the dentate gyrus of the hippocampus.

- Perera TD, *et al.* (2011) Necessity of hippocampal neurogenesis for the therapeutic action of antidepressants in adult nonhuman primates. PloS one 6(4):e17600.

- Pernhorst, K., Herms, S., Hoffmann, P., Cichon, S., Schulz, H., Sander, T., Schoch, S., Becker, A.J., and Grote, A. (2013). TLR4, ATF-3 and IL8 inflammation mediator expression correlates with seizure frequency in human epileptic brain tissue. Seizure 22, 675-678.

- Pernot, F., Heinrich, C., Barbier, L., Peinnequin, A., Carpentier, P., Dhote, F., *et al.* (2011). Inflammatory changes during epileptogenesis and spontaneous seizures in a mouse model of mesiotemporal lobe epilepsy. Epilepsia 52, 2315–2325. doi: 10.1111/j.1528-1167.2011.03273.

- Pickering, M., Cumiskey, D., and O'Connor, J.J. (2005). Actions of TNF-alpha on glutamatergic synaptic transmission in the central nervous system. Exp Physiol 90, 663-670.

- Pilegaard K, Ladefoged O. Total number of astrocytes in the molecular layer of the dentate gyrus of rats at different ages. Anal Quant Cytol Histol. 1996;18:279–285.

- Pilz G-A, *et al.* (2018) Live imaging of neurogenesis in the adult mouse hippocampus. Science (New York, N Y) 359(6376):658-662.

- Pirttilä TJ, Manninen A, Jutila L, Nissinen J, Kälviäinen R, Vapalahti M, Immonen A, Paljärvi L, Karkola K, Alafuzoff I, *et al.* Cystatin C expression is associated with granule cell dispersion in epilepsy. Ann. Neurol. 2005;58:211–223.

- Pleasure S. J., Collins A. E., Lowenstein D. H.(2000). Unique expression patterns of cell fate molecules delineate sequential stages of dentate gyrus development. J. Neurosci. 20, 6095-6105.

- Pluchino S, Quattrini A, Brambilla E, Gritti A, Salani G, Dina G, Galli R, Del CU, Amadio S, Bergami A, Furlan R, Comi G, Vescovi AL, Martino G. Injection of adult neurospheres induces recovery in a chronic model of multiple sclerosis. Nature. 2003;422:688–694.

- Prolla TA (2002) DNA microarray analysis of the aging brain. Chem Senses 27:299–306.

- Quirico-Santos, T., Meira, I.D., Gomes, A.C., Pereira, V.C., Pinto, M., Monteiro, M., Souza, J.M., and Alves -Leon, S.V. (2013). Resection of the epileptogenic lesion abolishes seizures and reduces inflammatory cytokines of patients with temporal lobe epilepsy. Journal of neuroimmunology 254, 125- 130.

- Rassendren, F., and Audinat, E. (2016). Purinergic signaling in epilepsy. Journal of neuroscience research 94, 781-793.

- Ravizza, T., Balosso, S., and Vezzani, A. (2011). Inflammation and prevention of epileptogenesis. Neurosci Lett 497, 223-230.

- Renault V. M., Rafalski V. A., Morgan A. A., Salih D. A., Brett J. O., Webb A. E., *et al.* . (2009). FoxO3 regulates neural stem cell homeostasis. Cell Stem Cell 5, 527–539. 10.1016/j.stem.2009.09.014.

- Riban V, Bouilleret V, Pham-Lê BT, Fritschy JM, Marescaux C, Depaulis A. Evolution of hippocampal epileptic activity during the development of hippocampal sclerosis in a mouse model of temporal lobe epilepsy. Neuroscience. 2002;112:101–111.

BIBLIOGRAPHY

- Rickmann M, Amaral DG, Cowan WM. Organization of radial glial cells during the development of the rat dentate gyrus. J. Comp. Neurol. 1987;264:449–479.

- Rolls A., Shechter R., London A., Ziv Y., Ronen A., Levy R., *et al.* (2007). Toll-like receptors modulate adult hippocampal neurogenesis. Nat. Cell Biol. 9, 1081–1088 10.1038/ncb1629.

- Rubinstein M, Westenbroek RE, Yu FH, Jones CJ, Scheuer T, Catterall WA. Genetic background modulates impaired excitability of inhibitory neurons in a mouse model of Dravet syndrome. Neurobiol Dis 2014; 73C: 106–17.

- Russo I, Barlati S, Bosetti F. Effects of neuroinflammation on the regenerative capacity of brain stem cells. Journal of Neurochemistry. 2011;116:947–956.

- S. Guo, M. Liu, R.R. Gonzalez-PerezRole of Notch and its oncogenic signaling crosstalk in breast cáncer Biochim. Biophys. Acta, 1815 (2011), p. 197.

- S.D. Tyner, S. Venkatachalam, J. Choi, S. Jones, N. Ghebranious, H. Igelmann, *et al.*p53 mutant mice that display early ageing-associated phenotypesNature, 415 (6867) (2002), pp. 45-53.

- Sahay A, Wilson DA, Hen R. Pattern separation: a common function for new neurons in hippocampus and olfactory bulb. Neuron. 2011;70:582–588.

- Sakauchi M, Oguni H, Kato I, Osawa M, Hirose S, *et al.* Mortality in Dravet syndrome: search for risk factors in Japanese patients. Epilepsia. 2011;52(2):50–4.

- Santarelli L, *et al.* (2003) Requirement of hippocampal neurogenesis for the behavioral effects of antidepressants. Science 301(5634):805-809.

- Savage, N. (2014). Epidemiology: The complexities of epilepsy. Nature 511, S2-3.

- Saxe MD, *et al.* (2006) Ablation of hippocampal neurogenesis impairs contextual fear conditioning and synaptic plasticity in the dentate gyrus. Proc Natl Acad Sci U S A 103(46):17501-17506.

- Scheff SW, Sullivan PG (1999) Cyclosporin A significantly ameliorates cortical damage following experimental traumatic brain injury in rodents. J Neurotrauma 16:783–92.

- Scheffer IE. Does genotype determine phenotype? Sodium channel mutations in Dravet syndrome and GEFS+ Neurology. 2011;76:588–9.

- *Schindelin*, J., *et al. (2012*) Fiji An Open-Source Platform for Biological-Image Analysis. Nature Methods, 9, 676-682.

- Schuele, S.U., and Luders, H.O. (2008). Intractable epilepsy: management and therapeutic alternatives. The Lancet Neurology 7, 514-524.
- Segi-Nishida E, Warner-Schmidt JL, & Duman RS (2008) Electroconvulsive seizure and VEGF increase the proliferation of neural stem-like cells in rat hippocampus. Proc Natl Acad Sci U S A 105(32):11352-11357.

- Seki T., Arai Y. (1995). Age-related production of new granule cells in the adult dentate gyrus. Neuroreport 6, 2479–2482.

- Semerci F, Choi WT, Bajic A, Thakkar A, Encinas JM, Depreux F, Segil N, Groves AK, Maletic-Savatic M1,2,4,10. (2017) Lunatic fringe-mediated Notch signaling regulates adult hippocampal neural stem cell maintenance. Elife. 2017 Jul 12;6. pii: e24660. doi: 10.7554/eLife.24660.

- Seri B, Garcia-Verdugo JM, McEwen BS, & Alvarez-Buylla A (2001) Astrocytes give rise to new neurons in the adult mammalian hippocampus. J Neurosci 21(18):7153-7160.

- Seri, B., Garcia-Verdugo, J.M., Collado-Morente, L., McEwen, B.S., and Alvarez-Buylla, A. (2004). Cell types, lineage, and architecture of the germinal zone in the adult dentate gyrus. J Comp Neurol 478, 359-378.

- Sharma, A.K., Reams, R.Y., Jordan, W.H., Miller, M.A., Thacker, H.L., and Snyder, P.W. (2007). Mesial temporal lobe epilepsy: pathogenesis, induced rodent models and lesions. Toxicol Pathol 35, 984-999.

- Sicinski P, Donaher JL, Geng Y, Parker SB, Gardner H, Park MY, Robker RL, Richards JS, McGinnis LK, Biggers JD, *et al.* Cyclin D2 is an FSH-responsive gene involved in gonadal cell proliferation and oncogenesis. Nature. 1996;384:470–474.

- Sierra, A., Martin-Suarez, S., Valcarcel-Martin, R., Pascual-Brazo, J., Aelvoet, S.A., Abiega, O., Deudero, J.J., Brewster, A.L., Bernales, I., Anderson, A.E., *et al.* (2015). Neuronal hyperactivity accelerates depletion of neural stem cells and impairs hippocampal neurogenesis. Cell Stem Cell 16, 488-503.

- Sievers J, Hartmann D, Pehlemann FW, Berry M. Development of astroglial cells in the proliferative matrices, the granule cell layer, and the hippocampal fissure of the hamster dentate gyrus. J Comp Neurol. 1992;320:1–32.

- Sloane JA, Hollander W, Rosene DL, Moss MB, Kemper T, Abraham CR (2000) Astrocytic hypertrophy and altered GFAP degradation with age in subcortical white matter of the rhesus monkey. Brain Res 862, 1–10.

- Snyder JS, Soumier A, Brewer M, Pickel J, & Cameron HA (2011) Adult hippocampal neurogenesis buffers stress responses and depressive behaviour. Nature 476(7361):458-461.

- Sofroniew MV, Vinters HV. Astrocytes: biology and pathology. Acta Neuropathol. 2010;119:7–35.

- Sofroniew MV. Molecular dissection of reactive astrogliosis and glial scar formation. Trends Neurosci. 2009;32:638–647.

- Song J, *et al.* (2012) Neuronal circuitry mechanism regulating adult quiescent neural stem-cell fate decision. Nature 489(7414):150-154.

BIBLIOGRAPHY

- Sorrells SF, *et al.* (2018) Human hippocampal neurogenesis drops sharply in children to undetectable levels in adults. Nature 555(7696):377-381.

- Spalding KL, Bergmann O, Alkass K, Bernard S, Salehpour M, Huttner HB, Boström E, Westerlund I, Vial C, Buchholz BA, *et al.* Dynamics of hippocampal neurogenesis in adult humans. Cell. 2013;153:1219–1227.

- Spalding KL, Bhardwaj RD, Buchholz BA, Druid H, & Frisen J (2005) Retrospective birth dating of cells in humans. Cell 122(1):133-143.

- Streit WJ, *et al.* Dystrophic microglia in the aging human brain. Glia. 2004;45:208–12.

- Suh H, Consiglio A, Ray J, Sawai T, D'Amour KA, Gage FH. *In vivo* fate analysis reveals the multipotent and self-renewal capacities of Sox2+ neural stem cells in the adult hippocampus. Cell Stem Cell. 2007;1:515–528.

- Sullivan PG, Keller JN, Mattson MP, Scheff SW (1999b)Traumatic brain injury alters synaptic homeostasis: implications for impaired mitochondrial and transport function. J Neurotrauma 15:789–98.

- Suzuki F, Junier MP, Guilhem D, Sorensen JC, Onteniente B. (1995) Morphogenetic effect of kainate on adult hippocampal neurons associated with a prolonged expression of brain-derived neurotrophic factor. Neuroscience 64:665–674.

- Tai C, Abe Y, Westenbroek RE, Scheuer T, Catterall WA. Impaired excitability of somatostatin- and parvalbumin-expressing cortical interneurons in a mouse model of Dravet syndrome. Proc Natl Acad Sci USA 2014; 111: E3139–48.

- Tatum, W.O.t. (2012). Mesial temporal lobe epilepsy. J Clin Neurophysiol 29, 356-365.

- Thurman DJ, Beghi E, Begley CE, Berg AT, Buchhalter JR, Ding D, Hesdorffer DC, Hauser WA, Kazis L, Kobau R, Kroner B, Labiner D, Liow K, Logroscino G, Medina MT, Newton CR, Parko K, Paschal A, Preux PM, Sander JW, Selassie A, Theodore W, Tomson T, Wiebe S. (2011) Standards for epidemiologic studies and surveillance of epilepsy. Epilepsia 52(Suppl. 7):2–26.

- Van Praag H, Schinder AF, Christie BR, Toni N, Palmer TD, Gage FH. Functional neurogenesis in the adult hippocampus. Nature. 2002;415:1030–1034.

- Vezzani, A. (2009). Pilocarpine -induced seizures revisited: what does the model mimic? Epilepsy currents / American Epilepsy Society 9, 146-148.

- Vezzani, A., Conti, M., De Luigi, A., Ravizza, T., Moneta, D., Marchesi, F., and De Simoni, M.G. (1999). Interleukin-1beta immunoreactivity and microglia are enhanced in the rat hippocampus by focal kainate application: functional evidence for enhancement of electrographic seizures. J Neurosci 19, 5054-5065.

▪ Vezzani, A., Friedman, A., and Dingledine, R.J. (2013b). The role of inflammation in epileptogenesis. Neuropharmacology 69, 16-24.

▪ Volmering E., Niehusmann P., Peeva V., Grote A., Zsurka G., Altmuller J., *et al.* . (2016). Neuropathological signs of inflammation correlate with mitochondrial DNA deletions in mesial temporal lobe epilepsy. Acta Neuropathol. [Epub ahead of print]. 10.1007/s00401-016-1561-1.

▪ Walker, T.L., Overall, R.W., Vogler, S., Sykes, A.M., Ruhwald, S., Lasse, D., Ichwan, M., Fabel, K., and Kempermann, G. (2016). Lysophosphatidic Acid Receptor Is a Functional Marker of Adult Hippocampal Precursor Cells. Stem Cell Reports 6, 552-565.

▪ Walter J, Keiner S, Witte OW, & Redecker C (2011) Age-related effects on hippocampal precursor cell subpopulations and neurogenesis. Neurobiol Aging 32(10):1906-1914.

▪ Wang J-W, David DJ, Monckton JE, Battaglia F, & Hen R (2008) Chronic fluoxetine stimulates maturation and synaptic plasticity of adult-born hippocampal granule cells. The Journal of neuroscience : the official journal of the Society for Neuroscience 28(6):1374-1384.

▪ Whitney, N. P., Eidem, T. M., Peng, H., Huang, Y., and Zheng, J. C. (2009). Inflammation mediates varying effects in neurogenesis: relevance to the pathogenesis of brain injury and neurodegenerative disorders. J. Neurochem. 108, 1343–1359.

▪ Widera D., Mikenberg I., Elvers M., Kaltschmidt C., Kaltschmidt B. (2006). Tumor necrosis factor α triggers proliferation of adult neural stem cells via IKK/NF-κB signaling. BMC Neurosci. 7:64. 10.1186/1471-2202-7-64.

▪ Wieser HG and ILAE Commission on Neurosurgery of Epilepsy. Mesial temporal lobe epilepsy with hippocampal sclerosis. Epilepsia 2004; 45:695–714.

▪ Yu FH, Mantegazza M, Westenbroek RE, Robbins CA, Kalume F, Burton KA, Spain WJ, McKnight GS, Scheuer T, Catterall WA. Reduced sodium current in GABAergic interneurons in a mouse model of severe myoclonic epilepsy in infancy. Nat Neurosci. 2006;9:1142–1149.

▪ Zattoni M, Mura ML, Deprez F, Schwendener RA, Engelhardt B, Frei K, Fritschy JM. (2011) Brain infiltration of leukocytes contributes to the pathophysiology of temporal lobe epilepsy. J Neurosci 31:4037–4050.

▪ Zhang CL, Zou Y, He W, Gage FH, & Evans RM (2008) A role for adult TLX-positive neural stem cells in learning and behaviour. Nature 451(7181):1004-1007.

▪ Zhao C, Deng W, Gage FH. Mechanisms and functional implications of adult neurogenesis. Cell. 2008;132:645–660.

▪ Zheng L-S, *et al.* (2014) Mechanisms for interferon-alpha-induced depression and neural stem cell dysfunction. Stem cell reports 3(1):73-84.

BIBLIOGRAPHY

- Ziebell F, Dehler S, Martin-Villalba A, & Marciniak-Czochra A (2018) Revealing age-related changes of adult hippocampal neurogenesis using mathematical models. Development 145(1).

- Zimmermann, H. (1999). Two novel families of ectonucleotidases: molecular structures, catalytic properties and a search for function. Trends Pharmacol Sci 20, 231-236.

- Zuberi SM, Brunklaus A, Birch R, Reavey E, Duncan J, Forbes GH.Genotype-henotype ssiciations in SCN1Arelated epilepsies.Neurology 2011; 76: 594–600.